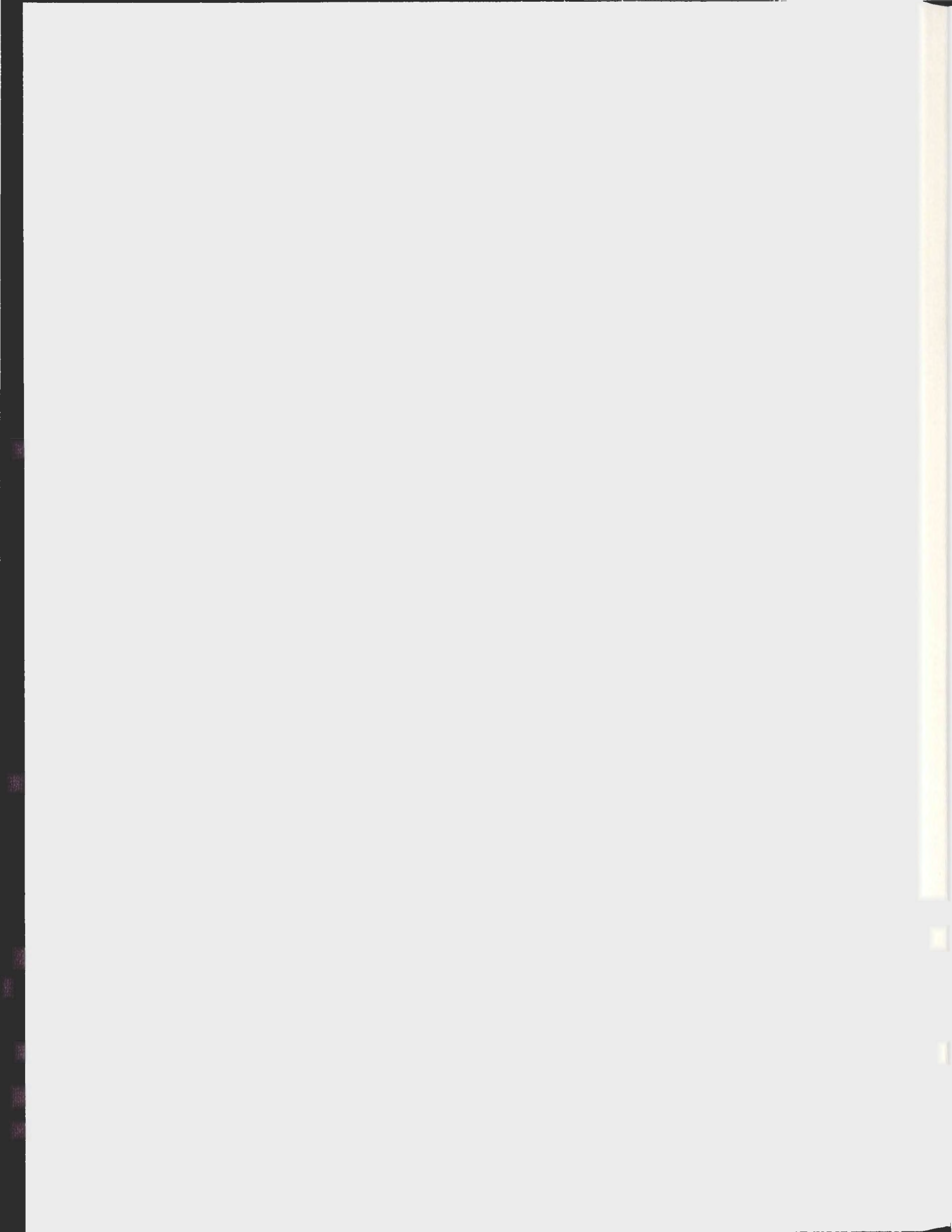


SLOW SKELETAL MUSCLE ACTIN:  
CONFIRMATION AND FURTHER INSIGHTS

ROBERT C.C. MERCER





**Slow skeletal muscle actin:  
Confirmation and further insights**

**Robert C.C. Mercer  
Department of Biochemistry  
Memorial University of Newfoundland  
St. John's, Canada**

This thesis is submitted in partial fulfilment of the requirements for the degree of Master of Science.

## Abstract

1) The 1° structures of three sarcomeric actin isoforms were inferred from cDNA sequences: Atlantic herring (*Clupea harengus*) fast skeletal muscle actin, Acc# GQ455648; Atlantic herring slow skeletal muscle actin, Acc# EF495203; and Atlantic Mackerel (*Scomber scombrus*) fast skeletal muscle actin, Acc# EF607093. The two herring skeletal muscle actin cDNAs possess different non-coding regions and are concluded to arise from different genes.

2) Sequence comparisons demonstrate that actin from a given type of skeletal muscle has been conserved across teleost evolution. Herring slow muscle actin and salmonid slow muscle actin (*Salmo trutta*; Acc# AF267426 [Mudalige et.al. 2007]) share a single substitution, Gln 354 Ala (herr:sal), while, in addition to this substitution the fast skeletal muscle actins from Atlantic herring and Atlantic salmon (*Salmo salar*; Acc# AF304406 [Mudalige et.al. 2007]) contain Ser 160 Thr for a total of two substitutions.

3) There are thirteen inferred substitutions between fast and slow skeletal muscle actins isolated from Atlantic herring, six that are non-conservative in nature. This is a record for two vertebrate sarcomeric actins. The replacements (non-conservative underlined) are: residues: 2, 3, 103, 155, 160, 165, 278, 281,

310, 329, 358, 360 and 363. Most of the heterogeneity occurs after residue 100. Also of note is the exchange of Gln (fast actin) for Asp (slow actin) at position 360, which endows the slow type isoform with a greater negative charge in the neutral pH range. Comparison with the actin found in the skeletal muscles of the rabbit demonstrates 11 replacements (five non-conservative) with herring slow skeletal muscle actin and four (one non-conservative) when compared to herring fast skeletal muscle.

4) Two skeletal muscle actins of non-identical net-charge were detected by alkaline urea PAGE in the slow skeletal muscle of the following species - mackerel and smelt - but not in other teleosts (halibut and tilapia), primitive fish (hagfish and lamprey), birds or amphibians.

5) Herring slow skeletal muscle G-actin (CaATP) is less resistant to thermal, and chemical, -induced denaturation (as monitored by electronic circular dichroism) than its fast muscle counterpart. Thermal melting temperatures (Tms) and [urea] unfolding midpoints, respectively, are: 50°C and 55°C; 3.5 M and 4.0 M. A rate of unfolding for slow skeletal muscle actin was determined, in the presence of 0.1 mM EDTA, to be  $6.5 \times 10^{-4} \text{ sec}^{-1}$ . The fast

skeletal muscle isolated from Atlantic mackerel has a  $T_m$  of 55°C and a midpoint of unfolding in the presence of urea of 4.0 M.

6) Fast skeletal muscle G-actin from Atlantic mackerel contains a non-conservative substitution in common with slow skeletal muscle actin: Ser 155 Ala (herring fast: mackerel fast/herring slow). This finding rules out the identity of this residue as a contributor to the observed instability.

7) Herring slow skeletal muscle G-actin (CaATP) is less resistant to cleavage by subtilisin and thrombin than the fast muscle counterpart. Subtilisin cleavage between residues 48 and 49 was confirmed by Edman sequencing of Western blotted peptides. Of the two actin isoforms, only slow skeletal muscle actin could be cleaved by thrombin. The fast skeletal muscle actin isolated from mackerel, in spite of the present substitutions, behaves as the other fast skeletal muscle actins when subjected to subtilisin and thrombin exposure.

8) Fluorescence spectra of all G-actins (Ca - 2'-deoxy 3' O- (N'-Methylantraniloyl) ATP) studied is characterized by emission maxima at 430 nm; demonstrating a virtual identity of the nucleotide binding pockets of the three isoforms. Emission intensity was reduced in the case of the slow muscle actin, consistent with it having a weaker affinity for the nucleotide.

### Acknowledgements

Above all, I wish to express my gratitude to my supervisor, Dr. David H. Heeley for his continuous encouragement and patience. The world of proteins is a complicated one; he has been my guide.

I would like to thank the members of my supervisory committee, Dr. Valerie Booth and Dr. David W Thompson for all the helpful discussions and insights.

Also, my thanks to Ms. Donna M. Jackman and Dr. Elizabeth Perry who have provided, on a number of occasions, essential technical expertise.

Many thanks to all my friends and family for their continued support. Special thanks go to my father, Bob Mercer, who spent some very early mornings helping to collect specimens and my brother, Jamison, for his encouragement and understanding. Finally, for my introduction to the world of science, I thank my mother, Marie Mercer.

## Table of Contents

Abstract	ii
Acknowledgments	v
Table of contents	vi
List of Abbreviations	ix
List of Figures	x
List of Tables	xii
<b>Chapter 1: Introduction</b>	<b>1</b>
1.0 An overview of muscle	1
1.1 Major sarcomeric proteins	7
1.1.1 Myosin	7
1.1.2 Troponin complex	9
1.1.2.1 Troponin C	10
1.1.2.2 Troponin I	12
1.1.2.3 Troponin T	13
1.1.3 Tropomyosin	14
1.1.4 Actin	16
1.2 Actin isoforms	22
1.3 Goals of study	26
<b>Chapter 2: Methods &amp; Materials</b>	<b>27</b>
2.1 RNA extraction	27
2.2 mRNA isolation	28
2.2.1 Annealing of probe	28
2.2.2 Stock solution preparation	28
2.2.3 Washing of Streptavidin-Paramagnetic Particles	29
2.2.4 Capture and washing of annealed Oligo(dt)-mRNA hybrids	29
2.2.5 Elution of mRNA	30
2.3 cDNA library construction	30
2.3.1 First strand synthesis	30
2.3.2 First strand yield	31
2.3.3 Second strand synthesis	32
2.3.4 Sal 1 adapter addition	33
2.3.5 Not 1 digestion	33
2.3.6 Column chromatography	34
2.3.7 Ligation of cDNA to the vector	35
2.4 E.coli transformation	35

2.5	cDNA library construction	36
2.5.1	Archive plates	36
2.5.2	Copy plates	36
2.6	cDNA library screening	37
2.6.1	Express dot-blot	37
2.6.2	Probe preparation	38
2.6.3	Dot-blot hybridization	38
2.7	DNA isolation and purification	40
2.8	Plasmid digestion	41
2.9	Southern transfer	41
2.10	DNA sequencing	42
2.11	Actin acetone powder	43
2.12	Actin preparation	44
2.13	Actin concentration determination	46
2.14	Electrophoretic methods	46
2.14.1	Sodium dodecyl sulphate polyacrylamide gel electrophoresis	46
2.14.2	Alkaline urea polyacrylamide gel electrophoresis	47
2.15	Electro blotting	47
2.16	Proteolytic methods	48
2.16.1	Subtilisin exposure	48
2.16.2	Thrombin exposure	49
2.17	Spectroscopic methods	49
2.17.1	Far and near ultra violet circular dichroism spectroscopy	49
2.17.2	Chemically induced unfolding	50
2.17.2.1	Urea induced unfolding	50
2.17.2.2	EDTA induced unfolding	50
2.17.3	Fluorescence spectroscopy	51
2.18	Data manipulation	51
2.18.1	cDNA sequences	51
2.18.2	Graphing	52

<b>Chapter 3: Results &amp; Discussion</b>	53
3.1 Nucleotide sequencing	53
3.2 Electrophoresis of isoactins	76
3.2.1 Alkaline urea PAGE	76
3.2.2 Limited proteolysis	84
3.2.2.1 Subtilisin exposure	84
3.2.2.2 Thrombin exposure	91
3.3 Spectroscopic techniques	93
3.3.1 Electronic circular dichroism	93
3.3.1.1 Thermal unfolding	93
3.3.1.2 Chemical unfolding	99
3.3.1.2.1 Urea induced unfolding	99
3.3.1.2.2 EDTA induced unfolding	104
3.3.2 Fluorescence spectroscopy	106
<b>Chapter 4: Conclusions &amp; Future Directions</b>	108
4.1 Conclusions	108
4.2 Phylogenetic analysis	115
4.3 Future Directions	119
References	121

## List of Abbreviations

ABP	Actin Binding Proteins
AMP	Ampicillin
ATP	Adenosine-5'-triphosphate
BSA	Bovine serum albumin
CD	Circular dichroism
cdNA	Complementary DNA
dCTP	Deoxycytidine triphosphate
DIG	Digoxigenin
DNA	Deoxyribonucleic acid
dNTP	Deoxyribonucleotide
DTT	Dithiothreitol
EDTA	Ethylenediaminetetraacetic acid
EtOH	Ethanol
F-actin	Filamentous actin
g	Gravity
G-actin	Globular actin
GTE	Glucose-Tris-EDTA buffer
kDa	kiloDalton
LB	Luria-Bertani broth
M	Mols/L
mRNA	Messenger RNA
PBS	Phosphate buffered saline
pI	Isoelectric point
PMSF	Phenylmethanesulphonylfluoride
RNA	Ribonucleic acid
Rpm	Revolutions per minute
RT	Room temperature
SA-PMP's	Streptavidin Paramagnetic Particles
SDS	Sodium dodecyl sulfate
SOC	Super optimal broth with catabolite repression
SSC	Saline sodium citrate
TE	Tris - EDTA buffer
TEN	Tris - EDTA - sodium chloride buffer
TM	Tropomyosin
Tn	Troponin
TnC	Troponin C (calcium)
TnI	Troponin I (inhibitory)
TnT	Troponin T (tropomyosin binding)
tRNA	Transfer RNA
TYPGN	A highly nutritious <i>E.coli</i> broth

List of Figures		Page #
Figure 1: Segregation of muscle fibre type in round bodied fish.		3
Figure 2: Structure of the striated muscle fibre.		6
Figure 3: cDNA sequence (Acc# EF495203) corresponding to the actin isoform found in the slow skeletal muscle of Atlantic herring ( <i>Clupea harengus</i> ).		54
Figure 4: Inferred amino acid sequence (immature) of the skeletal muscle actin found in the slow skeletal muscle of Atlantic herring.		55
Figure 5: cDNA sequence (Acc# GQ455648) corresponding to the actin isoform found in the fast skeletal muscle of Atlantic herring ( <i>Clupea harengus</i> ).		56
Figure 6: Inferred amino acid sequence (immature) of the skeletal muscle actin found in the fast skeletal muscle of Atlantic herring.		57
Figure 7: cDNA sequence (Acc # EF607093) corresponding to the actin isoform found in the fast skeletal muscle of Atlantic mackerel ( <i>Scomber scombrus</i> ).		58
Figure 8: Inferred amino acid sequence (immature) of the skeletal muscle actin found in the fast skeletal muscle of Atlantic mackerel.		59
Figure 9: Comparison of the cDNA sequences corresponding to the slow skeletal muscle actin isoforms isolated from Atlantic herring and Brown trout.		60
Figure 10: Comparison of the cDNA sequences corresponding to the fast skeletal muscle actin isoforms isolated from Atlantic herring and Atlantic salmon.		62
Figure 11: Comparison of the inferred actin amino acid sequences from the slow and fast skeletal muscles of Atlantic herring.		65
Figure 12: Comparison of the inferred actin amino acid sequences from the slow skeletal muscles of Atlantic herring and Brown trout.		69
Figure 13: Comparison of the inferred actin amino acid sequences from the fast skeletal muscles of Atlantic herring and Atlantic salmon.		70

Figure 14: Comparison of the inferred actin amino acid sequences from the fast skeletal muscles of Atlantic herring, Atlantic salmon and, Atlantic mackerel.	71
Figure 15: Location of substitutions in relation to the crystal structure of rabbit skeletal muscle actin.	73
Figure 16: Assessment of enrichment using SDS PAGE on actins isolated from the fast and slow skeletal muscles of Atlantic herring.	77
Figure 17: Alkaline urea PAGE of the fast and slow skeletal muscle actins isolated from Atlantic herring.	78
Figure 18: Alkaline urea PAGE of the fast and slow skeletal muscle actins isolated from Atlantic mackerel and Rainbow smelt.	81
Figure 19: Alkaline urea PAGE of skeletal muscle actin from Atlantic halibut ( <i>Hippoglossus hippoglossus</i> ) and tilapia (species unknown).	83
Figure 20: Differential susceptibility of actin isoforms isolated from Atlantic herring to limited proteolysis with subtilisin.	85
Figure 21: Edman sequencing of the 36 kDa peptide derived from subtilisin digestion of actin.	87
Figure 22: Limited proteolysis of actins from the skeletal muscle of Atlantic herring and the fast skeletal muscle actin from Atlantic mackerel.	90
Figure 23: Limited proteolysis of skeletal muscle actin isoforms from Atlantic herring using thrombin.	92
Figure 24: Thermally induced unfolding of the fast skeletal actin isoform from Atlantic herring as monitored by far-UV circular dichroism.	94
Figure 25: Thermally induced unfolding of the slow skeletal actin isoform from Atlantic herring as monitored by far-UV circular dichroism.	95
Figure 26: Thermally induced unfolding of the skeletal muscle isoforms of actin isolated from the muscles of Atlantic herring plotted as the percent overall change in ellipticity.	96

Figure 27: Thermally induced unfolding of the fast skeletal actin isoform from Atlantic mackerel as monitored by far-UV circular dichroism.	97
Figure 28: Dependence of relative ellipticity of actin isolated from Atlantic herring on the concentration of urea present.	101
Figure 29: Dependence of the relative ellipticity of actin isolated from Atlantic mackerel upon concentration of urea present.	103
Figure 30: EDTA induced unfolding of actin isoforms isolated from the fast and slow skeletal muscles of Atlantic herring.	105
Figure 31: Emission spectra of mant-ATP bound to various skeletal muscle actin isoforms.	107
Figure 32: Phylogenetic analysis of <i>teleost</i> fish for the presence of slow skeletal muscle actin.	116

### List of Tables

Table 1: Summary of results for the three skeletal muscle actins compared to the skeletal muscle actin isolated from rabbit.	66
--	----

# Chapter 1

## Introduction

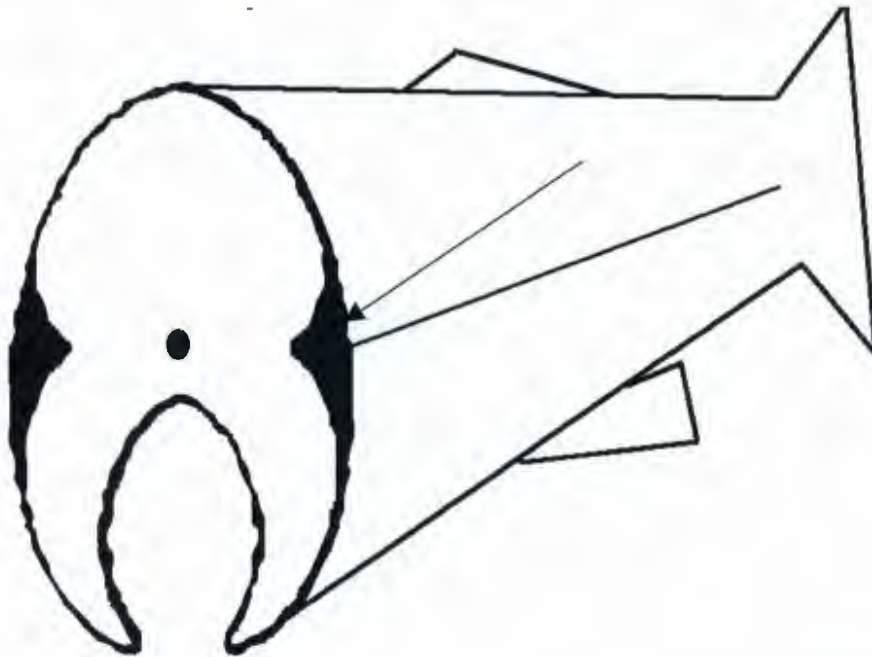
### 1.0 An overview of muscle

There are a number of criteria that must be met before something can be defined as alive: the ability to maintain homeostasis, organisation, metabolism, growth, adaptation, response to stimuli and the ability to reproduce. Without motion, much of this would be impossible. It is an absolutely essential process for all life on every size scale. Movement can be imperceptible to the human eye, when a cell divides in two; or, on the other end of the spectrum, it can be obvious when observing a predator catch its prey, a sprinter completing a race in mere seconds or a bird beginning flight. Very few proteins are responsible for a cell's and, by extension, an organism's movement. Simply put, the proteins actin and tubulin form 'tracks' upon which the motor proteins (myosin, kinesin and dynein) 'walk'. While the 'track' proteins form the roads upon which the motor proteins 'drive', the motor proteins themselves 'burn' ATP, adenosine triphosphate, transforming its stored energy into movement. For over sixty years these processes have been studied extensively [Engelhardt & Ljubimowa 1939; Straub 1942; Huxley & Niedergerke 1954; Huxley & Hanson 1954]. In that time the mechanisms of muscle contraction have been the focus of the most attention and are, therefore, the best understood.

There are two main forms of muscle: striated (cardiac and skeletal) and unstriated (smooth muscle) [MacIntosh 2006]. The classification is based upon visual inspection under a light microscope: the presence of light and dark bands or stripes is indicative of striated muscle while the absence of this banding pattern is characteristic of smooth muscle. Only striated muscle can be found in the voluntary skeletal muscles. This muscle type is innervated by the somatic nervous system and under the conscious control of the organism. The involuntary muscles, smooth and cardiac, are under control of the autonomic nervous system.

Teleost fish, the organisms that are host to the protein isoforms that are the focus of this thesis, like other vertebrates, contain diverse muscle fibre types. Unlike other vertebrates, however, their fast and slow skeletal muscle fibres are highly segregated from one another. Slow contracting, or red, skeletal muscle fibres are confined to a narrow strip along the lateral line with a wedge-like insertion into body of the fish (Figure 1) [Johnston 2001].

Figure 1: Segregation of muscle fibre type in round bodied fish.



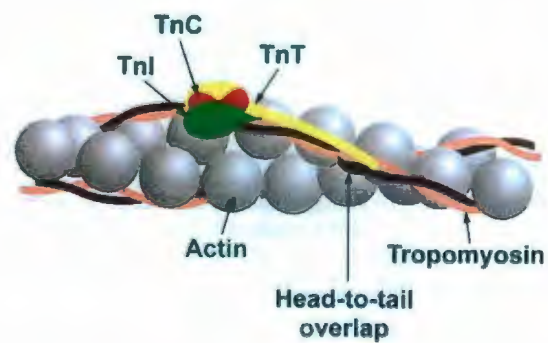
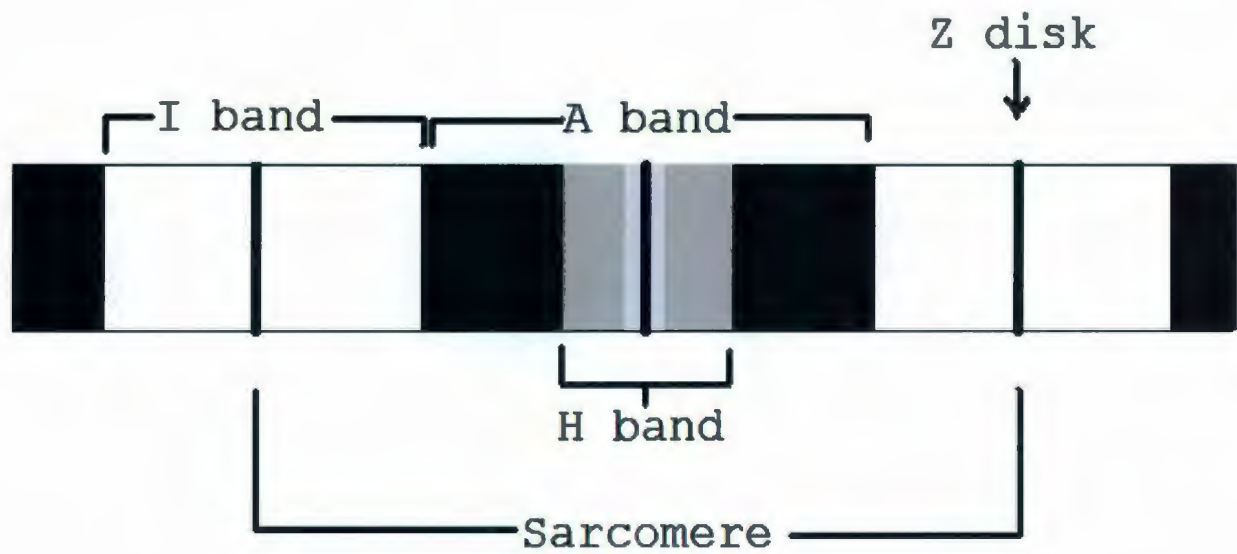
Arrow indicates slow skeletal muscle. Fast skeletal muscle is represented by the lighter shaded region.

Slow muscle fibres are smaller in diameter than their fast (white) fibre counterparts (25-45µm as opposed to 50-100µm). They usually account for less than 10% of total muscle and have never been found to account for more than 30% [Johnston 2001]. Slow fibres synthesise ATP predominantly by oxidative phosphorylation of ADP, saving carbohydrates for the glycolytic pathway used by tissues that cannot readily utilise pyruvate, fatty acids or ketone bodies [Hess 1970]. These fibres are richer in myoglobin, cytochromes and mitochondria than their fast counterparts, which gives them their dark appearance. Slow (oxidative) muscle fibres are employed in long term, low intensity sustained swimming, such as migration, where the cost of locomotion is low and economical and, as such, they are more resistant to fatigue than their fast counterparts [Morgan & Proske 1984]. Fast contracting muscle, on the other hand, is used in situations where the need for maximum power output exceeds the need for economical energy use; fast start swimming activities such as catching prey or avoiding predators and the uphill battle of the salmon as it returns to its birthplace to mate. While oxidative phosphorylation can be utilised by fast muscle, the primary energy source is the breakdown of glycogen while at the same time utilising small amounts of cytosolic ATP and phosphocreatine. In some teleost species, intermediate (pink) muscle is found between the fast and slow skeletal muscle fibres. As the name suggests, the characteristics of these intermediate skeletal muscle fibres are midway between those of fast and slow

skeletal muscle fibres. In cases of isoform specific expression in the various muscle fibre types, intermediate skeletal muscle fibres will utilise a mixture of protein isoforms.

Muscle fibres are multinucleated cells that, while in diameter measuring 10 - 100  $\mu\text{m}$ , can be several cm in length [Squire 1990]. Made of parallel bundles of myofibrils (Greek origin; *myos* meaning muscle), of which there are about one thousand in an individual fibre, skeletal (striated) muscle is given its striped appearance by the in register alignment of the repeating myofibrillar unit, the sarcomere (Greek; *sarkos* meaning flesh). Sarcomeres are bordered by two dense Z disks with a dark A band (itself with a light H zone which contains the M line) in the center and two light I bands between the A band and the two Z disks (Figure 2). It was found by electron microscopy that the A and I bands represent areas of greater and lesser density, respectively. The thick (15 nm diameter) and thin (6 nm diameter) filaments that make up the sarcomere cause this difference in density, giving the cells their striated appearance [Huxley & Niedergerke 1954; Huxley & Hanson 1954]. A bands are more dense as they are regions of thick and thin filament overlap while the I bands are due to thin filaments only and are therefore less dense.

Figure 2: Structure of the striated muscle fibre.



Thin filament structure taken from Heeley *et al.* 1987.

While the mechanism of skeletal muscle contraction is outside the scope of this thesis, a general description of filament structure is useful when discussing the individual components. The thick filament is formed by the motor protein myosin in a staggered array to optimise thin filament binding. The thin filament is constructed primarily of globular actin polymerized into a left handed coil; tropomyosin is found polymerized in a head to tail fashion forming a string that wraps around the actin filament, covering the myosin binding sites (Figure 2). The troponin complex (TnC, TnT, TnI) which binds to both actin and tropomyosin, is responsible for moving tropomyosin away from the myosin binding sites upon the reception of the proper stimulus, allowing for myosin binding and contraction [Greeves 1999; Perry 2001; Gomes et al. 2002].

## **1.1 Major sarcomeric proteins**

### **1.1.1.0 Myosin**

Myosins are a large (over 15 members) and diverse family of proteins that undergo dynamic conformational changes upon ATP hydrolysis, triggered by binding to actin filaments [Berg et al 2001, Lionikas & Larsson 2006]. First discovered in 1864 by Kuhne, but not reported as an enzyme until 1939 [Engelhardt & Ljubimowa 1939], myosin is ubiquitous in all eukaryotic cells. It is found in highest concentration in striated muscle where it composes almost 50% of the total protein [Lyons et al. 1990]. Due

to the large quantities in which it can be prepared, most research was performed on muscle myosin up until cloning methods made all myosins accessible. The current discussion will focus on the muscle myosins whose role it is to pull actin filaments closer together, shortening the sarcomere and, by extension, the entire muscle.

Sarcomeric myosin (or myosin II) is a hexameric protein composed of two heavy chains (171-241 kDa) and four light chains (15-30 kDa); two regulatory light chains (RLC) and two essential light chains (ELC). The heavy chain of myosin was shown [Karn *et al.* 1983] to have a pI of ~ 5.5 and a roughly equal number of positively and negatively charged residues. All 20 of the standard amino acids are represented in the sequence, which contains over 50% polar residues with tryptophan and cysteine being found in the lowest quantity [Karn *et al.* 1983]. The substructure of sarcomeric myosin, that of two heads which are joined by a long tail, was elucidated by electron microscopy [Lowey & Cohen 1962; Lowey *et al.* 1969]. Under controlled *in vitro* conditions, limited proteolytic cleavage can occur within the neck region generating a soluble head portion [Mueller & Perry 1962, Weeds & Taylor 1975], the so-called subfragment-1. This particular fragment retains the capability of binding to actin and hydrolysing ATP. Further, unlike the native molecule, it was soluble and has, therefore, been extensively used over the years in biochemical studies [Lymn & Taylor 1971].

Subsequent structural studies [Vibert & Cohen 1988, Rayment *et al.* 1993] showed that the globular head is comprised of three domains: one each of 50 kDa, 25 kDa and, 20 kDa. Two light chains, one of each type, associate with the 20 kDa neck region while the site of ATP and actin binding is the role of the 50 kDa component which is further divided into upper and lower subdomains [Houdusse *et al.* 2000]. The cleft formed between these subdomains has been shown to bind strongly to actin when closed and weakly when open; mirroring the cycle of ATP hydrolysis that takes place during contraction [Conibear *et al.* 2003]. The two C-terminal regions of myosin II associate as a coiled coil to form the tail, which can spontaneously form filaments when exposed to solutions of low ionic strength [Schwaiger *et al.* 2002]. These filaments arrange themselves with half the heads pointing away from the other half so that there is a bare region in the center where no crossbridges can be formed with actin [Harford & Squire 1986].

#### 1.1.2.0 Troponin complex

Cardiac and skeletal muscles have myosin (contraction) regulatory systems that differ markedly from that found in smooth muscle and non-muscle cells.  $\text{Ca}^{2+}$  regulates vertebrate skeletal muscle contraction through binding to a regulatory protein complex known as troponin (Tn). Discovered in 1965 by Ebashi [Ebashi & Kodama 1965; Ebashi *et al.* 1968], Tn is composed of three subunits: the

calcium binding subunit, TnC; the tropomyosin binding subunit, TnT; and the inhibitory subunit, TnI [Greaser & Gergely 1971, 1973]. The quaternary structure of the Tn complex can be divided into two domains: TnC, TnI and the C-terminal one third of TnT form a globular domain and the remainder of TnT forms a highly extended tail [Ohtsuki 1979; Pato *et al.* 1981; White *et al.* 1987; Ohtsuki 2007]. The 3D structure of the core domain of Tn (Ca<sup>2+</sup> saturated) is primarily composed of  $\alpha$  helices and can be further divided into structurally distinct subdomains; the regulatory head (TnC residues 3-84 and TnI residues 150-159) and the IT arm (TnC residues 93-161, TnI residues 42-136 and TnT residues 203-271) [Herzberg & James 1988; Gagné *et al.* 1995; Filatov *et al.* 1999; Takeda *et al.* 2003]. For the purposes of this discussion the three subunits will be addressed separately and the binding between them will be discussed.

#### 1.1.2.1 Troponin C

Troponin C (TnC) is the smallest of the three troponin subunits. It is composed of about 160 residues; with a molecular weight of about 18 kDa [Head & Perry 1974; Collins *et al.* 1977] and a pI of 4.1-4.4 [Hearthorne & Driezen 1972]. A dumbbelled shaped protein, TnC is composed of two Ca<sup>2+</sup> binding domains, each capable of binding a divalent cation at two sites, that are separated by an alpha helical linker. Like other Ca<sup>2+</sup> binding proteins each binding domain in TnC is composed of an EF hand motif - a helix-loop-helix structure. Numbered I-IV starting at the N-terminus

sites I and II are low affinity sites specific for  $\text{Ca}^{2+}$  while III and IV are high affinity sites that are capable of binding  $\text{Mg}^{2+}$  in addition to  $\text{Ca}^{2+}$  [Ikemoto 1974; Ikemoto *et al.* 1974; Leavis *et al.* 1978; Sin *et al.* 1978]. An EF hand binds divalent metal ions by coordinating it with six charged residues located in a twelve residue loop region that is flanked by two alpha helices (hence, helix-turn-helix). Returning our attention to TnC, sites I, II, III and IV are flanked by helices A & B, C & D, E & F and, G & H respectively [Collins *et al.* 1973; Kretsinger & Barry 1975]. The previously mentioned linker between the two TnC domains is located between helices D and E. In addition to a high glutamic and aspartic acid content used to bind divalent cations, TnC contains only two tyrosine residues, a single residue of proline, cysteine and histidine and no tryptophan [Collins *et al.* 1977; Zot & Potter 1987]. It was shown that the  $\text{Ca}^{2+}$  binding of the high affinity sites (III and IV) results in a release that is too slow to contribute to the dynamic nature of contractile regulation. As such, these two C-terminal binding sites are thought to anchor TnC in the Tn complex and are always saturated with divalent metal cations under physiological conditions [Ohtsuki & Morimoto 2008].

Like other thin filament proteins, TnC expression is unique to the particular muscle type where it is found. Cardiac TnC (cTnC) is found in cardiac muscle and slow skeletal muscle while skeletal TnC (sTnC) is expressed solely in fast skeletal muscle.

It is important to note that in cTnC site I is incapable of binding  $\text{Ca}^{2+}$  due to sequence substitutions.  $\text{Ca}^{2+}$  binding is the switch that triggers muscle contraction; the size of the conformational change upon  $\text{Ca}^{2+}$  binding is considerably larger for sTnC when compared to cTnC [Spyracopoulos et al. 1997].

#### 1.1.2.2 Troponin I

First isolated by Hartshorne and Mueller in 1968 and independently by Schaub and Perry the following year, troponin I (TnI) inhibits the actin activated  $\text{Mg}^{2+}$  dependent ATPase activity of myosin by interacting with actin and tropomyosin [Van Eyk et al. 1993]. A basic protein, it is composed of about 180 amino acids giving it a molecular weight of 21 kDa. It has a pI of 9.3 due to an unusually high content of charged residues; 44 positive and 35 negative in addition to three cysteine, two tyrosine and one tryptophan [Wilkinson 1974; Grand & Wilkinson 1976]. Upon the binding of  $\text{Ca}^{2+}$  by TnC, TnI is pulled from actin, relieving the inhibition of the myosin ATPase. Residues 104-115 (gly-lys-phe-lys-arg-pro-pro-lys-arg-arg-val-arg) are the minimum fragment required for the binding of this 'main inhibitory region' to actin [Talbot & Hodges 1981]. When  $\text{Ca}^{2+}$  is not bound to TnC, TnI is predominantly bound to TM and actin. There are three known genes coding for three distinct isoforms of TnI: cardiac, fast skeletal and slow skeletal muscles. These isoforms are highly homologous with the exception of one peculiarity: cTnI has a N-terminal extension of 32 amino acids [Van Eerd & Takahashi 1976].

This extension is present across species and has been shown to have two adjacent serine residues phosphorylated by protein kinase A in response to adrenergic stimulation of the heart [Zhang *et al.* 1995]. This modification has been demonstrated to lower the  $Ca^{2+}$  sensitivity of force development and to increase the rate of force relaxation [Zhang *et al.* 1995]. Interestingly, while slow TnI is the dominant cardiac isoform during the foetal development of the mouse, to be completely replaced by nine months of age, mice lacking cTnI died of acute heart failure after just eighteen days [Huang *et al.* 1999].

#### 1.1.2.3 Troponin T

Troponin T (TnT) is the largest member of the Tn complex with a molecular weight ranging from 31-36 kDa, about 250 - 300 residues, depending on the source where a particular isoform is found (cardiac TnT typically contains more amino acids than skeletal TnT.). TnT is a highly charged, structurally asymmetric molecule; there is an almost equal content of glutamic and aspartic acid residues in the N-terminal half of the molecule while positively charged residues prevail at the C-terminal half giving the molecule a pI of 9.1 [Pearlstone *et al.* 1976, Pearlstone & Smillie 1976]. TnT is capable of binding tropomyosin at two sites at least, acting as the anchor of the troponin complex to tropomyosin. Structural studies show that the C-terminal one third of TnT is located near residue 190 of tropomyosin while the N-terminal region, that forms the tail of

the Tn complex, bridges the overlap region of adjoining tropomyosin molecules [White *et al.* 1987; Goonasekara & Heeley 2009]. The primary role of TnT is to anchor the Tn complex to the thin filament by binding TnI and TnC through its C-terminal portion and binding tropomyosin with the N-terminal segment. Unfortunately, TnT is of low solubility making *in vitro* studies difficult. However, two large soluble fragments can be prepared by mild treatment with chymotrypsin resulting in TnT1 (residues 1-158) and TnT2 (residues 159-259) [Pearlstone *et al.* 1979].

#### 1.1.3.0 Tropomyosin

Discovered by Bailey in the 1940's [Bailey 1946; Bailey 1948], skeletal muscle tropomyosin (TM) is a member of a large family of proteins that is widely distributed among eukaryotic cells. However, it was not until the 1960s that a role for TM in muscle contraction was demonstrated [Ebashi 1963]. The length of TM varies in vertebrates; there is a high molecular weight group with 274-284 amino acids and a low molecular weight group composed of 245-251 residues [Perry 2001]. Regardless of the overall length of the molecule, all TMs have multiples of ~40 amino acids that are responsible for the interactions with the monomers in an actin filament. Most pertinent to the current discussion is TM in the thin filament of vertebrate skeletal (and smooth) muscle where it plays a regulatory role in the contractile process [Spudich & Watt 1971].

Through the use of alternative promoters and RNA splicing the four identified TM genes in mammals (TMP1, TMP2, TMP3 & TMP4) are responsible for over twenty isoforms [Lees-Miller & Helfman 1991]. The most extensively studied skeletal muscle TM is that from rabbit fast muscle where it makes up ~3% of the total protein. The two dominant TM isoforms found in skeletal muscle, the protein products of TMP1 and TMP2, are respectively named  $\alpha$ -TM and  $\beta$ -TM. Both of the skeletal muscle isoforms are members of the high molecular weight group and are composed of 284 amino acids [Stone & Smillie 1978; Mak *et al.* 1980]. The most notable difference in primary structure between the  $\alpha$  and  $\beta$  TMs is the cysteine content:  $\alpha$ -TM has a single cysteine residue while the  $\beta$  isoform has two [Mak *et al.* 1980]. Tropomyosin exists as a dimer of two 33 kDa subunits that are 100%  $\alpha$ -helical; the dimer is a left handed coil of the two  $\alpha$  helices - the coiled-coil whose formation is entirely dependent on 1° structure. A repeating heptad *a-b-c-d-e-f-g* [McLachlan & Stewart 1975] with non-polar residues dominating positions *a* and *d* form a hydrophobic seam wrapping around the monomer (since an  $\alpha$  helix encompasses 3.6 residues per turn, this hydrophobic seam does not run parallel to the axis of the helix). This is a very important feature as it allows the two subunits of the dimeric TM to spontaneously coil around each other forming the coiled-coil. This can be clearly seen when subjecting TM to heat denaturation. A heat stable protein, the two subunits will dissociate when heated to 60°C but

will reassociate when cooled [Graceffa & Lehrer 1980; 1984]. It is known that both subunits are orientated the same way in the coiled-coil structure [Betcher-Lange & Lehrer 1978]. That is, both of the N-termini (and C-termini) are at the same end of the dimer [Johnson & Smillie 1975]. While all TMs appear capable of polymerization, it is more obvious in the muscle TMs. At physiological pH, the N-terminus of TM will have a net positive charge while the C-terminus will have a net negative charge. This results in an overlap of ~ 10 residues on either end of the molecule that is based, in part, on electrostatic interactions when the thin filament is formed [Caspar *et al.* 1969; Smillie 1976; Greenfeld *et al.* 2006]. This allows TM to form a continuous chain wrapping around the actin filament that, when properly controlled by the Tn complex, can block or expose the myosin binding sites on actin to either inhibit or allow for contraction.

#### 1.1.4.0 Actin

Actin is one of the most abundant eukaryotic proteins. In striated muscle it accounts for ~20% of total protein. Aside from one known exception, the *nematode* sperm, actin is ubiquitous in all eukaryotic cells. The mature, class II actin, found in striated muscle is comprised of 375 amino acids [Elzinga *et al.* 1973; Collins & Elzinga 1975]. The initiating methionine and following cysteine are both acetylated and removed (this is slightly different in class I actins - section 1.2) before the N-

terminus is permanently acetylated [Martin & Rubenstein 1987] and the 73<sup>rd</sup> residue, histidine, is methylated [Huszar & Elzinga 1971; Weihing & Korn 1972]. In addition to its abundance, actin is one of the most highly conserved proteins known throughout evolution. Astonishingly, the skeletal muscle actin isolated from chicken (*Gallus gallus*, Acc#P68139) and human (*Homo sapiens*, Acc#NP\_001091) have identical 1° structures. A protein of roughly 42 kDa, actin has a pI of 5.4-5.9 due to a roughly equal number of positively and negatively charged residues [Elzinga et al. 1973]. In addition, actin contains 16 tyrosine, 12 phenylalanine, nine histidine, five cysteine and four tryptophan residues (all four tryptophan located in subdomain one).

Isolated in 1942 by Bruno F. Straub as a soluble component of muscle acetone powder, actin was so named due to its ability to activate myosin [Straub 1942]. The protein exists in two forms: monomeric, globular actin (G-actin) and polymeric, filamentous actin (F-actin). This transition is accompanied by the hydrolysis of adenosine triphosphate (ATP) at a high affinity-binding site located within the central cleft of the protein [Kabsch et al. 1990] that also binds a divalent cation, believed to be Mg<sup>2+</sup> *in vivo*. In addition to this high affinity site, there are several other low affinity sites for the same cation scattered about the molecule [Zimmerle et al. 1987; Selden et al. 1989; Estes et al. 1992].

To form the core of the thin filament, actin must polymerize; a process that is regulated by a large number of actin binding proteins (ABPs) which are in turn regulated by signal transduction pathways. F-actin is further organised by other ABPs that can cross-link, cap, bundle or attach the filaments to the cell membrane [Kabsch & Vandekerckhove 1992]. While highly regulated *in vivo*, actin is capable of spontaneous polymerisation *in vitro* when exposed to ionic conditions believed to exist within the cell (50 mM KCl, pH 7.00 and 1 mM  $Mg^{2+}$ ). Typical actin preparations result in  $Ca^{2+}$  bound actin due to the use of  $CaCl_2$  in the extraction buffer. This practice results in a higher critical concentration for actin polymerisation (0.1 mM when binding  $Ca^{2+}$  and 0.1  $\mu M$  when binding  $Mg^{2+}$ ) which allows for solutions of G-actin to be kept at higher concentrations [Estes et al. 1991].

F-actin is, intrinsically, a highly dynamic structure due to the actin ATPase; the turnover of an actin filament has been measured in the order of minutes [Pollard & Cooper 1986]. Hydrolysis of ATP occurs after incorporation of a monomer into the filament: what is initially ATP-F-actin, will, over time, become ADP-F-actin. Monomer exchange is ~20 fold faster at the barbed end (subdomains one and three) of the filament compared to the pointed end (subdomains two and four) [Pollard 1986]; there is a higher probability that the subunits (actin monomers) at the pointed end have hydrolysed ATP before the next subunit is

incorporated - the opposite is true at the barbed end. As both ends share the same pool of monomeric actin, there is a net gain of monomers at the barbed end (ATP bound) and a net loss at the pointed end (ADP bound). ATP-actin incorporated at the barbed end is effectively shuttled along the filament to the pointed end where it is released as ADP-actin. This phenomenon is referred to as head-to-tail assembly or treadmilling [Wang 1985]. ADP-G-actin will not reassemble into filaments in any significant numbers until the ADP has been switched for ATP. The unassisted exchange rate is slow ( $0.003 \text{ s}^{-1}$ ) but it can be either increased by positive modulators or decreased by negative ones such as profilin and thymosin, respectively [Goldschmidt-Clermont et al. 1992].

While there are a very large number of identified ABPs, most fall into a much smaller number of families. The major functional groupings of the ABPs are as follows: motor (myosins), filament stabilising (tropomyosins), filament destabilising (cofilins), crosslinking (parallel, antiparallel and disordered), end-binding (capping, nucleation and anchorage), filament severing (gelsolin family) and monomer binding (sequestering and regulatory; as discussed above) [Pollard & Cooper 1986].

When the first atomic-resolution structure of actin was solved [Kabsch et al. 1990] it allowed for the wealth of biochemical and physical data to be interpreted with a new frame of reference.

To form crystals suitable for x-ray diffraction it was necessary to bind actin to DNaseI; otherwise the protein polymerised under the necessary crystallizing conditions. Fortunately there was a high-resolution structure of DNaseI available that made interpretation of the raw data easier [Suck *et al.*, 1984; Oefner & Suck, 1986]. While many other actin bound structures have been published in the ensuing years [Kabsch *et al.* 1990; McLaughlin *et al.* 1993; Schutt *et al.* 1993; Robinson *et al.* 1999] and more recently those of free, uncomplexed, G-actin [Otterbein *et al.* 2001; Graceffa & Dominguez 2003; Rould *et al.* 2006] they agree on the main structural elements of the actin molecule. Actin is composed of two domains, traditionally referred to as the large and small domain. These structures reveal that the two domains contain roughly the same amount of amino acids and can be each broken down into two subdomains; the 'large' domain consists of subdomains three and four while the 'small' domain is comprised of subdomains one and two. The residues that form these subdomains are as follows: subdomain one, 1-32, 70-144, 338-372; subdomain two, 33-69; subdomain three, 145-180 and 270-337; subdomain four, 181-269. The last three residues of the protein have, in most structures, either not been resolved or cleaved to prevent polymerisation. With a structure of actin in hand it became evident that subdomains one and three, between which there is a 'hinge' involved with the supposed opening and closing of the cleft, had identical topology. Each subdomain comprised a five stranded  $\beta$ -pleated sheet built from a  $\beta$  meander and a right-

handed  $\beta\alpha\beta$  structure; a strong indication of a gene duplication event. Interestingly, the amino acid composition of these two subdomains has little homology; it was inferred from this that each must have evolved independently to perform separate functions. Even more startling was the realisation that this conserved topology was identical to that of hexokinase and the N-terminal ATPase fragment of the 70 kDa bovine heat shock cognate protein (HSC70) [Kabsch & Holmes 1995; Hurley 1996]. HSC70 had been shown to have prokaryotic homologues which indicated that actin too has a prokaryotic ancestor. It has been demonstrated that MreB, the long elusive actin precursor, is capable of forming distinct filaments just below the cell surface of all non-spherical bacteria [Bork *et al.* 1992]. While there is little sequence homology, the 3° structure is startlingly similar to eukaryotic actin. When considered, this is of little surprise; since the functions performed by actin are so absolutely essential that all eukaryotic cells express it, prokaryotes must have a functional equivalent.

Returning to actin, while the published structures do agree on most aspects of the molecule, certain aspects of the true structure remain controversial. The nature of the binding cleft remains a question as it has been crystallised in both the open and closed states with both ATP and ADP. It appears that this cleft closes during polymerisation, which indicates that the opening and closing does indeed have something to do with

nucleotide exchange. Also, there is a collection of solution data demonstrating intramolecular changes in actin when bound to either ATP or ADP. Specifically, the susceptibility of the DNaseI binding loop (residues 39-55, subdomain two) to subtilisin changes dramatically with the identity of the bound nucleotide [Strzelecka-Golaszewska et al. 1992]. Yet, most crystal structures, with the exception of the work of Otterbien et al. in 2001 show little difference in the structure of the DNaseI binding loop located in subdomain two. In the Otterbien structure, this loop is a short  $\alpha$ -helix while in the others (excluding the original [Kabsch et al. 1990] where it is ordered due to binding DNaseI) it is not resolved and therefore concluded to be of a disordered nature, freely accessible to enzymatic cleavage. Clearly there is a discrepancy between the solution and crystal data that must be resolved.

## 1.2 Actin isoforms

The actin family comprises a small number of members. Heterogeneity was first demonstrated by isoelectric focusing and two dimensional electrophoresis [Whalen et al. 1976; Rubenstein & Spudich 1977; Zechel & Weber 1978] and peptide mapping [Lu & Elzinga 1977, Vandekerckhove & Weber 1978; 1981]. The number of residues that are acetylated and exolytically removed during post-translational modification is used as one criterion for the classification of the various actin isoforms. Class one actins

have only the initiating methionine removed while class two actins undergo two rounds of acetylation and removal; met-cys. Regardless of the class, all actins have a negatively charged amino acid that is acetylated as the first residue in the mature protein [Rubenstein & Martin 1983]. In vertebrates, class one actins are found primarily in microfilaments ( $\beta$ -cytoplasmic and  $\gamma$ 1-cytoplasmic) and class two actins are used in muscle ( $\alpha$ -skeletal,  $\alpha$ -aortic smooth,  $\alpha$ -cardiac and  $\gamma$ 2-enteric smooth) [DeNofrio *et al.* 1989]. Functional diversity appears to be the reason for this large number of actin genes. Each of the listed isoforms is found in specialised tissues [Otey *et al.* 1988] with more than one being utilized in a single cell.

In stark contrast to the other contractile proteins, no difference has been reported between actins isolated from different types of skeletal muscle [Vandekerckhove & Weber 1979]. That is, slow and fast skeletal muscles are assumed to function with exactly the same actin isoform (recall the 100% identity of the skeletal muscle actins from chicken and human!). This situation, which was viewed as being consistent with the high conservation of actin, was recently thrown into question, however [Mudalige *et al.* 2007]. In view of the report by Mudalige *et al.*, one of the goals of the current work was to thoroughly examine a variety of vertebrate slow skeletal muscles for their actin content. Clear evidence is presented which invalidates the one skeletal muscle isoactin rule [Mercer *et al.* 2009].

When comparing the over 180 actin sequences available from SwissProt, some interesting trends emerge. Even though substitutions are distributed throughout actin and no single residue can act as an indicator of function or location in a cell, certain regions are more variable than others. Generally, muscle actins tend to have four negatively charged residues at the extreme amino terminus (mature protein) opposed to the two or three found in other actins. This is believed to be involved in the more rapid or less compliant binding of myosin (and other ABPs) to various actin isoforms [Mounier & Sparrow 1997]. Other regions of high variability are as follows: residues 39-55 the DNaseI binding loop, residues 187-199 a helix involved in TM binding, residues 223-235 a small helix close to the filament axis, residues 260-280 the putative hydrophobic plug involved in interstrand interactions and, residues 316-325 a major self assembly site [Pollard & Cooper 1986; Kabsch & Vandekerckhove 1992]. By the end of the 1990s, 27 residues (7.2%) of the 375 found in actin were invariant in all actins [Sheterline et al. 1998]. This number has been continuously lowered as subsequent editions of that text have been published. On this point, residue 160, previously considered invariant, is shown to differ amongst actin sequences presented herein.

Moreover, this thesis demonstrates an unexpected level of heterogeneity for a vertebrate skeletal muscle actin. In fact the sequence of slow skeletal muscle actin from Atlantic herring

(compared to other sarcomeric actins such as fast muscle actin from same source), establishes a substitution record of thirteen replacements. The differing properties of this isoform in relation to its fast skeletal muscle counterpart will be discussed in detail in the following sections. Again it is important to note that the two actin isoforms display a level of heterogeneity that is unprecedented for a skeletal muscle actin. These differences in the 1° structure of the protein result in a marked decrease in conformational stability and biochemical properties such as rate of polymerisation [unpublished results from the Heeley laboratory] and nucleotide exchange rates [Mudalige *et al.* 2007]. As outlined in the goals of the current work, establishing the identified slow skeletal muscle actin as a bona fide isoform is of the utmost importance as the possibility exists that it could represent a singular 'freak of nature'.

## 1.4 Goals of study

- Determine the legitimacy of slow skeletal muscle actin as a true actin isoform.
  
- Map the distribution of slow skeletal muscle actin in vertebrates.
  
- Characterise the conformational stability of the actins identified in this work.
  
- Relate differences in conformational stability to heterogeneity of actin amino acid sequences.
  
- Incorporate the findings of this work into a phylogenetic tree of vertebrate skeletal muscle actins.

## Chapter 2

### Methods & Materials

#### 2.1 RNA extraction

A living Atlantic herring (obtained with the help of Robert Porter, a local fisherman) and an Atlantic mackerel (caught by the author with a fishing rod) were brought back to the laboratory for total RNA extraction of isolated muscle samples. TRIzol reagent (Invitrogen - cat. No. 15596-018) was used; the method will be described briefly. Fast (from herring) and slow (herring and mackerel) muscle tissue was taken from the specimen and homogenized with 1.0 ml TRIzol for every 0.1 g of tissue (2.0 g of muscle and 20.0 ml of TRIzol) using a 40 V Polytron homogenizer in a sterile, 50 ml polypropylene tube. Samples were incubated at room temperature (RT) for five minutes to allow for complete dissociation of nucleoprotein complexes. 0.2 ml of chloroform (Sigma, molecular biology grade - cat. No. C2432) was added for every 1.0 ml TRIzol. The tubes were capped and shaken by hand for 15 seconds and incubated at RT for another three minutes. The samples were then centrifuged at 12,000 x g for 15 minutes at 4°C. The colorless, upper aqueous phase was transferred to a new sterile tube and the RNA was precipitated using 0.5 ml isopropanol (Sigma, molecular biology grade - cat. No. I9516) for every 1.0 ml TRIzol. Samples were incubated at RT for another 10 minutes and centrifuged at 12,000 x g for 10 minutes at 4°C. The supernatant was poured off and the pellet

washed with at least 1.0 ml of 75% ethanol (EtOH) for every 1.0 ml TRIzol used in the initial homogenization. This was vortexed and centrifuged at 7,500 x g for five minutes at 4°C. The supernatant was poured off and the pellet was allowed to dry at RT for 10 minutes before being re dissolved in 0.1 ml RNase free deionized water (dH<sub>2</sub>O).

## **2.2 mRNA isolation**

For mRNA isolation, the PolyAtract<sup>®</sup> system II (Promega - cat. no. Z5200) was used. The procedure will be described.

### *2.2.1 Annealing of probe*

1.5 mg of total RNA and RNase free water was combined in a sterile, RNase free 3 ml tube to a final volume of 2.43 ml. The tube was incubated in a 65°C water bath for 10 minutes. 10 µl of Biotinylated-Oligo (dt) probe was added along with 60 µl of 20X standard saline citrate (SSC: 3 M NaCl, 300 mM sodium citrate). This was gently rocked to mix, and incubated at RT until completely cooled (~ 30 minutes).

### *2.2.2 Stock solution preparation*

10.0 ml sterile 0.5X SSC - combine 250 µl 20X SSC and bring to 10.0 ml with RNase-free water in a sterile, RNase free tube. The second solution (10.0 ml sterile 0.1X SSC) was prepared by

combining 50  $\mu$ l of 20X SSC with 9.95 ml RNase free water in a sterile, RNase free tube.

### *2.2.3 Washing of Streptavidin-Paramagnetic Particles*

The SA-PMPs are provided at a concentration of 1 mg/ml in a solution of PBS, 1 mg/ml BSA and 0.02% sodium azide in a 3 ml tube. This solution was necessary for the long-term stability of the SA-PMPs. For each isolation one tube of SA-PMPs was resuspended by gently flicking and then captured by placing it in a magnetic stand. Once the SA-PMPs were collected on the side of the tube (~ 30 seconds), the supernatant was carefully removed without disturbing the particles. The SA-PMPs were washed three times with 0.5X SSC (1.5 ml each time) and captured using the magnetic stand to remove the supernatant after each wash. The SA-PMPs needed to be completely resuspended for proper function; particles that appeared to be "clumped" and that could not be resuspended were discarded. The SA-PMPs were then resuspended in 0.5 ml of 0.5X SSC. The mRNA isolation procedures were carried out within 30 minutes of the washings in order to insure optimal performance and they could not be reused.

### *2.2.4 Capture and washing of annealed Oligo(dt)-mRNA hybrids*

The entire contents of the annealing reaction were added to the tube containing the washed and resuspended SA-PMPs. The mixture was gently inverted every one to two minutes to ensure proper mixing while incubating at RT for 10 minutes. The tube was

placed in the magnetic stand to capture the SA-PMPs so the supernatant could be removed. This supernatant was saved until confirmation that sufficient binding of mRNA had occurred. The particles were washed four times with 0.1X SSC (1.5 ml per wash) by once again flicking the tube to resuspend the particles between each wash.

#### *2.2.5 Elution of mRNA*

After the washes were complete and all the supernatant was removed, the SA-PMPs were resuspended in 1.0 ml of RNase-free water. The particles were captured using the magnetic stand and the mRNA containing supernatant was transferred to a provided, sterile 2 ml user tube.

### **2.3 cDNA library construction**

To create the cDNA library the SuperScript™ Plasmid System with Gateway® Technology for cDNA synthesis and Cloning (Invitrogen - cat.no.18248-013/039) was used.

#### *2.3.1 First strand synthesis*

Starting with the maximum amount (5 µg) of mRNA: 5 µl of nuclease free water, 2 µl Not 1 primer-adapter (0.5 µg/µl) and 5 µl of mRNA (1 µg/µl) were added to a sterile, 1.5 ml microcentrifuge tube. After heating to 70°C for 10 minutes the tube was quick chilled on ice and its contents collected by brief

centrifugation. 4  $\mu$ l of the 5x first strand buffer, 2  $\mu$ l of 0.1 M dithiothreitol (DDT), 1  $\mu$ l of a 10 mM dNTP mix and, 1  $\mu$ l of  $\alpha$ -<sup>32</sup>P dCTP (PerkinElmer - cat.no. BLU513H250UC - 1  $\mu$ Ci/ $\mu$ l) was added to the tube and the contents were mixed by vortex, collected by centrifugation and placed at 37°C for two minutes. 5  $\mu$ l of SuperScript™ II reverse transcriptase (200 units/ $\mu$ l) was added and the contents gently mixed by pipette and incubated at 37°C for one hour (final volume of 20  $\mu$ l). The tube was placed on ice to terminate the reaction.

### *2.3.2 First strand yield*

2  $\mu$ l was removed from the first strand reaction tube and placed in another microcentrifuge tube containing 43  $\mu$ l of 0.02 M ethylenediaminetetraacetic acid (EDTA - pH 7.50) and 5  $\mu$ l of the control, yeast transfer RNA (tRNA). 10  $\mu$ l aliquots of the diluted sample were spotted onto two glass fiber filters (Whatman cat.no. 1827-024). One filter was allowed to dry at RT to determine the specific activity of the  $\alpha$ -<sup>32</sup>P dCTP. The other filter was washed three times (five minutes each time) in a beaker containing 50.0 ml of ice cold 10% (wt/vol) trichloroacetic acid (TCA - Sigma cat.no. T6399) and 1% (wt/vol) sodium pyrophosphate. The filter was washed a fourth time at RT with 95% EtOH for two minutes and dried at RT. Both filters were placed in standard scintillant (Fischer - cat.no. SX16-4) and counted in plastic vials on the <sup>32</sup>P channel.

### 2.3.3 Second strand synthesis

93  $\mu$ l of nuclease free water, 30  $\mu$ l of 5x second strand buffer, 3  $\mu$ l of the 10 mM dNTP mix, 1  $\mu$ l of *E.coli* DNA ligase (10 units/ $\mu$ l), 4  $\mu$ l *E.coli* DNA polymerase (10 units/ $\mu$ l), 1  $\mu$ l *E.coli* RNase H (2 units/ $\mu$ l) and the 18  $\mu$ l remaining from the first strand reaction were added to a new, sterile, 1.5 ml microcentrifuge tube (final volume 150  $\mu$ l). The tube was vortexed and its contents collected by brief centrifugation. The reaction was incubated at 16°C for two hours. 2  $\mu$ l of T4 DNA polymerase (5 units/ $\mu$ l) was added to the reaction and it was allowed to incubate at 16°C for another five minutes before adding 10  $\mu$ l of 0.5 M EDTA and being placed on ice. 150  $\mu$ l of phenol:chloroform:isoamyl alcohol (25:24:1) was added and followed by thorough vortexing. After centrifugation at 14,000 x g for five minutes at RT, 140  $\mu$ l of the upper, aqueous layer was removed and transferred to a fresh 1.5 ml microcentrifuge tube. 70  $\mu$ l of sterile 7.5 M ammonium acetate and 500  $\mu$ l absolute EtOH (-20°C) was added, followed by thorough vortexing and centrifuged at 14,000 x g for 20 minutes at RT. The supernatant was removed and the pellet overlaid with 500  $\mu$ l of 70% EtOH (-20°C) and centrifuged at 14,000 x g for two minutes at RT. The supernatant was discarded and the pellet allowed to dry at 37°C for 10 minutes.

#### 2.3.4 *Sal 1* adapter addition

25  $\mu$ l nuclease free water, 10  $\mu$ l 5x T4 DNA ligase buffer, 10  $\mu$ l *Sal 1* adapters (1  $\mu$ g/ $\mu$ l) and 5  $\mu$ l T4 DNA ligase was added on ice to the dried cDNA pellet leaving a final volume of 50  $\mu$ l. After gentle mixing the reaction was incubated for 20 hours at 16°C. 50  $\mu$ l of phenol:chloroform:isoamyl alcohol (25:24:1) was added and followed by thorough vortexing. After centrifugation at 14,000 x g for five minutes at RT, 45  $\mu$ l of the upper, aqueous layer was removed and transferred to a fresh 1.5 ml microcentrifuge tube. 25  $\mu$ l of sterile 7.5 M ammonium acetate and 150  $\mu$ l absolute EtOH (-20°C) was added, followed by thorough vortexing and centrifuged at 14,000 x g for 20 minutes at RT. The supernatant was removed and the pellet overlaid with 500  $\mu$ l of 70% EtOH (-20°C) and centrifuged at 14,000 x g for two minutes at RT. The supernatant was discarded and the pellet allowed to dry at 37°C for 10 minutes.

#### 2.3.5 *Not 1* digestion

41  $\mu$ l nuclease free water, 5  $\mu$ l REact 3 buffer and 4  $\mu$ l *Not 1* (15 units/ $\mu$ l) was added to the dried cDNA for a total volume of 50  $\mu$ l. After mixing the reaction was allowed to incubate at 37°C for two hours. 50  $\mu$ l of phenol:chloroform:isoamyl alcohol (25:24:1) was added and followed by thorough vortexing. After centrifugation at 14,000 x g for five minutes at RT, 45  $\mu$ l of the upper, aqueous layer was removed and transferred to a fresh 1.5 ml microcentrifuge tube. 25  $\mu$ l of sterile 7.5 M ammonium acetate

and 150  $\mu$ l absolute EtOH (-20°C) was added, followed by thorough vortexing and centrifuged at 14,000 x g for 20 minutes at RT. The supernatant was removed and the pellet overlaid with 500  $\mu$ l of 70% EtOH (-20°C) and centrifuged at 14,000 x g for two minutes at RT. The supernatant was discarded and the pellet allowed to dry at 37°C for 10 minutes.

### *2.3.6 Column chromatography*

The following was performed at RT. The cDNA pellet was dissolved in 100  $\mu$ l of TEN buffer (10 mM Tris-HCl (pH 7.50), 0.1 mM EDTA, 25 mM NaCl; autoclaved) and allowed to hydrate on ice. While the pellet was hydrating a prepackaged 1.0 ml column was placed in a support and allowed to drain (20% EtOH). 800  $\mu$ l of TEN buffer were allowed to pass through the column four times for a total volume of 3.2 ml. After labeling 20 microcentrifuge tubes (1-20) the entire cDNA sample was loaded onto the column and the entire effluent was collected in tube 1. 100  $\mu$ l of TEN buffer were added and allowed to drain into tube 2. After this, each 100  $\mu$ l TEN buffer aliquot was collected dropwise (one in each tube) until all tubes were used. Volumes were measured with an automatic pipette and any tubes used after 550  $\mu$ l total collected volume were discarded as smaller cDNA molecules predominate in these fractions. The remaining tubes were counted without scintillant on the H<sup>3</sup> channel and using a formula provided with the kit the amount of cDNA in each tube was calculated. To continue with the procedure it was necessary to have 10 ng of

cDNA in less than 14  $\mu$ l TEN buffer. Otherwise the following was performed: 0.5 volumes of sterile 7.5 M ammonium acetate and two volumes absolute EtOH (-20°C) were added, followed by thorough vortexing and centrifugation at 14,000 x g for 20 minutes at RT. The supernatant was removed and the pellet overlaid with 500  $\mu$ l of 70% EtOH (-20°C) and centrifuged at 14,000 x g for two minutes at RT. The supernatant was discarded and the pellet allowed to dry at 37°C for 10 minutes and dissolved in 10  $\mu$ l TEN buffer.

#### 2.3.7 Ligation of cDNA to the vector

4  $\mu$ l 5x T4 DNA ligase buffer, 1  $\mu$ l NotI-SalI-cut pSPORT1 vector (50 ng/ $\mu$ l), 10  $\mu$ l cDNA (1 ng/ $\mu$ l) and 4  $\mu$ l nuclease free water were added to a 1.5 ml microcentrifuge tube (total volume 19  $\mu$ l). 1  $\mu$ l of T4 DNA ligase was added, the reaction was mixed by pipette and allowed to incubate overnight at 4°C.

## 2.4 E.coli transformation

Competent DH5 $\alpha$  *E.coli* cells (Invitrogen cat.no.18258-12) were removed from storage at -70C and allowed to thaw on wet ice. 100  $\mu$ l aliquots were placed in chilled 1.5 ml microcentrifuge tubes. 5  $\mu$ l (roughly 12.5 ng) of vector was added to the cells along with 1.0 ml SOC medium (2% wt/vol bacto-tryptone, 0.5% wt/vol bacto-yeast extract, 10 mM NaCl, 2.5 mM KCl, 10 mM MgCl<sub>2</sub>, 10 mM MgSO<sub>4</sub>, pH 7.00 with NaOH, sterile, 20 mM glucose). The cells are incubated at 37°C for one hour with 225 rpm shaking. The

transformed cell culture was then plated on LB medium (Sigma cat.no. L-3022) plates containing 100 µg/ml ampicillin (AMP) and allowed to grow overnight at 37°C.

## **2.5 cDNA library construction**

### *2.5.1 Archive plates*

200 µl TYPGN media (2% tryptone, 1% yeast extract, 0.5% sodium phosphate, 0.8% glycerol, 1% potassium nitrate, wt/vol, autoclaved, 100 µg/ml AMP) was added per well with a multichannel pipette to 96-well, round bottom plates (Costar cat.no. - 3790). Each well was inoculated with a recombinant *E.coli* colony taken from a selection plate with a sterile toothpick. The plates were covered with a pressure sensitive film (Costar cat.no. 6524) to minimize evaporation and incubated overnight at 37°C, 225 rpm. 100 µl of 2x glycerol (65% glycerol w/v, 0.1 M MgSO<sub>4</sub>, 0.025 M Tris-HCl, pH 8.00) was added to the archive plates after replication and they were recovered with film and stored at -70°C.

### *2.5.2 Copy plates*

200 µl TYPGN (with AMP) are added per well in another 96-well, round-bottom plate. The bacterial cells are transferred from the archive plate to the copy plate using a 96-well replicator which maintains the configuration of the archive plate and this

technique also minimizes cross-contamination as all 96 wells are inoculated in one step. The copy plate is covered in pressure sensitive film, grown over night at 37°C in a shaker and stored at -20°C until needed.

## **2.6 cDNA library screening**

### *2.6.1 Express dot-blot*

A nylon membrane (Gelman Sciences cat.no. 66481 - 0.45 µm) and filter paper (Whatman cat.no. 3030917) were cut into dimensions to fit the 96-well dot-blot manifold apparatus. The filter paper is wetted with 2x standard saline citrate (0.3 M NaCl, 30 mM sodium citrate) and placed below the membrane which has been soaked with 10% sodium dodecyl sulfate (SDS). 50 µl of the *E.coli* suspension were transferred to the dot-blot apparatus using a multichannel pipette, keeping the archive plate's original orientation. The liquid was removed by applying a vacuum, the bacteria were lysed and the DNA denatured by adding 200 µl of a saline-sodium hydroxide solution (0.5 M NaOH, 1.5 M NaCl). After five minutes the vacuum was reapplied to remove the solution. The samples were neutralized by adding 200 µl of a saline-Tris solution (1.5 M NaCl, 0.5 M Tris-HCl, pH 8.00) and after five minutes the vacuum was again applied. The nylon membrane was removed, floated on 4x SSC for two minutes, air dried at RT and baked at 80°C for two hours.

### *2.6.2 Probe preparation*

The DIG DNA Labeling and Detection Kit (Boehringer Mannheim cat.no.1093 657) was used to create a digoxigenin-dUTP full-length actin nucleotide probe that was used to screen the cDNA libraries. The procedure will be outlined below.

1 to 3 µg of template DNA (obtained from a previous library) was denatured in a boiling water bath for 10 minutes and chilled in an ice/NaCl water bath. While on ice the following reactants were added to the tube: 2 µl hexanucleotide mix, 2 µl dNTP mixture, nuclease free water to bring the reaction volume to 19 µl and 1 µl klenow enzyme. The mixture was centrifuged briefly to pool reagents and incubated at 37°C for one hour. To stop the reaction, 2 µl of 0.2 M EDTA was added (pH 8.00). The labeled DNA was precipitated by the addition of 2.5 µl of 4.0 M LiCl and 75 µl of -20°C absolute EtOH. After vortexing and a quick spin to pool reagents, the tube was placed at -20°C for one hour. After this, the tube was spun at 12,000 x g for 15 minutes at RT and the pellet was washed with 50 µl of -20°C absolute EtOH, dried for 10 minutes at 37°C and redissolved in 50 µl nuclease free water.

### *2.6.3 Dot-blot hybridization*

The membranes were incubated at 60°C for two hours in 10.0 ml of pre-hybridization solution (5X SSC, 0.001% laryl sarcosine, 0.8%

SDS and 0.5% blocking reagent supplied from the Boehringer-Mannheim DNA Labeling and Detection Kit). This was followed by a 24-hour (minimum) incubation at 60°C in 10.0 ml of hybridization solution (pre-hybridization solution containing the DIG labeled actin nucleotide probe). The hybridized membranes were then washed twice for 15 minutes at RT in 1X SSC & 0.5% SDS (wt/vol), three times for 20 minutes at 60°C in 0.5X SSC & 0.5% SDS (wt/vol) and finally two more washes for 10 minutes at RT in 0.5X SSC.

The following procedure is carried out at RT. The washed membrane was rinsed briefly in buffer 1 (100 mM Tris - HCl pH 7.50 and 150 mM NaCl) followed by a wash with 100.0 ml of buffer 2 (buffer 1 with 0.5% (wt/vol) blocking reagent) with shaking for 30 minutes. The membrane was briefly rinsed in buffer 1 and then shaken again for 30 minutes with 40.0 ml of buffer 1 and 8 µl of antibody conjugate (Digoxigenin - AP Fab fragments ref. # 11 093 274 910, Boehringer Mannheim) This was followed by two 15 minute washes in 100.0 ml of buffer 1 and a two minute wash in 20.0 ml of buffer 3 (100 mM Tris-HCl pH 9.50, 100 mM NaCl and 50 mM MgCl<sub>2</sub>). The membrane was incubated overnight in the dark with 10.0 ml of the color solution (10.0 ml buffer 3, 45 µl Nitroblue tetrazolium solution (Promega, cat# S380C), 35 µl 5-bromo-4-chloro-3-indolyl phosphate solution (Promega, cat# S381C)). The reaction was stopped by soaking the membrane in TE buffer (10 mM Tris-HCl pH 8.00, 1 mM EDTA).

## 2.7 DNA isolation and purification

Before and after confirmation of positive clones, identified colonies from copy plates were inoculated in 5.0 ml LB broth (with 100 µg/ml AMP) overnight at 37°C. The cells were collected sequentially in a sterile 1.5 ml microfuge tube with three successive centrifugations at 10,000 X g for two minutes at RT, discarding supernatant after each spin. The pellet was resuspended in 200 µl GTE and 400 µl NaOH/SDS were added to lyse the cells (four inversions ensured all cells were lysed). 300 µl of KAcF was added and mixed well until a flocculent precipitate was formed throughout the solution. The tubes were centrifuged at 10,000 X g for five minutes at RT. The supernatant was removed (750-800 µl) and placed in a new, sterile, microfuge tube. DNA was extracted with an equal volume of phenol:chloroform (1:1) (5 µl:5 µl). The aqueous phase was transferred to a sterile 1.5 ml microfuge tube and 0.5X the volume of 7.5 M ammonium acetate was added along with 0.6X the volume of cold isopropanol. The contents of the tube were thoroughly mixed. The tubes were then centrifuged at 10,000 X g for 10 minutes at RT. The isopropanol was removed, taking care not to disturb the pellet. The pellet was then washed with cold 70% ethanol and centrifuged at 10,000 X g for five minutes at RT. The ethanol was drained and the pellet was allowed to air dry for

10 minutes at RT. The DNA was then resuspended in 50  $\mu$ l TE buffer.

## **2.8 Plasmid digestion**

The provided vector has restriction sites for BamHI and HindIII located on either side of the ligation points. Taking advantage of this, isolated plasmids were digested with these two restriction enzymes over night at 37°C. Digestions were then run on a 0.8% agarose gel (wt/vol) at 120 V for one hour and then subjected to either insert retrieval (for probe preparation) or southern transfer (for insert size estimation).

## **2.9 Southern transfer**

Southern transfer gave an indication of the insert size of clones identified by express dot-blot. Briefly, the gel was inverted in a glass dish with 400.0 ml of 0.25 M HCl while shaking for 15 minutes at RT. NaOH (500.0 ml, 0.4 M) was used as the transfer solution. The apparatus was left overnight at RT to ensure complete transfer of DNA. The membrane was then neutralized with 200.0 ml of neutralizing solution (0.2 M Tris pH 7.50, 2X SSC) for one minute and allowed to air dry. The membranes were hybridized and immunodetected as described in section 2.6.3.

## 2.10 DNA sequencing

Sequencing was performed in the CREAT genomics lab at Memorial University of Newfoundland. The lab uses an Applied Biosystems ABI3730xl sequencer that is automatic aside from some preliminary operator set-up. For each sample, 2  $\mu$ l of 5X sequencing buffer, 0.5  $\mu$ l of sequencing mix, 2  $\mu$ l of the appropriate primer (T7, M13 forward, M13 reverse, actin1, actin2 and, actin3 - actin specific primers designed in the Heeley lab by Donna M. Jackman, made by GIBCOBRL) at a concentration of 1.6 pmol/ $\mu$ l, the appropriate volume of DNA template (to reach at least 500 pmol) and ddH<sub>2</sub>O to reach a total volume of 20  $\mu$ l was added at RT. pGEM sequencing was performed as a control. The samples were vortexed and spun in a table top microfuge for one minute to pool reagents. A 9800 thermocycler (Applied biosystems) was used to anneal the probes to the DNA with the following program: 96°C for six minutes, followed by 25 cycles of 96°C for 10 seconds, 50°C for five seconds and 60°C for four minutes. The samples are then kept at 4°C until retrieved from the thermocycler. The samples were again vortexed and spun at RT. The DNA was precipitated by adding 5  $\mu$ l EDTA (125 mM. pH 8.00) and 65  $\mu$ l of 95% ethanol. The samples were left overnight at 4°C protected from light. The samples were then centrifuged at 3,000 x g for 30 minutes at RT and a paper towel was placed over the top of the open tubes, which were inverted and then centrifuged for 40 seconds at 200 x g at RT to remove all supernatant. A wash was performed with 150

µl of 70% ethanol and centrifuged at 3,000 x g for 15 minutes at RT. The supernatant was then discarded by centrifugation as previously described and the samples were allowed to air dry for 15 minutes under a fume hood at RT to ensure complete removal of the EtOH. The samples were then resuspended in 15 µl of Hi-Di formamide (Applied Biosystems cat. No. 4311320). Finally, they were loaded into the ABI 3730xl for sequencing.

## **2.11 Actin acetone powder**

This procedure was performed on swimming muscle obtained from the following fish: Atlantic herring (*Clupea harengus*), Atlantic mackerel (*Scomber scombrus*), Rainbow smelt (*Osmerus mordax*), Atlantic halibut (*Hippoglossus hippoglossus*), tilapia, hagfish and lamprey (final three species unknown).

500.0 g of ground muscle (fresh) was stirred for 30 minutes in 6.0 L of cold, deionized water with 2 mM phenylmethanesulphonylfluoride (PMSF), a serine protease inhibitor, and allowed to settle for an additional 30 minutes. The filtrate was spun in a Beckman J6-HC centrifuge at 4,200 rpm and 4°C for five minutes. The residue was resuspended in 1.5 L of 4°C, 0.4% (wt/vol) NaHCO<sub>3</sub> at pH 8.00 and stirred for 15 minutes. This was followed by another centrifugation of 4,200 rpm for 10 minutes at 4°C. This washing and spinning step was repeated at the same temperature, pH and speed with 0.05 M Na<sub>2</sub>CO<sub>3</sub>

and 0.05 M NaHCO<sub>3</sub>. The filtrate was stirred at 4°C in 0.2 mM CaCl<sub>2</sub> for two minutes and centrifuged a final time at 4,200 rpm for 10 minutes at 4°C. The residue was now removed from the centrifuge bottles and stirred for 2 minutes in 1.5 L of 4°C 95% (vol/vol) EtOH. It is important to note that this step should be repeated once or even twice when working with muscle of high lipid content. EtOH was removed by filtering with cheesecloth and the residue was resuspended in 1.5 L of -20°C acetone and stirred for 2 minutes. This step was repeated three times to ensure the removal of the EtOH and any remaining water. The residue was then allowed to dry under a fume hood over night.

## **2.12 Actin preparation**

4.0 L of actin extraction buffer (AEB) was prepared first: 2 mM Tris-HCl, 0.2 mM CaCl<sub>2</sub>, 0.2 mM ATP, 0.1 mM DTT, pH 8.00 at 4°C. 0.01% (wt/vol) NaN<sub>3</sub> is added to the buffer to prevent bacterial growth. 10.0 g of acetone powder was stirred in 200.0 ml of AEB for 30 minutes in the cold room (4-7°C) with solid DTT added to a final concentration of 0.5 mM. The residue was centrifuged at 4,200 rpm for 15 minutes at 4°C in a Beckman J6-HC. The actin-containing supernatant was poured off and kept while the residue was washed with 100.0 ml of AEB. The supernatant was passed through a Whatman number 1 filter (cat. No 1001 090) and the soaked muscle acetone powder was allowed to drain. It is of importance to note here that not all 300.0 ml of AEB will be

collected. It is also very important to avoid excessive frothing, as this will denature the protein. The sample was then filtered through 8  $\mu\text{m}$ , 0.45  $\mu\text{m}$  and 0.22  $\mu\text{m}$  filters and the final filtrate volume measured. Actin in the filtrate was polymerized at room temperature by the addition of 50 mM KCl and 2 mM  $\text{MgCl}_2$  (solid salts were used to minimise dilution) with stirring for at least one hour. Solid KCl was then added to a final concentration of 0.8 M and the solution was stirred for a further 90 minutes at room temperature. The now filamentous actin was centrifuged at 45,000 rpm with a Beckman 70Ti rotor at 4°C. The supernatant was decanted but kept for analysis by SDS-PAGE. The button-shaped pellets were collected with a spatula and immersed in ~15 ml AEB, disrupted by gently breaking the pellets between finger and thumb and placed in AEB to dialyze for at least two to three days. The buffer should be changed once a day but twice is preferable. The solution was centrifuged at 45,000 rpm in the Beckman 70Ti rotor for 90 minutes and the G-actin containing supernatant was removed with a Pasteur pipette and stored at 4°C in the presence of 0.01% (wt/vol)  $\text{NaN}_3$ . The level of actin enrichment was visually assessed by SDS PAGE.

## 2.13 Actin concentration determination

Actin concentration was determined in a Beckman DU-64 Spectrophotometer. An extinction coefficient of 0.694 for a 1 mg/ml solution (290 nm) was used for actin [Johnson & Taylor 1978]. The instrument was calibrated with dH<sub>2</sub>O and the absorbance of the buffer (either TRIS or HEPES) was subtracted. In addition, absorbance readings at 320 nm were recorded and used to correct for light scattering. All absorbance readings at 290 nm were within the range of 0.1-1.0.

## 2.14 Electrophoretic methods

### 2.14.1 Sodium dodecyl sulphate polyacrylamide gel electrophoresis (SDS-PAGE)

All separating gels used were 12% (wt/vol) acrylamide (Biorad, 161-0107) diluted from a stock solution (30% wt/vol acrylamide and 0.8% (wt/vol) bis acrylamide (Sigma, M-7279)) with separating buffer (0.75 M Tris-HCl, 0.21 % (wt/vol) SDS, pH 8.80 using conc. HCl). Solutions were polymerized with 20 µl N, N, N', N'-tetramethylethylenediamine (TEMED: Promega cat. # V3161) and 100 µl of a 10% (wt/vol) solution of ammonium persulfate (Promega cat.# V3131). Stacking gels were diluted to 3% (wt.vol) from the same stock solutions and polymerized with 75 µl of ammonium persulfate and 20 µl of TEMED. Bio-Rad mini-Protean II apparatus [Bio-Rad, Richmond, CA] was used for electrophoresis. Gels were

7.0 cm long, 10.0 cm wide and either 1.0 mm or 0.75 mm thick. All gels were run at 180 V for 45 minutes and stained in 0.25% (wt/vol) Coomassie Brilliant Blue R-250 (Bio-Rad), 50% (vol/vol) methanol and 10% (vol/vol) acetic acid and destained in 15% (vol/vol) acetic acid and 20% (vol/vol) methanol.

#### *2.14.2 Alkaline urea PAGE*

Alkaline urea-polyacrylamide gels were comprised of 10% (wt/vol) acrylamide diluted from the same stock solution in 8% (vol/vol) 12X glycine buffer (1.49 M glycine and 0.24 M Tris-HCl) and 8.0 M urea [Perrie & Perry 1970]. All protein samples were dissolved in a freshly made solution of saturated urea (RT, ~10 M), containing DTT and Bromophenol blue to a final dilution of ~ 1 mg/ml. Urea gels were pre run for 15 minutes at 220 V and samples were loaded immediately after flushing the wells with the running buffer using a Pasteur pipette. Electrophoresis was carried out at 220 V for 700 volt hours. The gel was stained and destained as previously described.

## **2.15 Electro blotting**

Protein transfer was carried out after either SDS-PAGE or alkaline urea PAGE to polyvinylidene difluoride [PVDF] membrane. The gel and membrane were soaked in transfer buffer [10 mM CAPS, pH 11.00 in 10% [vol/vol] methanol] for 30 minutes, assembled into a sandwich and electrophoresed for two and a half hours at 60 V

at RT in transfer buffer. To confirm complete transfer of protein, the gel was stained with Coomassie Brilliant Blue R250 as outlined in section 2.2.1. The membrane was briefly stained using 0.025% [wt/vol] Coomassie Brilliant Blue R250 in 40% [vol/vol] methanol and destained in 50% [vol/vol] methanol. Membranes were then allowed to air-dry before submission for Edman sequencing (Advanced Protein Technology Center, University of Toronto).

## **2.16 Proteolytic methods**

### *2.16.1 Subtilisin digestion*

Actin was digested with subtilisin (Sigma cat.# P-5380) at a 1:1000 (wt/wt) enzyme to substrate ratio at 24°C. Digestions were carried out in actin extraction buffer at a final actin concentration of ~ 1mg/ml. At specific time intervals aliquots were removed and diluted to a final actin concentration of ~ 0.5 mg/ml with SDS sample buffer (2% SDS (wt/vol), 80 mM Tris pH 6.80, 10% glycerol (wt/vol)) containing bromophenol blue (0.01% (wt/vol) - Schwarz/Mann Biotech, 805732) and 1 mM PMSF before being placed in a boiling water bath for 10 minutes. About 4 µg of actin was loaded into each well and the gel was run, stained and destained as previously described.

### 2.16.2 *Thrombin digestion*

A 1:65 (m/m) enzyme to substrate ratio at 24°C was used to digest the actin isoforms with thrombin (Sigma cat.# T-6884). Other than the change of enzyme and ratio the remaining procedure is exactly that of the subtilisin digestion.

## 2.17 **Spectroscopic methods**

### 2.17.1 *Far and near ultra violet circular dichroism spectroscopy*

Electronic circular dichroism spectra were recorded in the near [250-340 nm] and far-ultraviolet region [190-300 nm] using a Jasco-810 spectropolarimeter. It was typical to use protein concentrations of ~ 1.0 mg/ml and ~ 4mg/ml in the far and near-UV, respectively. When thermally denaturing actin it was necessary to perform an overnight dialysis in HEPES buffer (5 mM Hepes, 0.2 mM CaCl<sub>2</sub>, 0.2 mM ATP, 0.01% [wt/vol] NaN<sub>3</sub> and 2 mM DTT, pH 8.00 at 4°C) to avoid unwanted changes in pH that would accompany the heating of TRIS buffer. All temperature control (5 - 75°C) was maintained by a CTC-345 circulating water bath. Water-jacketed cells varying in light path 0.1 mm (far-UV) and 5 mm (near-UV) were used. The heating rate was varied from 30°C/hr to 60°C/hr to ensure the protein solutions were at equilibrium. The scanning speed of the instrument was set at 100 nm/minute with normal sensitivity. The temperature-dependence of the signal at 222 nm [far-UV] and 292 nm [near-UV] was observed by

continuous monitoring at these wavelengths between 5-75°C. The melting temperature ( $T_m$ ) was then obtained by converting the progress curve  $\{[\theta]_{222}$  or  $[\theta]_{292}$  vs.  $T\}$  to the first differential form  $d[\theta]_{222}$  or  $d[\theta]_{292}/dT$  vs.  $T$ .

## **2.17.2 Chemically induced unfolding**

### *2.17.2.1 Urea induced unfolding*

Electronic circular dichroism spectra in the far-UV spectra of Ca-G-actin [ $\sim 2.0$  mg/ml] were recorded as a function of urea concentration from 0.0 M to 6.0 M in 0.5 M intervals allowing 30 minutes exposure to urea before recording. The stock concentration of urea was 8.0 M (in actin extraction buffer) and was prepared fresh and gravity filtered with a #1 Whatman filter paper each time. Experiments were carried out at RT. The ellipticity at 222 nm was then plotted versus [urea].

### *2.17.2.2 EDTA induced unfolding*

EDTA (Biorad, 161-0729) was added to a  $\sim 1$  mg/ml solution of actin to a final concentration of 1 mM (100 mM stock solution) and loaded into a 0.2 mm water jacketed cell. After 30 seconds, the instrument was started and allowed to record the ellipticity change at 222 nm, as previously described, for two hours. The temperature was maintained at 25°C by the circulating waterbath. The change in ellipticity was presented against time (rather than temperature) and rates of unfolding were determined.

### **2.17.3 Fluorescence spectroscopy**

A ~ 2 mg/ml solution of Ca-G-actin was depleted of excess ATP by incubation with Dowex A 1-8x 20%[v/v] (Biorad, 140-1443) for about 30 minutes on ice while gently rocking. Samples were then syringe filtered through a 0.2  $\mu\text{m}$  Millipore filter and incubated with N-methylantraniloyl-5' triphosphate (mant-ATP; a generous gift from Dr. Howard White, Eastern Virginia Medical School) at 4°C for two hours at a final actin concentration of 15  $\mu\text{M}$  and 1  $\mu\text{M}$  mant-ATP. Visible spectra were recorded on all samples before and after excited state measurements to ensure that the samples did not photodegrade. Mant-ATP was excited at 340 nm and emission was measured at 440 nm. A wavelength scan from 360 nm to 600 nm was carried out using a Photon Technology International (PTI) model QM-2001-6 QuantaMaster emission spectrometer equipped with a Hamamatsu R-928 photomultiplier tube housed in a Products for Research Inc PC177CE refrigerated chamber. All emission spectra were collected with a 1 mm slit width, 90° to excitation source and are uncorrected for instrument response.

## **2.18 Data manipulation**

### *2.18.1 cDNA sequences*

All sequences were analyzed using FinchTV (freely available from geospiza) to visualize the electrophoretograms and to perform BLAST searches.

### 2.18.2 *Graphing*

All graphs presented have been constructed using Graphpad Prism in addition to any normalization or subtraction procedures (as indicated in figure legends).

## Chapter 3

# Results & Discussion

### 3.1 Nucleotide sequencing

cDNA libraries were constructed and screened as described in section 2.1. Plasmids from positive clones were isolated and 1° structures were inferred from the obtained nucleotide sequences. In total, three actin isoforms were sequenced in this work: Atlantic herring slow skeletal muscle actin (*Clupea harengus* Acc# EF495203) (Figures 3 & 4), Atlantic herring fast skeletal muscle actin (Acc# GQ455648) (Figures 5 & 6) and, Atlantic mackerel fast skeletal muscle actin (*Scomber scombrus* Acc# EF607093) (Figures 7 & 8). Sequences from Atlantic herring were confirmed by separate clones in the same library.

This work represents the second finding of an actin isoform specific to slow skeletal muscle, the first [Mudalige *et al.* 2007] being found in the skeletal muscles of *salmonid* fish (slow muscle Acc #AF267496 isolated from *Salmo trutta*, Brown trout; fast muscle Acc #AF304406 isolated from *Salmo salar*, Atlantic salmon). Comparing the fast and slow herring skeletal muscle actin cDNA sequences with those from salmonid fish (Figures 9 & 10) demonstrates that the two sequences are highly conserved; at the nucleotide level there is 89% homology between the two slow sequences and 92% homology between the fast sequences.

Figure 3: cDNA sequence (Acc# EF495203) corresponding to the actin isoform found in the slow skeletal muscle of Atlantic herring (*Clupea harengus*).

```

1 AAGCACGTGA GCCTCCTCTC CTAAGTGTGC AGGTCTACAA CCGTCTGAGT AAAGATGTGT
61 GATGAGGAAG AGACTACCGC TCTGGTGTGT GACAACGGCT CTGGCCTGGT CAAGGCAGGG
121 TTCGCCGAG ATGATGCCCC AAGAGCTGTC TTCCCCCCA TTGTTGGCCG TCCCCGCCAT
181 CAGGGTGTGA TGGTGGGTAT GGGACAGAAG GACAGCTATG TAGGAGACGA GGCTCAGAGC
241 AAGAGAGGTA TCCTGACCCT GAAATACCCC ATCGAGCACG GCATCATCAC CAACTGGGAC
301 GACATGGAGA AGATCTGGCA TCACACCTTC TACAATGAGC TGCGTGTGGC CCCCAGGAG
361 CACCCCGTCC TGCTGACTGA GGCTCCCCTC AACCCCAAGG CCAACAGAGA GAAGATGACC
421 CAGATTATGT TTGAAACCTT CAACGTTCCA GCTATGTATG TAGCCATCCA AGCTGTGCTC
481 TCCCTCTACG CTTCCTGGCCG TACCACTGGT ATGTGTCTGG ATGCTGGTGA TGGTGTGACC
541 CACAATGTGC CAGTATATGA AGGCTATGCT CTGCCTCATG CCATCATGAG GCTGGATCTG
601 GCTGGCCGTG ACCTGACTGA CTACCTCATG AAGATCCTCA CAGAGAGAGG CTACAGCTTT
661 GTCACCACCG CCGAGCGTGA GATTGTCCGG GACATCAAGG AGAAGCTGTG CTACGTGGCT
721 CTGGACTTTG AGAATGAGAT GGCCACTGCT GCCTCTTCCT CCTCCCTGGA GAAGTCCTAT
781 GAGTTGCCCG ATGGCCAAGT CATTACCATC GGTAACGAGA GGTTCGCTG TCCCGAGACC
841 CTTTTCCAGC CCTCTTTCAT TGGTATGGAG TCTGCTGGAA TCCATGAGAC CACATACAAC
901 GGCATCATGA AGTGTGACAT TGACATCCGT AAGGACCTGT ACGCCAACAA TGTGCTCTCT
961 GGCGGTACCA CCATGTACCC AGGTATCGGT GACCGTATGC AGAAAGAGAT CACAGCCCTG
1021 GCTCCCAGCA CCATGAAGAT CAAGATGATT GCTCCACCTG AGCGTAAAGTA CTCTGTATGG
1081 ATCGGTGGCT CTATCTTGGC TTCCCTGTCC ACTTTCCAGC AGATGTGGAT CAGCAAGGAT
1141 GAGTATGAAG AGGCTGGACC TTCCATTGTC CACAGGAAGT GCTTCTAAAC ACACCATGTG
1201 TATATGTTCA TGTACTTACA CACATTTTCT CACATCCTTT AACTTTTAAC TTTCATCCAC
1261 ATTATTTCTT TCAAGCTAAA TTTCCATTGT CTCCAGTGTC ACTCTCCATC TTGATTTTAA
1321 TTGCACATGT GTTGTCTCTA ACCACTGTGA ATCACTGTTT ATTCCCTCCC TTTTGTTAAT
1381 CTCACAATAA AACTTCTAA TCCCCAAAA AAAAAAAAAA A

```

Untranslated regions indicated as **bold** and underlined.  
Translated region comprised of nucleotides 55-1188.

Figure 4: Inferred amino acid sequence (immature) of the skeletal muscle actin found in the slow skeletal muscle of Atlantic herring.

1	20	40
MCDEEETTALVCDNGSGLVK		AGFAGDDAPRAVFPSIVGRP
41	60	80
RHQGVVMVGMGQKDSYVGDEA		QSKRGILTTLKYPIEHGIITN
81	100	120
WDDMEKIWHHTFYNELRVAP		EEHPVLLTEAPLNPKANREK
121	140	160
MTQIMFETFNVPAMYVAIQ		VLSLYASGRRTTGIVLDAGDG
161	180	200
VTHNVPVYEGYALPHAIMRL		DLAGRDLTDYLMKILTERGY
201	220	240
SFVTTAEREIVRDIKEKLCY		VALDFENEMATAASSSSLEK
241	260	280
SYELPDGQVITIGNERFRCP		ETLFQPSFIGMESAGIHETT
281	300	320
YNGIMKCDIDIRKDLYANNV		LSGGTTMYPGIGDRMQKEIT
321	340	360
ALAPSTMKIKMIAPPERKYS		VWIGGSILASLSTFQQMWIS
361	377	
KDEYEEAGPSIVHRKCF		

Single letter code: Ala (A), Arg (R), Asn (N), Asp (D), Cys (C), Glu (E), Gln (Q), Gly (G), His (H), Ile (I), Leu (L), Lys (K), Met (M), Phe (F), Pro (P), Ser (S), Thr (T), Trp (W), Tyr (Y), Val (V). Immature actin 377 amino acids, mature actin is comprised of 375 amino acids due to the post translational removal of the met-cys at the amino terminal end.

Figure 5: cDNA sequence (Acc# GQ455648) corresponding to the actin isoform found in the fast skeletal muscle of Atlantic herring (*Clupea harengus*).

```

1 CCACGCGTCC GAGCAGCGGT TGAACTACTA GGCAGGAAAC TCCACAGTAT CCATCAAGAT
61 GTGTGACGAC GACGAGACTA CCGCTCTTGT GTGCGACAAC GGCTCCGGCC TTGTGAAAGC
121 TGGCTTTGCC GGTGATGACG CCCCAGGGC TGTATTCCCC TCCATTGTGG GCCGTCCTCG
181 TCACCAGGGT GTGATGGTCG GTATGGGACA GAAGGACTCC TACGTAGGAG ATGAGGCTCA
241 GAGCAAGAGA GGTATCCTGA CTCTGAAGTA CCCCATTGAG CACGGTATCA TCACCAACTG
301 GGATGATATG GAGAAGATCT GGCATCACAC CTTCTACAAT GAGCTGCGTG TGGCACCCGA
361 GGAGCACCCC ACCCTGCTCA CAGAGGCCCC CCTGAAACCCC AAGGCCAACA GAGAGAAGAT
421 GACCCAGATC ATGTTTGAGA CCTTCAACGT CCCAGCCATG TATGTGGCCA TCCAGGCTGT
481 GCTGTCCCTG TACGCCTCTG GCCGTACCAC TGGTATCGTG CTGGACTCCG GTGATGGTGT
541 GTCTCACAAT GTCCCCATCT ATGAGGGTTA TGCTCTCCCC CATGCCATCA TGCGTCTGGA
601 TCTGGCTGGT CGCGATCTGA CTGATTACCT GATGAAGATC CTGACAGAGC GTGGTTACTC
661 TTTCTGTGACA ACCGCTGAGC GTGAGATCGT GCGCGACATC AAGGAGAAGT TGTGCTATGT
721 GGCTCTGGAC TTCGAGAATG AGATGGCAAC CGCTGCCTCC TCCTCCTCTC TGGAGAAGAG
781 CTACGAGCTC CCCGACGGTC AGGTCATTAC CATTGGTAAT GAACGTTTCC GTTGCCCTGA
841 GACCCCTTTC CAGCCTTCCT TCATTGGTAT GGAGTCTGCT GGTATTCATG AGACTGCCTA
901 CAACAGCATC ATGAAGTGCG ACATTGACAT CAGGAAGGAC CTGTACGCCA ACAATGTCTT
961 GTCCGGTGGT ACCACCATGT ACCCTGGTAT TGCTGACAGG ATGCAGAAGG AGATCACTGC
1021 TCTGGCCCCC AGCACCATGA AGATCAAGAT CATTGCCCCA CCTGAGCGTA AGTACTCCGT
1081 CTGGATTGGT GGCTCCATCC TGGCTTCCCT GTCCACCTTC CAGCAGATGT GGATCACCAA
1141 ACAGGAGTAC GATGAGGCAG GCCCCAGCAT TGTCACCGC AAATGCTTCT AAGCGAACGA
1201 ATCACCCCAT GGATCATTTC TTGCTCAGGA ACCAACGACA GCCCGCTGCT GTTATTATGG
1261 GACAATTTTG TACAAGTTTT TTTTCCAGCC AACGATTTGT TTTACAATGA CGCGAAACTG
1321 AGAGGATTTT AGCCTCTACA AACACATCAA GAAATGTCAT CCTTTGAATG TATGCTTGTA
1381 GAGGGTGCAA GCAACCTAAC TGGGGAACAT CAGGGTTATA GACTGTTGCC TTGCTTGTAT
1441 TCTTAAAGTT GGTCAATTGT AGTCTATTA TCGGTTCTAT CTTCCAGATC AATTAACACC
1501 AACAGGAAAT AAAACTTATG AACTATAAAA AAAAAAAAAA AAA

```

Untranslated regions indicated as **bold** and underlined.  
Translated region comprised of nucleotides 59-1192.

Figure 6: Inferred amino acid sequence (immature) of the skeletal muscle actin found in the fast skeletal muscle of Atlantic herring.

1	20	40
MCDDDQTTALVCDNGSGLVK		AGFAGDDAPRAVFPISIVGRP
41	60	80
RHQGVVMVGMGQKDSYVGDEA		QSKRGILTLKYPIEHGIITN
81	100	120
WDDMEKIWHHTFYNELRVAP		EEHPTLLTEAPLNPKANREK
121	140	160
MTQIMFETFNPAMYVAIQ		VLSELYASGRRTTGIVLDSGDG
161	180	200
VSHNVPIYEGYALPHAIMRL		DLAGRDLTDYLMKILTERGY
201	220	240
SFVTTAEREIVRDIKEKLCY		VALDFENEMATAASSSSLEK
241	260	280
SYELPDGQVITIGNERFRCP		ETLFQPSFIGMESAGIHETA
281	300	320
YNSIMKCDIDIRKDLYANNV		LSGGTTMYPGIADRMQKEIT
321	340	360
ALAPSTMKIKIIAPPERKYS		VWIGGSILASLSTFQQMWIT
361	377	
KQEYDEAGPSIVHRKCF		

Single letter code: Ala (A), Arg (R), Asn (N), Asp (D), Cys (C), Glu (E), Gln (Q), Gly (G), His (H), Ile (I), Leu (L), Lys (K), Met (M), Phe (F), Pro (P), Ser (S), Thr (T), Trp (W), Tyr (Y), Val (V). Immature actin 377 amino acids, mature actin is comprised of 375 amino acids due to the post translational removal of the met-cys at the amino terminal end.

Figure 7: cDNA sequence (Acc # EF607093) corresponding to the actin isoform found in the fast skeletal muscle of Atlantic mackerel (*Scomber scombrus*).

```

1   TACGCCTGCA GGTACCGGTC CGGAATTCCC GGGTCGACCC ACGCGTCCGG CAGTAGCACT
61  GGTTGGGGTTG TTCTCTCCAA GCCGCAGACA CTCTCCTAAG AAGCCATCAT GTGTGACGAC
121 GATGAAACTA CCGCTCTTGT GTGCGACAAC GGCTCCGGCC TTGTGAAAGC TGGCTTCGCC
181 GGAGATGATG CCCCCAGGGC CGTGTTCCCC TCCATCGTCG GCCGCCCTCG TCACCAGGGT
241 GTCATGGTCG GTATGGGTCA GAAGGACTCC TACGTGGCG ACGAGGCCCA GAGCAAGAGA
301 GGTATCCTGA CTCTGAAGTA CCCCATTGAG CACGGTATCA TCACCAACTG GGACGACATG
361 GAGAAGATCT GGCACCACAC CTTCTACAAC GAGCTGAGAG TGGCCCCCGA GGAGCACCCC
421 ACCCTGCTCA CTGAAGCCCC ACTGAACCCC AAGGCTAACA GGGAGAAAAT GACCCAGATC
481 ATGTTTGAGA CCTTCAACGT CCCCGCCATG TATGTGGCCA TCCAGGCTGT GCTGTCCCTG
541 TACGCTTCCG GCCGTACCAC CGGTATTGTG CTGGATGCTG GTGATGGTGT GACCCACAAC
601 GTCCCAGTCT ATGAGGGTTA CGCCCTGCCC CACGCCATCA TGCGTCTGGA TCTGGCTGGT
661 CGCGATCTGA CCGACTACCT GATGAAGATC CTGACTGAGC GTGGCTACTC CTTCGTGACA
721 ACCGCTGAAC GTGAGATCGT GCGCGACATC AAGGAGAAGC TGTGCTATGT GGCTCTGGAC
781 TTTGAGAATG AGATGGCCAC CGCTGCCTCC TCCTCCTCCC TGGAGAAGAG CTACGAGCTT
841 CCCAGCGGTC AGGTCATCAC CATCGGTAAC GAGAGGTTCC GTTGCCCTGA GACCCCTCTTC
901 CAGCCTTCTT TCATTGGTAT GGAGTCTGCT GGTATCCATG AGACCGCCTA CAACAGCATC
961 ATGAAGTGGC ACATTGACAT CCGTAAGGAT CTGTACGCCA ACAATGTCTT CTCCGGTGGT
1021 ACCACCATGT ACCCTGGTAT TGCTGACCGT ATGCAGAAGG AAATCACTGC TCTGGCCCCC
1081 AGCACCATGA AGATCAAGAT CATTGCTCCT CCCGAGAGGA AGTACTCCGT CTGGATCGGT
1141 GGCTCCATCC TGGCTTCCCT GTCCACCTTC CAGCAGATGT GGATCTCCAA GCAGGAGTAC
1201 GACGAGGCAG GCCCCAGCAT TGTCCACAGG AAGTGCTTCT AAATCCTCCA TCTTCTACTC
1261 CTGCTTCTCC ATCATTATCA CCACCAGCTA TCTGGAGATC AAGCGAGGAG GAGGATCAAC
1321 CTATGCGACA CAGCAACACT CTGCTGTCAA TGGACTGTCT GTCTGCGCTG TTGACATTTT
1381 TATGCATTTT TTTATCGTTA TAAAATGTGC ATATTTTTAT GGCTGTCTGT TGTC

```

Untranslated regions indicated as **bold** and underlined.  
Translated region comprised of nucleotides 109-1242.

Figure 8: Inferred amino acid sequence (immature) of the skeletal muscle actin found in the fast skeletal muscle of Atlantic mackerel.

1	20	40
MCDDDETTALVCDNGSGLVK		AGFAGDDAPRAVFPSIVGRP
41	60	80
RHQGVVMVGMGQKDSYVGDEA		QSKRGILTLKYPIEHGIITN
81	101	120
WDDMEKIWHHTFYNELRVAP		EEHPTLLTEAPLNPKANREK
121	140	160
MTQIMFETFNVPAMYVAIQ		VLSLYASGRTTGIVLDAGDG
161	180	200
VTHNVPVYEGYALPHAIMRL		DLAGRDLTDYLMKILTERGY
201	221	240
SFVTTAEREIVRDIKEKLCY		VALDFENEMATAASSSSLEK
241	261	280
SYELPDGQVITIGNERFRCP		ETLFQPSFIGMESAGIHETA
281	300	320
YNSIMKCDIDIRKDLYANNV		LSGGTTMYPGIADRMQKEIT
321	340	360
ALAPSTMKIKIIAPPERKYS		VWIGGSILASLSTFQQMWIS
361	377	
KQEYDEAGPSIVHRKCF		

Single letter code: Ala (A), Arg (R), Asn (N), Asp (D), Cys (C), Glu (E), Gln (Q), Gly (G), His (H), Ile (I), Leu (L), Lys (K), Met (M), Phe (F), Pro (P), Ser (S), Thr (T), Trp (W), Tyr (Y), Val (V). Immature actin 377 amino acids, mature actin is comprised of 375 amino acids due to the post translational removal of the met-cys at the amino terminal end.

Figure 9: Comparison of the cDNA sequences corresponding to the slow skeletal muscle actin isoforms isolated from Atlantic herring and Brown trout.

1	<u>AAGCACGTGA</u>	<u>GCCTCCTCTC</u>	<u>CTAAGTGTGC</u>	<u>AGGTCTACAA</u>	<u>CCGTCTGAGT</u>	<u>AAAGATGTGT</u>
	taaccaccg	cctcctgtcc	agctctccag	ggccacagt	aaccagactc	aaccatgtgt
61	GATGAGGAAG	AGACTACCGC	TCTGGTGTGT	GACAACGGCT	CTGGCCTGGT	CAAGGCAGGG
	gacgaggaag	agacaacagc	cttgggtatgc	gacaacggct	caggactggt	gaaggctggc
121	TTCGCCGGAG	ATGATGCCCC	AAGAGCTGTC	TTCCCCCTCA	TTGTTGGCCG	TCCCCGCCAT
	ttcgccggtg	acgatgcccc	cagggcagtg	ttccccctca	ttgtggggcg	cccccgcat
181	CAGGGTGTGA	TGGTGGGTAT	GGGACAGAAG	GACAGCTATG	TAGGAGACGA	GGCTCAGAGC
	cagggggtga	tggtgggtat	gggtcagaaa	gactcctatg	taggagacga	ggccagagc
241	AAGAGAGGTA	TCCTGACCCT	GAAATACCCC	ATCGAGCACG	GCATCATCAC	CAACTGGGAC
	aagagaggta	tcctgaccct	caagtacccc	attgagcacg	gcatcataac	taactgggac
301	GACATGGAGA	AGATCTGGCA	TCACACCTTC	TACAATGAGC	TGCGTGTGGC	CCCCGAGGAG
	gacatggaga	agatctggca	tcataccttc	tacaatgagc	ttcgtgtggc	acctgaggag
361	CACCCCGTCC	TGCTGACTGA	GGCTCCCCTC	AACCCCAAGG	CCAACAGAGA	GAAGATGACC
	caccctgtcc	tgctcactga	ggccccactc	aaccccaagg	ccaacagaga	gaagatgacc
421	CAGATTATGT	TTGAAACCTT	CAACGTTCCA	GCTATGTATG	TAGCCATCCA	AGCTGTGCTC
	cagatcatgt	ttgagacctt	caacgtgcca	gctatgtatg	tggccatcca	ggctgtgctg
481	TCCCTCTACG	CTTCTGGCCG	TACCACTGGT	ATTGTGCTGG	ATGCTGGTGA	TGGTGTGACC
	tccctgtacg	cctctggctg	taccacaggt	attgtgctgg	acgctggcga	tggtgtgacc
541	CACAATGTGC	CAGTATATGA	AGGCTATGCT	CTGCCTCATG	CCATCATGAG	GCTGGATCTG
	cacaacgtgc	ccgtatatga	gggttatgcc	tgccccatg	ccatcatgag	actggacttg
601	GCTGGCCGTG	ACCTGACTGA	CTACCTCATG	AAGATCCTCA	CAGAGAGAGG	CTACAGCTTT
	gctggccgtg	acctgactga	ctacctgatg	aagatcctca	ctgagagagg	ctactctttc
661	GTCACCACCG	CCGAGCGTGA	GATTGTCCGG	GACATCAAGG	AGAAGCTGTG	CTACGTGGCT
	gtcaccaccg	ctgagagaga	gattgtgcgt	gacatcaagg	agaagctgtg	ctacgtggct
721	CTGGACTTTG	AGAATGAGAT	GGCCACTGCT	GCCTCTTCCT	CCTCCCTGGA	GAAGTCCTAT
	ctggactttg	agaatgagat	ggccaccgct	gcctctctct	cctctctgga	gaagtcctat
781	GAGTTGCCCG	ATGGCCAAGT	CATTACCATC	GGTAACGAGA	GGTTCCGCTG	TCCCGAGACC
	gagttgcccg	atggtcaggt	catcaccatc	ggtaacgaga	ggttccggtg	cccagaaacc
841	CTTTTCCAGC	CCTCTTTCAT	TGGTATGGAG	TCTGCTGGAA	TCCATGAGAC	CACATACAAC
	cttttccagc	cctctttcat	tggtatggag	tctgctggaa	tccatgagac	cacatacaac
901	GGCATCATGA	AGTGTGACAT	TGACATCCGT	AAGGACCTGT	ACGCCAACAA	TGTGCTCTCT
	ggcatcatga	agtgtgacat	tgacatccgt	aaggacctgt	acgccaaaca	tgtcttgtcc
961	GGCGGTACCA	CCATGTACCC	AGGTATCGGT	GACCGTATGC	AGAAAGAGAT	CACAGCCCTG
	ggcggtacca	ccatgtaccc	aggtatcggg	gaccgcatgc	agaaggaaat	cacagccctg

1021 GCTCCAGCA CCATGAAGAT CAAGATGATT GCTCCACCTG AGCGTAAGTA CTCTGTATGG  
 gccccagca caatgaagat caagatgatt gccccctg agcgtaagta ctcagtctgg

1081 ATCGGTGGCT CTATCTTGGC TTCCCTGTCC ACTTCCAGC AGATGTGGAT CAGCAAGGAT  
 atcggcgct ccatcctggc ctccctgtcc acctccagg ccatgtggat cagcaaagat

1141 GAGTATGAAG AGGCTGGACC TTCCATTGTC CACAGGAAGT GCTTCTAAAC ACACCATGTG  
 gagtatgagg aggccggacc ctcaatcgtc cacagaaagt gcttctaatt tctctctcca

1201 TATATGTTCA TGTACTTACA CACATTTCT CACATCCTT AACTTTAAC TTTCATCCAC  
 actgtcaact gtccccaaat atttgcctc tgcctattct catctctcta atccccaca

1261 ATTATTTCTT TCAAGCTAAA TTCCATTGT CTCCAGTGT ACTCTCCATC TTGATTTAA  
 ataaccatt gtaattgtt actatttgt caacgtccc aaagaatctg tattatcagt

1321 TTGCACATGT GTTGTCTCA ACCACTGTGA ATCACTGTT ATTCCCTCCC TTTTGTTAAT  
 ctctaacca caaataccat tgtaattgt tactatttgt gcaacgttcc caaagaatct

1381 CTCACAATAA ATACTTCTAA TCCCCAAAA AAAAAAAAAA A  
 gtattatcag gatattgcta aataaattaa ttctgacttt t

cDNA sequence obtained from Atlantic herring is in CAPITALS, that from Brown trout in lowercase. Untranslated regions are **bold** and underlined for the herring sequence. Brown trout accession number AF267496 [Mudalige et al 2007]. These sequences have 89% homology. Only overlapping sequence is shown here.

Figure 10: Comparison of the cDNA sequences corresponding to the fast skeletal muscle actin isoforms isolated from Atlantic herring and Atlantic salmon.

1	<u>CCACGCGTCC</u>	<u>GAGCAGCGGT</u>	<u>TGAACTACTA</u>	<u>GGCAGGAAAC</u>	<u>TCCACAGTAT</u>	<u>CCATCAAGAT</u>
	actgtaaccc	accgcctcct	gtccagctct	ccagggccca	cagtaaccag	actcaaccat
61	GTGTGACGAC	GACGAGACTA	CCGCTCTTGT	GTGCGACAAC	GGCTCCGGCC	TTGTGAAAGC
	gtgtgacgag	gaagagacaa	cagccttggg	atgcgacaac	ggctcaggac	tgggtaaggg
121	TGGCTTTGCC	GGTGATGACG	CCCCAGGGC	TGTATTCCCC	TCCATTGTGG	GCCGTCCTCG
	tggcttcgcc	ggtgacgatg	ccccagggc	agtgttcccc	tccattgtgg	ggcgcccccg
181	TCACCAGGGT	GTGATGGTCG	GTATGGGACA	GAAGGACTCC	TACGTAGGAG	ATGAGGCTCA
	tcatcagggg	gtgatgggtg	gtatgggtca	gaaagactcc	tatgtaggag	acgagggcca
241	GAGCAAGAGA	GGTATCCTGA	CTCTGAAGTA	CCCCATTGAG	CACGGTATCA	TCACCAACTG
	gagcaagaga	ggtatcctga	ccctcaagta	ccccattgag	cacggcatca	taactaactg
301	GGATGATATG	GAGAAGATCT	GGCATCACAC	CTTCTACAAT	GAGCTGCGTG	TGGCACCCGA
	ggacgacatg	gagaagatct	ggcatcatac	cttctacaat	gagcttcgtg	tggcacctga
361	GGAGCACCCC	ACCCTGCTCA	CAGAGGCCCC	CCTGAACCCC	AAGGCCAACA	GAGAGAAGAT
	ggagcaccc	gtcctgctca	ctgaggcccc	actcaacccc	aaggccaaca	gagagaagat
421	GACCCAGATC	ATGTTTGAGA	CCTTCAACGT	CCCAGCCATG	TATGTGGCCA	TCCAGGCTGT
	gaccagatc	atgtttgaga	ccttcaacgt	gccagctatg	tatgtggcca	tccaggctgt
481	GCTGTCCCTG	TACGCCTCTG	GCCGTACCAC	TGGTATCGTG	CTGGACTCCG	GTGATGGTGT
	gctgtccctg	tacgcctctg	gtcgtaccac	aggtattgtg	ctggacgctg	gcgatgggtg
541	GTCTCACAAT	GTCCCCATCT	ATGAGGGTTA	TGCTCTCCCC	CATGCCATCA	TGCGTCTGGA
	gaccacaac	gtccccatct	atgagggtta	tgccttgccc	catgccaatca	tgagactgga
601	TCTGGCTGGT	CGCGATCTGA	CTGATTACCT	GATGAAGATC	CTGACAGAGC	GTGGTTACTC
	cttggctggg	agagacctga	ctgactacct	gatgaagatc	ctcactgaga	gaggctactc
661	TTTCGTGACA	ACCGCTGAGC	GTGAGATCGT	GCGCGACATC	AAGGAGAAGT	TGTGCTATGT
	tttcgtcacc	accgctgaga	gagagattgt	gcgtgacatc	aaggagaagc	tgtgctacgt
721	GGCTCTGGAC	TTCGAGAATG	AGATGGCAAC	CGCTGCCTCC	TCCTCCTCTC	TGGAGAAGAG
	ggctctggac	tttgagaatg	agatggccac	cgctgcctcc	tcctcctctc	tggagaagtc
781	CTACGAGCTC	CCCGACGGTC	AGGTCATTAC	CATTGGTAAT	GAACGTTTCC	GTTGCCCTGA
	ctatgagttg	cccgatggtc	aggatcatcac	catcggtaac	gagaggttcc	gttgcccaga
841	GACCCTCTTC	CAGCCTTCCT	TCATTGGTAT	GGAGTCTGCT	GGTATTCATG	AGACTGCCTA
	aaccctcttc	cagccttcct	tcattggcat	ggagtccgct	ggtatccatg	agaccacata
901	CAACAGCATC	ATGAAGTGCG	ACATTGACAT	CAGGAAGGAC	CTGTACGCCA	ACAATGTCTT
	caacagcatc	atgaagtgcg	acattgacat	ccgtaaggac	ctgtacgccca	acaatgtctt
961	GTCCGGTGGT	ACCACCATGT	ACCCTGGTAT	TGCTGACAGG	ATGCAGAAGG	AGATCACTGC
	gtccgggtgg	accaccatgt	accctggtat	cggtgaccgc	atgcagaagg	aatcacagc

1021 TCTGGCCCC AGCACCATGA AGATCAAGAT CATTGCCCCA CCTGAGCGTA AGTACTCCGT  
 cctggcccc agcacaatga agatcaagat gattgcccc cctgagcgta agtactcagt  
 1081 CTGGATTGGT GGCTCCATCC TGGCTTCCCT GTCCACCTTC CAGCAGATGT GGATCACCAA  
 ctggatcggc ggctccatcc tggctccct gtccaccttc caggccatgt ggatcagcaa  
 1141 ACAGGAGTAC GATGAGGCAG GCCCCAGCAT TGTCCACCGC AAATGCTTCT AAGCGAACGA  
 agatgagtat gaggaggccg gacctcaat cgtccacaga aagtgttct aatttctctc  
 1201 ATCACCCCAT GGATCATTTT TTGCTCAGGA ACCAACGACA GCCCGCTGCT GTTATTATGG  
 tccaactgtc aactgtcccc aaatatttgc tctctgtcta ttctcatctc tctaattccc  
 1261 GACAATTTTG TACAAGTTT TTTCCAGCC AACGATTGT TTACAATGA CGCGAACTG  
 acaaataacc cattgtaatt gtttactatt tgtgcaacgt tcccaaagaa tctgtattat  
 1321 AGAGGATTTT AGCCTCTACA AACACATCAA GAAATGTCAT CCTTTGAATG TATGCTTGTA  
 cagtctctaa tccacaaata ccattgtaat tgtttactat ttgtgcaacg ttcccaaaga  
 1381 GAGGGTGCAA GCAACCTAAC TGGGGAACAT CAGGGTTATA GACTGT  
 atctgtatta tcaggatatt gctaaataaa ttaattctga cttttg

cDNA sequence obtained from Atlantic herring is in CAPITALS, that from Atlantic salmon in lowercase. Untranslated regions are **bold** and underlined for the herring sequence. Atlantic salmon accession number AF304406 [Mudalige *et al* 2007]. These sequences have 92% homology. Only overlapping sequence shown here.

During the discussion of the inferred amino acid sequences keep in mind the identical 1° structures between the skeletal muscle actins of humans and chicken. In the instance of these teleost fish, the heterogeneity exceeds 3% (Figure 11). A total of 13 inferred amino acid substitutions, six of those being non-conservative in nature, are noted when comparing the slow skeletal muscle actin from either source to the fast skeletal muscle actin from the same species. The substitutions are as follows (Atlantic herring; non-conservative underlined and in bold): Asp 2 Glu, Asp 3 Glu, **Thr 103 Val**, **Ser 155 Ala**, Ser 160 Thr, Ile 205 Val, **Ala 278 Thr**, **Ser 281 Gly**, **Ala 310 Gly**, Ile 329 Met, Thr 358 Ser, **Gln 360 Asp**, Asp 363 Glu (fast:slow). Interestingly, most of these substitutions are not located in the regions of actin where heterogeneity is most common. The exceptions to this are residues two and three, which are at the extreme amino terminus and residue 278, found in the hydrophobic plug. With regards to residue 278, the slow skeletal muscle actin isoform has threonine at this position, as does actin isolated from rabbit, the fast has alanine. So while this is indeed a non-conservative substitution its contribution to the observed instability can likely be ruled out as it is the fast skeletal muscle actin isoform that is heterogeneous at this residue compared to rabbit - an isoform with the same stability (Table 1).

Figure 11: Comparison of the inferred (immature) actin amino acid sequences from the slow and fast skeletal muscles of Atlantic herring.

Herr fast	MCDDDQTTALVCDNGSGLVKAGFAGDDAPRAVFPSIVGRP	40
Herr Slow	MCDEEETTALVCDNGSGLVKAGFAGDDAPRAVFPSIVGRP	
Herr fast	RHQGVVMVGMGQKDSYVGDEAQSKRGILTLYPIEHGIITN	80
Herr Slow	RHQGVVMVGMGQKDSYVGDEAQSKRGILTLYPIEHGIITN	
Herr fast	WDDMEKIWHHTFYNELRVAPEEHPVLLTEAPLNPKANREK	120
Herr Slow	WDDMEKIWHHTFYNELRVAPEEHPVLLTEAPLNPKANREK	
Herr fast	MTQIMFETFNVPAMYVAIQAVLSLYASGRRTGIVLDAGDG	160
Herr Slow	MTQIMFETFNVPAMYVAIQAVLSLYASGRRTGIVLDAGDG	
Herr fast	VSHNVPIYEGYALPHAIMRLDLAGRDLTDYLMKILTERGY	200
Herr Slow	VTHNVPVYEGYALPHAIMRLDLAGRDLTDYLMKILTERGY	
Herr fast	SFVTTAEREIVRDIKEKLCYVALDFENEMATAASSSSLEK	240
Herr Slow	SFVTTAEREIVRDIKEKLCYVALDFENEMATAASSSSLEK	
Herr fast	SYELPDGQVITIGNERFRCPETLFQPSFIGMESAGIHETA	280
Herr Slow	SYELPDGQVITIGNERFRCPETLFQPSFIGMESAGIHETI	
Herr fast	YNSIMKCDIDIRKDLYANNVLSGGTTMYPGIADRMQKEIT	320
Herr Slow	YNSIMKCDIDIRKDLYANNVLSGGTTMYPGIADRMQKEIT	
Herr fast	ALAPSTMKIKI I I APPERKYSVWIGGSILASLSTFQQMWIT	360
Herr Slow	ALAPSTMKIKI M I APPERKYSVWIGGSILASLSTFQQMWIS	
Herr fast	KLEYDEAGPSIVHRKCF	377
Herr Slow	KLEYEEAGPSIVHRKCF	

Substitutions are highlighted as follows: conservative substitutions in yellow, non conservative (defined as a changes in charge, hydrophobicity or glycine content) highlighted in blue and, substitutions of special interest in red (all of which are non-conservative).

Table 1: Summary of results for the three skeletal muscle actins compared to the skeletal muscle actin isolated from rabbit.

The fourteen positions of heterogeneity with rabbit skeletal muscle actin are listed. Residues numbered as mature actin. Non-conservative substitutions are in *italics*, underlined, and **bold**. Non conservative substitutions are defined by a change in polarity, charge or glycine content. Information pertaining to the salmonid fast and slow actin isoforms taken from Mudalige et al. 2007. Thermal unfolding experiments resulted in the following Tms: Herr fast  $55.26^{\circ}\text{C} \pm 0.709^{\circ}\text{C}$ ; Herr slow  $49.74^{\circ}\text{C} \pm 0.599^{\circ}\text{C}$ ; Mack fast  $54.94^{\circ}\text{C} \pm 0.688^{\circ}\text{C}$  presented Tms to the nearest  $^{\circ}\text{C}$ . Thermal unfolding experiments were repeated at least three times with different (n=5) protein preparations. Information pertaining to rabbit actin taken from Strzelecka-Golaszewska et al. 1985.

Amino Acid	Sal fast	Sal slow	Herr fast	Herr slow	Mack fast	Rabbit
2	Asp	Glu	Asp	Glu	Asp	Glu
3	Asp	Glu	Asp	Glu	Asp	Asp
103	Thr	<u>Val</u>	Thr	<u>Val</u>	Thr	Thr
155	Ser	<u>Ala</u>	Ser	<u>Ala</u>	<u>Ala</u>	Ser
160	Thr	Thr	Ser	Thr	Thr	Thr
165	Ile	Val	Ile	Val	Ile	Ile
278	<u>Ala</u>	Thr	<u>Ala</u>	Thr	<u>Ala</u>	Thr
281	Ser	<u>Gly</u>	Ser	<u>Gly</u>	Ser	Ser
299	Leu	Leu	Leu	Leu	Leu	Met
310	Ala	<u>Gly</u>	Ala	<u>Gly</u>	Ala	Ala
329	Ile	Met	Ile	Met	Ile	Ile
354	<u>Ala</u>	<u>Ala</u>	Gln	Gln	Gln	Gln
358	Thr	Ser	Thr	Ser	Ser	Thr
360	Gln	<u>Asp</u>	Gln	<u>Asp</u>	Gln	Gln
363	Asp	Glu	Asp	Glu	Asp	Asp
Tm	55°C	45°C	55°C	50°C	55°C	55°C
[urea]	4M	3M	4M	3.5M	4M	4M

When comparing both fast or slow skeletal muscle actins a different situation is presented - one more typical of actin. The single inferred substitution between the two slow actin isoforms identified in teleost fish (Figure 12) Gln 354 Ala (herr:sal) demonstrated that slow skeletal muscle actin is conserved across teleost evolution as *cupeloformes* and *salmonids* are distantly related fish orders (See Chapt. 4, Figure 32). The two fast actins (Figure 13) exhibit a slightly higher level of heterogeneity; the non-conservative substitution Gln 354 Ala (herr:sal) and a second, Ser 160 Thr (herr:sal - a conserved substitution). Although slightly more heterogeneous, it can also be said that the fast specific actin isoform is conserved across teleost evolution. Perhaps most importantly, as there is now a second sequence, slow skeletal muscle actin can now be considered a *bona fide* actin isoform and not simply a lone occurrence.

An ideal situation to document the contribution of single residues to the stability of actin has presented itself. Interestingly, amino acid 354 seems to be conserved within species as opposed to within actin isotype. In *clupleoforms*, glutamine occupies this position while in *salmonid* fish it is alanine (Table 1). Most importantly, as this is the only substitution between the two identified slow skeletal muscle actins, any differences in the nature of the protein isolated from the two species can be attributed to this residue. Comparison of the three fast skeletal muscle isoforms (Figure 14)

Figure 12: Comparison of the inferred (immature) actin amino acid sequences from the slow skeletal muscles of Atlantic herring and Brown trout.

Herr Slow	MCDEEETALVCDNGSGLVKAGFAGDDAPRAVFPSIVGRP	40
Sal Slow	MCDEEETALVCDNGSGLVKAGFAGDDAPRAVFPSIVGRP	
Herr Slow	RHQGVMVGMGQKDSYVGDEAQSKRGILTLKYPIEHGIITN	80
Sal Slow	RHQGVMVGMGQKDSYVGDEAQSKRGILTLKYPIEHGIITN	
Herr Slow	WDDMEKIWHHTFYNELRVAPEEHPVLLTEAPLNPKANREK	120
Sal Slow	WDDMEKIWHHTFYNELRVAPEEHPVLLTEAPLNPKANREK	
Herr Slow	MTQIMFETFNVPAMYVAIQAVLSLYASGRRTGIVLDAGDG	160
Sal Slow	MTQIMFETFNVPAMYVAIQAVLSLYASGRRTGIVLDAGDG	
Herr Slow	VTHNVPVYEGYALPHAIMRLDLAGRDLTDYLMKILTERGY	200
Sal Slow	VTHNVPVYEGYALPHAIMRLDLAGRDLTDYLMKILTERGY	
Herr Slow	SFVTTAEREIVRDIKEKLCYVALDFENEMATAASSSSLEK	240
Sal Slow	SFVTTAEREIVRDIKEKLCYVALDFENEMATAASSSSLEK	
Herr Slow	SYELPDGQVITIGNERFRCPETLFQPSFIGMESAGIHETT	280
Sal Slow	SYELPDGQVITIGNERFRCPETLFQPSFIGMESAGIHETT	
Herr Slow	YNGIMKCDIDIRKDLYANNVLSGGTTMYPGIGDRMQKEIT	320
Sal Slow	YNGIMKCDIDIRKDLYANNVLSGGTTMYPGIGDRMQKEIT	
Herr Slow	ALAPSTMKIKMIAPPERKYSVWIGGSILASLSTFQ MWIS	360
Sal Slow	ALAPSTMKIKMIAPPERKYSVWIGGSILASLSTFQ MWIS	
Herr Slow	KDEYEEAGPSIVHRKCF	377
Sal Slow	KDEYEEAGPSIVHRKCF	

Substitutions are highlighted in red are of special interest and are non-conservative in nature. Sequence of salmon slow skeletal muscle actin taken from Mudalige et al. 2007.

Figure 13: Comparison of the inferred (immature) actin amino acid sequences from the fast skeletal muscles of Atlantic herring and Atlantic salmon.

Herr fast	MCDDDQTTALVCDNGSGLVKAGFAGDDAPRAVFPSIVGRP	40
Sal Fast	MCDDDETTALVCDNGSGLVKAGFAGDDAPRAVFPSIVGRP	
Herr fast	RHQGVVMVGMGQKDSYVGDEAQSKRGILTLKYPIEHGIITN	80
Sal Fast	RHQGVVMVGMGQKDSYVGDEAQSKRGILTLKYPIEHGIITN	
Herr fast	WDDMEKIWHHTFYNELRVAPEEHPTLLTEAPLNPKANREK	120
Sal Fast	WDDMEKIWHHTFYNELRVAPEEHPTLLTEAPLNPKANREK	
Herr fast	MTQIMFETFNVPAMYVAIQAVLSLYASGRRTGIVLDSGDG	160
Sal Fast	MTQIMFETFNVPAMYVAIQAVLSLYASGRRTGIVLDSGDG	
Herr fast	VSHNVPIYEGYALPHAIMRLDLAGRDLTDYLMKILTERGY	200
Sal Fast	VTHNVPIYEGYALPHAIMRLDLAGRDLTDYLMKILTERGY	
Herr fast	SFVTTAEREIVRDIKEKLCYVALDFENEMATAASSSSLEK	240
Sal Fast	SFVTTAEREIVRDIKEKLCYVALDFENEMATAASSSSLEK	
Herr fast	SYELPDGQVITIGNERFRCPETLFQPSFIGMESAGIHETA	280
Sal Fast	SYELPDGQVITIGNERFRCPETLFQPSFIGMESAGIHETA	
Herr fast	YNSIMKCDIDIRKDLYANNVLSGGTTMYPGIADRMQKEIT	320
Sal Fast	YNSIMKCDIDIRKDLYANNVLSGGTTMYPGIADRMQKEIT	
Herr fast	ALAPSTMKIKIIAPPERKYSVWIGGSILASLSTFQ MWIT	
Sal Fast	ALAPSTMKIKIIAPPERKYSVWIGGSILASLSTFQ MWIT	
Herr fast	KQEYDEAGPSIVHRKCF	377
Sal Fast	KQEYDEAGPSIVHRKCF	

Substitutions are highlighted as follows: conservative substitutions in yellow, non-conservative substitutions of special interest in red. Sequence of salmon fast skeletal muscle actin taken from Mudalige et al. 2007.

Figure 14: Comparison of the inferred (immature) actin amino acid sequences from the fast skeletal muscles of Atlantic herring, Atlantic salmon and, Atlantic mackerel.

Herr fast	MCDDDQTTALVCDNGSGLVKAGFAGDDAPRAVFPSIVGRP	40
Sal Fast	MCDDDETTALVCDNGSGLVKAGFAGDDAPRAVFPSIVGRP	
Mack fast	MCDDDETTALVCDNGSGLVKAGFAGDDAPRAVFPSIVGRP	
Herr fast	RHQGVVMVGMGQKDSYVGDEAQSKRGILTLKYPIEHGIITN	80
Sal Fast	RHQGVVMVGMGQKDSYVGDEAQSKRGILTLKYPIEHGIITN	
Mack fast	RHQGVVMVGMGQKDSYVGDEAQSKRGILTLKYPIEHGIITN	
Herr fast	WDDMEKIWHHTFYNELRVAPEEHPTLLTEAPLNPKANREK	120
Sal Fast	WDDMEKIWHHTFYNELRVAPEEHPTLLTEAPLNPKANREK	
Mack fast	WDDMEKIWHHTFYNELRVAPEEHPTLLTEAPLNPKANREK	
Herr fast	MTQIMFETFNVPAMYVAIQAVLSLYASGRITGIVLDSGDG	160
Sal Fast	MTQIMFETFNVPAMYVAIQAVLSLYASGRITGIVLDSGDG	
Mack fast	MTQIMFETFNVPAMYVAIQAVLSLYASGRITGIVLDSGDG	
Herr fast	VSHNVPIYEGYALPHAIMRLDLAGRDLTDYLMKILTERGY	200
Sal Fast	VTHNVPIYEGYALPHAIMRLDLAGRDLTDYLMKILTERGY	
Mack fast	VTHNVPVYEGYALPHAIMRLDLAGRDLTDYLMKILTERGY	
Herr fast	SFVTTAEREIVRDIKEKLCYVALDFENEMATAASSSSLEK	240
Sal Fast	SFVTTAEREIVRDIKEKLCYVALDFENEMATAASSSSLEK	
Mack fast	SFVTTAEREIVRDIKEKLCYVALDFENEMATAASSSSLEK	
Herr fast	SYELPDGQVITIGNERFRCPETLFQPSFIGMESAGIHETA	280
Sal Fast	SYELPDGQVITIGNERFRCPETLFQPSFIGMESAGIHETA	
Mack fast	SYELPDGQVITIGNERFRCPETLFQPSFIGMESAGIHETA	
Herr fast	YNSIMKCDIDIRKDLYANNVLSGGTTMYPGIADRMQKEIT	320
Sal Fast	YNSIMKCDIDIRKDLYANNVLSGGTTMYPGIADRMQKEIT	
Mack fast	YNSIMKCDIDIRKDLYANNVLSGGTTMYPGIADRMQKEIT	
Herr fast	ALAPSTMKIKIIAPPERKYSVWIGGSILASLSTFQAMWIT	
Sal Fast	ALAPSTMKIKIIAPPERKYSVWIGGSILASLSTFQAMWIT	
Mack fast	ALAPSTMKIKIIAPPERKYSVWIGGSILASLSTFQAMWIS	
Herr fast	KQEYDEAGPSIVHRKCF	377
Sal Fast	KQEYDEAGPSIVHRKCF	
Mack fast	KQEYDEAGPSIVHRKCF	

Substitutions are highlighted as follows: conservative substitutions in yellow, non-conservative substitutions of special interest in red. Sequence of salmon fast skeletal muscle actin taken from Mudalige et al. 2007.

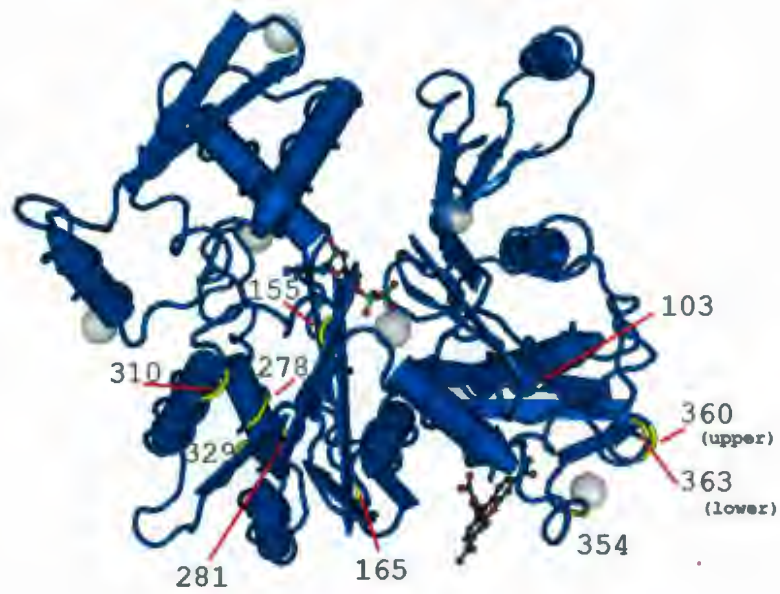
reveals four substitutions (two non-conservative) between the *salmonid* and *percomorph* isoforms and four substitutions (one non-conserved) between the *clupleoform* and *percomorph* isoforms. The fast skeletal muscle actin isolated from mackerel contains the previously mentioned Ser 155 Ala replacement but not the charge substitution Gln 360 Asp. Because of this, the mackerel fast skeletal muscle actin will allow for the relative contribution of Ser 155 Ala to be determined. It is important to mention that the fast skeletal muscle actin isoform identified in Atlantic mackerel came from a slow skeletal muscle library. This will be addressed further in section 3.2.1.

As mentioned in the introduction, there are many published crystal structures of actin. The locations of all substitutions documented herein were mapped on the structure obtained by Otterbein *et al.* in 2001 and presented in Figure 15. It can be seen that all substitutions are limited to subdomains one and three. The crystal structure of actin shows that residue 155 points away from the central cleft, unable to contribute to nucleotide or divalent cation binding.

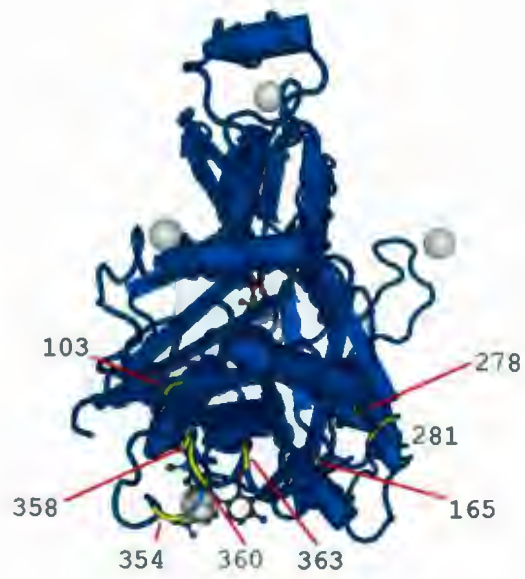
Figure 15: Location of substitutions in relation to the crystal structure of rabbit skeletal muscle actin.

Crystal structure obtained by Otterbein, *et al.* Science 293, 708 (2001). PDB file can be accessed with the ID: 1J6Z. The first three residues have been removed and are not indicated. All identified substitutions are highlighted in yellow and associated numbers are indicated with red lines where necessary. A) Front view of actin: subdomain 1 - lower right; subdomain 2 - upper right; subdomain 3 - lower left; subdomain 4 - upper left. B) View of actin from the right side: subdomain 1 - bottom; subdomain 2 - top. C) View of actin from behind: subdomain 1 - lower left; subdomain 2 - upper left; subdomain 3 - lower right; subdomain 4 - upper right. D) View of actin from the left side: subdomain 3 - bottom; subdomain 4 - top.

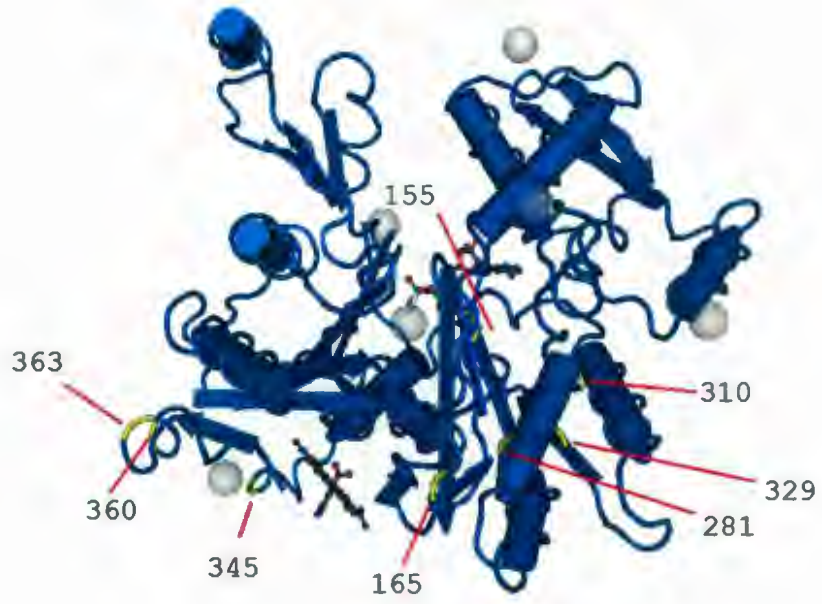
**A**



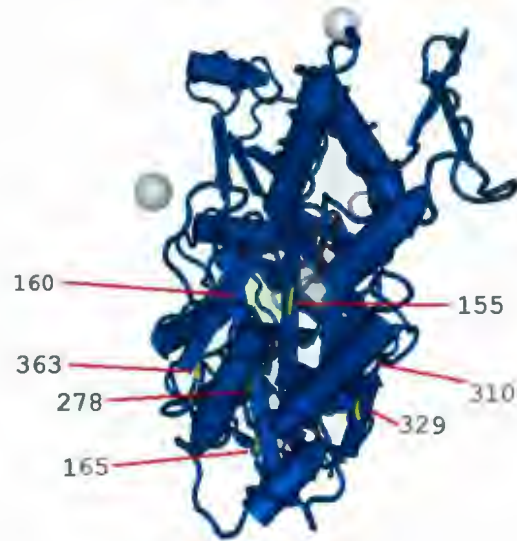
**B**



C



D



## 3.2 Electrophoresis of isoactins

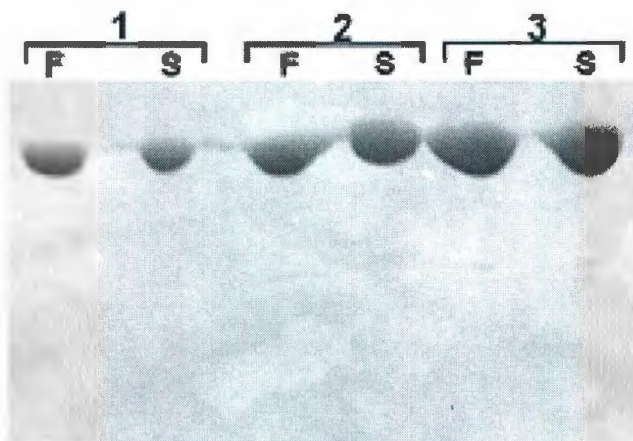
In total, actin was prepared from the fast and slow skeletal muscles of seven different species of fish. All preparations were done by rounds of polymerization /depolymerization according to the method of Spudich & Watt (1971). The concentration of all actins was determined using UV spectroscopy and level of enrichment (as well as concentration) was assessed by SDS-PAGE (Figure 16).

### 3.2.1 Alkaline urea PAGE

Alkaline urea PAGE is a powerful electrophoretic technique capable of separating two proteins of virtually identical mass with a single difference in charge. Unlike SDS PAGE, the intrinsic charge of the protein or peptides is left intact. This method was useful in this study for two reasons: to confirm the charge substitution that had been inferred from nucleotide sequencing and, similarly, as a rough tool to screen for the presence of a charge substituted actin without entering into a nucleotide sequencing effort.

Figure 17 shows a Coomassie Blue stained gel of the fast and slow skeletal muscle actins found in Atlantic herring. The resolving power of urea PAGE is further demonstrated by the right lane where the sample loaded was a mixture of both isoforms. Urea PAGE was used to screen for charge variants in the following fish: Rainbow smelt, *Osmerus mordax*; Atlantic mackerel, *Scomber*

Figure 16: Assessment of enrichment using SDS PAGE of actins isolated from the fast and slow skeletal muscles of Atlantic herring.



Electrophoresis was performed with 12% polyacrylamide gels (SDS) and 180 V was applied for 45 minutes. Gels stained using Comassie Brilliant Blue R-250. S: slow skeletal muscle actin. F: fast skeletal muscle actin. Numbers indicate the following: 1 - 1.5  $\mu\text{g}$  protein loaded; 2 - 3 $\mu\text{g}$  protein loaded; 3 - 4.5  $\mu\text{g}$  of protein loaded. Higher loading in the group 3 was to verify the high enrichment of actins isolated with the outlined procedure.

Figure 17: Alkaline urea PAGE of the fast and slow skeletal muscle actins isolated from Atlantic herring.

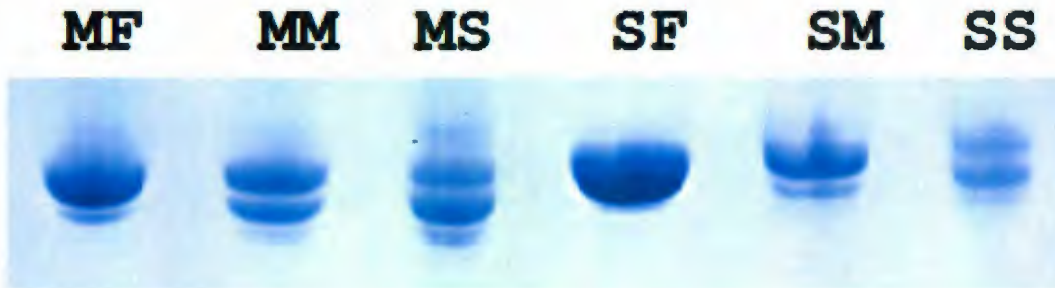


Inset of an alkaline urea 10% polyacrylamide gel. Electrophoresis was at 220 V for three hours after a 15 minute pre-run at the same voltage [Perrie and Perry 1970]. All samples dispersed at RT in saturated urea, freshly prepared with 0.2 mM DTT to a final protein concentration of ~ 0.5 mg/ml. Gel staining/destaining is identical to the SDS gels. 2-4  $\mu$ g of protein loaded. Lane 1 - fast skeletal muscle actin; Lane 2 - slow skeletal muscle actin; Lane 3 - 50:50 mix of fast and slow skeletal muscle actin.

*Scombrus* (Figure 18); Atlantic halibut, *Hippoglossus hippoglossus*; tilapia (Figure 19) and hagfish and lamprey (final three species unknown, data not shown for hagfish or lamprey). With the exception of smelt and mackerel, there was no indication of a charge substituted actin isoform in the slow skeletal muscle of any of these fish. This result infers that while slow skeletal muscle actin is conserved across species (as shown by nucleotide sequencing) it is not necessarily employed across species. Figure 18 shows the results of the analysis of the smelt and mackerel skeletal muscle actin isoforms. It is noteworthy that the slow skeletal muscle samples from mackerel and smelt do not appear to be homogeneous in this gel system. In the case of actin isolated from smelt this could be due to contamination with intermediate, or pink, muscle as the species is quite small and separation of the two muscle types was more difficult. This is unlikely to be the case for Atlantic mackerel as there were greater quantities of acetone powder used in multiple preparations, as opposed to the lone preparation in the case of smelt. In addition, the fast skeletal muscle actin sequence obtained from Atlantic mackerel was found in a slow muscle cDNA library. This information combined with the heterogeneity observed here indicates that the slow skeletal muscle in Atlantic mackerel utilizes two distinct  $\alpha$ -actin isoforms. Regardless, the finding of a charge substituted actin in the slow skeletal muscle of Atlantic mackerel confirms that

the inferred actin sequence (Acc # EF607093) corresponds to a fast skeletal muscle actin.

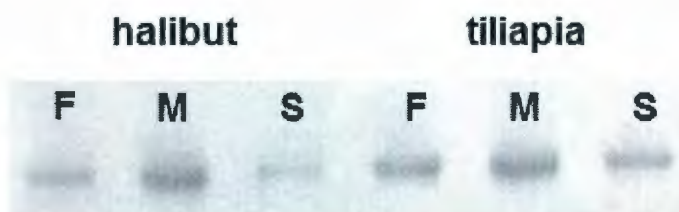
Figure 18: Alkaline urea PAGE of the fast and slow skeletal muscle actins isolated from Atlantic mackerel and Rainbow smelt.



Inset of an alkaline urea 10% polyacrylamide gel. Electrophoresis was at 220 V for three hours after a 15 minute pre-run at the same voltage [Perrie and Perry 1970]. All samples dispersed at RT in saturated urea, freshly prepared with 0.2 mM DTT to a final protein concentration of ~ 0.5 mg/ml. Gel staining/destaining is identical to the SDS gels. 6  $\mu$ g of protein loaded. MF - mackerel fast actin; MM - 50:50 mix of mackerel fast and slow actin; MS - mackerel slow actin; SF - smelt fast actin; SM - 50:50 mix of smelt fast and slow actin; SS - smelt slow actin. The extra band that is found under each sample is possibly an artifact of electrophoresis in the presence of urea.

While a powerful technique, urea PAGE is not without limitations. Charge substitutions can be identified but no information as to the location of those substitutions is given. Nor can it give any information about the identities of the other 374 amino acids. Urea PAGE analysis of halibut and tilapia fast and slow skeletal muscle actins is presented in Figure 19. There is no evidence of a charge variant actin isoform as was detected before (Figures 17 & 18) nor was there evidence of its presence in the other studied fish species (data not shown). The same result is obtained over a range of sample loadings, indicating that a minor component (in addition to the major component) is not present. This does not preclude the possibility that the actin utilized in these muscles is heterogeneous; they do, however, have the same net charge. Given that there was a collection of sequenced actins (ie fast and slow skeletal muscle actins from Atlantic herring and Atlantic salmon as well as the fast skeletal muscle actin found in Atlantic mackerel) at our disposal with sufficient amounts of muscle acetone powder, the unsequenced actins were not used for the remainder of the study.

Figure 19: Alkaline urea PAGE of skeletal muscle actin from Atlantic halibut (*Hippoglossus hippoglossus*) and tilapia (species unknown).



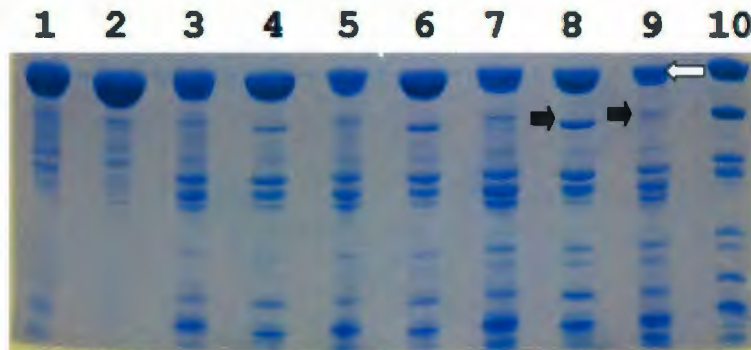
Inset of an alkaline urea 10% polyacrylamide gel. Electrophoresis was at 220 V for three hours after a 15 minute pre-run at the same voltage [Perrie and Perry 1970]. All samples dispersed at RT in saturated urea, freshly prepared with 0.2 mM DTT to a final protein concentration of ~ 0.5 mg/ml. Gel staining/destaining is identical to the SDS gels. 2-4  $\mu$ g of protein loaded. F - fast skeletal muscle actin; M - 50:50 mix of fast and slow skeletal muscle actin; S - slow skeletal muscle actin. Species is indicated above the lanes.

### 3.2.2 Limited proteolysis

#### 3.2.2.1 Subtilisin exposure

Before the first crystal structure of actin [Kabsch et al. 1990] proteolysis had been used for some time as a crude but informative method to probe for regions of disorder within the actin molecule. A typical subtilisin digestion of actin (source: *Oryctolagus cuniculus*, rabbit) results in the generation of a ~6 kDa N-terminal fragment and a 36 kDa C-terminal fragment (the equivalent peptide from herring is indicated by black arrows in Figure 20) [Schwyter et al 1989]. The very specific production of this high molecular weight peptide by subtilisin in the DNaseI binding loop at Met 47/Gly 48 and the functional consequences of this cleavage have been well documented [Schwyter et al. 1989, Strzelecka-Golaszewska et al. 1992, Crosbie et al. 1994, Vahdat et al. 1995, Ooi & Mihashi 1996]. With this in mind, the fast and slow isoforms of skeletal muscle actin from Atlantic herring were exposed to subtilisin in the hopes of identifying regions of relative instability (Figure 20). At room temperature, different patterns of digestion are observed by SDS PAGE (Figure 20). The rate of slow skeletal muscle actin digestion is, qualitatively, greater compared to the fast. In addition, lower molecular weight peptides dominate the banding for the slow actin while the distribution for the fast isoactin is more uniform; neither gave a typical banding pattern when digesting actin with subtilisin.

Figure 20: Differential susceptibility of actin isoforms isolated from Atlantic herring to limited proteolysis with subtilisin.



A 1:1000 (mass:mass) subtilisin to substrate ratio was used at RT. 15  $\mu$ g of subtilisin-exposed G-actin in 2 mM Tris, 0.2 mM  $\text{CaCl}_2$ , 0.2 mM ATP, 0.1 mM DTT, 0.01%  $\text{NaN}_3$ , pH 8.00 was loaded onto a 12% polyacrylamide gel (SDS) and 180 V was applied for 45 minutes. Gels stained using Coomassie Brilliant Blue R-250. Slow skeletal muscle actin - odd numbers (0 min, 5 min, 10 min, 20 min, 40 min respectively). Fast skeletal muscle actin - even numbers (0 min, 5 min, 10 min, 20 min, 40 min respectively). Arrows indicate the peptide subjected to Edman based sequencing that is known from other experiments to have a molecular mass of about 36 kDa. The other polypeptides observed in lanes 1 and 2 are due to the incomplete inhibition of subtilisin in the presence of 2 mM PMSF and 10 minutes boiling in the presence of SDS. The difference in the apparent size of the peptides in lane 10 is attributed to an 'end' migration effect.

The smaller molecular weight peptides observed in lanes 1 and 2 are due to the incomplete inhibition of subtilisin in 2 mM PMSF and 10 minutes boiling in the presence of SDS as they are not present in samples before exposure to protease

Returning to the present work, the differential band intensity and mobility of the 36 kDa species prompted an Edman based sequencing effort to identify the peptide in both isoforms. The results are presented in Figure 21 and clearly demonstrate that both peptides are formed by cleavage between Met 47/Gly 48. The differential mobility can be most easily explained by cleavage of some C-terminal residues from the slow skeletal muscle actin that does not occur with the fast. It can also be noted that there is a rapid accumulation of a high molecular weight peptide just under slow actin that is absent in the fast sample (Indicated by the white arrow in Figure 20).

The 36 kDa peptide can be clearly seen to accumulate in the fast actin sample while it is much less intense in the slow skeletal muscle actin sample (Figure 20) which is indicative of differential stability. Solution studies have established that the nucleotide bound to actin (ADP or ATP) [Strzelecka-Golaszewska *et al.* 1992] results in distinct intramolecular structural changes in the DNaseI binding loop (residues 38-52,

Figure 21: Edman sequencing of the 36 kDa peptide derived from subtilisin digestion of actin.

	48	49	50	51	52	53	54	55	56	57	58	59	60	61	62
Fast	G/S	Q	Q	D	S/G/P	Y	V	G	G	E	A	Q	S/G	G	R
Slow	G	Q	X	D	S/D	Y	V	G	D	E/D	A	Q	S	S	R
Known	G	Q	K	D	S	Y	V	G	D	E	A	Q	S	K	R

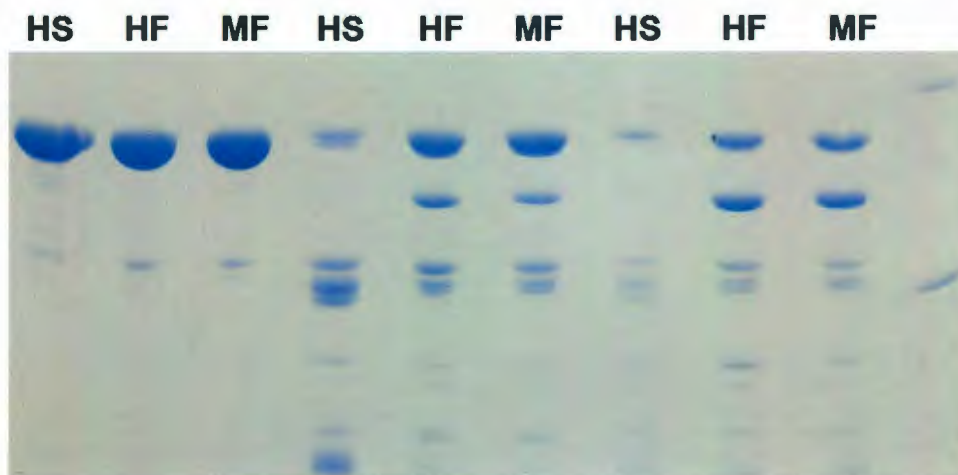
All letters represent amino acid identities with the exception of X, which indicates an inconclusive cycle. Residues with more than one assignment are presented according to abundance (highest/intermediate/least). The known actin sequence is taken from the inferred amino acid sequences presented earlier in this work (Figures 4,6 & 8).

subdomain 2 [Borovikov *et al.* 2000]). This is demonstrated by a change in the DNaseI loop's susceptibility to subtilisin digestion. It has been shown [Crosbie *et al.* 1994] that perturbations in the C-terminus, such as cleavage of the last few residues or the covalent attachment of a reporter probe to cys 374, does not affect digestion at the DNaseI binding loop. In the same work, however, it was demonstrated that binding of DNaseI at this loop exposes new cleavage sites; a 40 kDa species arises due to cleavage at 62/63 and 68/69 when exposed to trypsin. So while it is conceivable that an amino acid substitution at either of these locations could affect the susceptibility of the DNaseI binding loop to proteolysis, it remains a contentious issue as these findings are not in line with all of the structural data available. So, while the digestion pattern for both actins is difficult to explain fully it can nevertheless be concluded from these experiments that the slow isoform has adopted a 'looser' 3° conformation than its fast counterpart making it more easily accessible to the enzyme.

Figure 22 presents the subtilisin exposure of the two skeletal muscle actin isoforms from Atlantic herring as well as the fast skeletal muscle actin from Atlantic mackerel. The digestion of the fast skeletal muscle actin isoform found in mackerel is indistinguishable from that of the fast actin found in herring. While this is, admittedly, a crude method it is the first indication in this work that the identity of residue 155 (Ala in

mackerel fast and herring slow, Ser in herring fast) is of little consequence to the 3° structure of actin.

Figure 22: Limited proteolysis of actins from the skeletal muscle of Atlantic herring and the fast skeletal muscle actin from Atlantic mackerel.

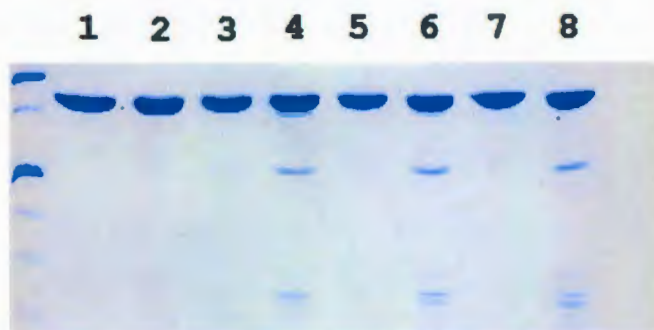


A 1:1000 (mass:mass) subtilisin to substrate ratio was used at RT. 10  $\mu\text{g}$  of subtilisin exposed G-actin in 2 mM Tris, 0.2 mM  $\text{CaCl}_2$ , 0.2 mM ATP, 0.1 mM DTT, 0.01%  $\text{NaN}_3$ , pH 8.00 was loaded onto a 12% polyacrylamide gel (SDS) and 180 V was applied for 45 minutes. Gels stained using Coomassie Brilliant Blue R-250. HS - herring slow skeletal muscle actin; HF - herring fast skeletal muscle actin; MF - mackerel fast skeletal muscle actin. Ignoring the molecular weight marker, the three leftmost samples were digested for 0 min, center three 20 min; rightmost three 40 min. Molecular mass markers in the right most lane correspond to peptides of 50 and 25 kDa.

#### 3.2.2.2 Thrombin exposure

Although little is known about the cleavage of actin by thrombin, it was noted in 1974 by Muszbek & Laki that it can indeed occur under certain conditions. When actin is purified without added  $\text{Ca}^{2+}$ , left in the  $\text{Mg}^{2+}$  bound form, the cleavage is allowed to proceed, albeit slowly. When  $\text{Ca}^{2+}$  is added to the extraction buffer, there is no detectable cleavage of actin. Removal of bound nucleotide (in the presence of 50% sucrose for stabilization) increases the rate of cleavage as does the addition of EDTA to actin prepared in the presence of  $\text{Ca}^{2+}$ . In these previous studies, it was found that actin is initially cleaved into a 37 and 5 kDa fragments. As the reaction proceeded, the 37 kDa peptide was further degraded to peptides of 27 and 10 kDas. All actins used in this study were prepared according to the traditional method of Spudich and Watt [Spudich & Watt 1971] using solutions with excess  $\text{Ca}^{2+}$ . The results presented in Figure 23 clearly show that, at RT and a mass to mass ratio of 1:65 (enz:sub), slow skeletal muscle actin is digested in the presence of  $\text{Ca}^{2+}$  while fast skeletal muscle actin is not. All previously documented peptide species are visible. Given the documented interconnectivity of distant regions of actin the explanation for this cleavage is hard to discern. What can be said with certainty is that the slow skeletal muscle actin isoform identified in this study can be digested by thrombin, under the employed conditions, while its fast counterpart cannot, suggesting that slow skeletal muscle actin has adopted a 3°

Figure 23: Limited proteolysis of skeletal muscle actin isoforms from Atlantic herring using thrombin.



A 1:65 (mass:mass) thrombin to actin ratio was used at RT. 15  $\mu$ g of thrombin exposed G-actin in 2 mM Tris, 0.2 mM  $\text{CaCl}_2$ , 0.2 mM ATP, 0.1 mM DTT, 0.01%  $\text{NaN}_3$ , pH 8.00 was loaded onto a 12% polyacrylamide gel (SDS) and 180 V was applied for 45 minutes. Gels stained using Coomassie Brilliant Blue R-250. Slow skeletal muscle actin - even numbers (0 min, 30 min, 60 min, 120 min respectively). Fast skeletal muscle actin - odd numbers (0 min, 30 min, 160 min, 120 min respectively). Molecular mass markers in the left most lane correspond to peptides of 50, 37, 25, 20, 15 and 10 kDa.

structure similar to that of EDTA exposed actin. As with the subtilisin digestion, this is indicative of a looser 3° structure. In short, the complete lack of fast actin digestion upon exposure to thrombin underlines the consequences of the substitutions found in the actin utilized in the slow skeletal muscle of *teleost* fish.

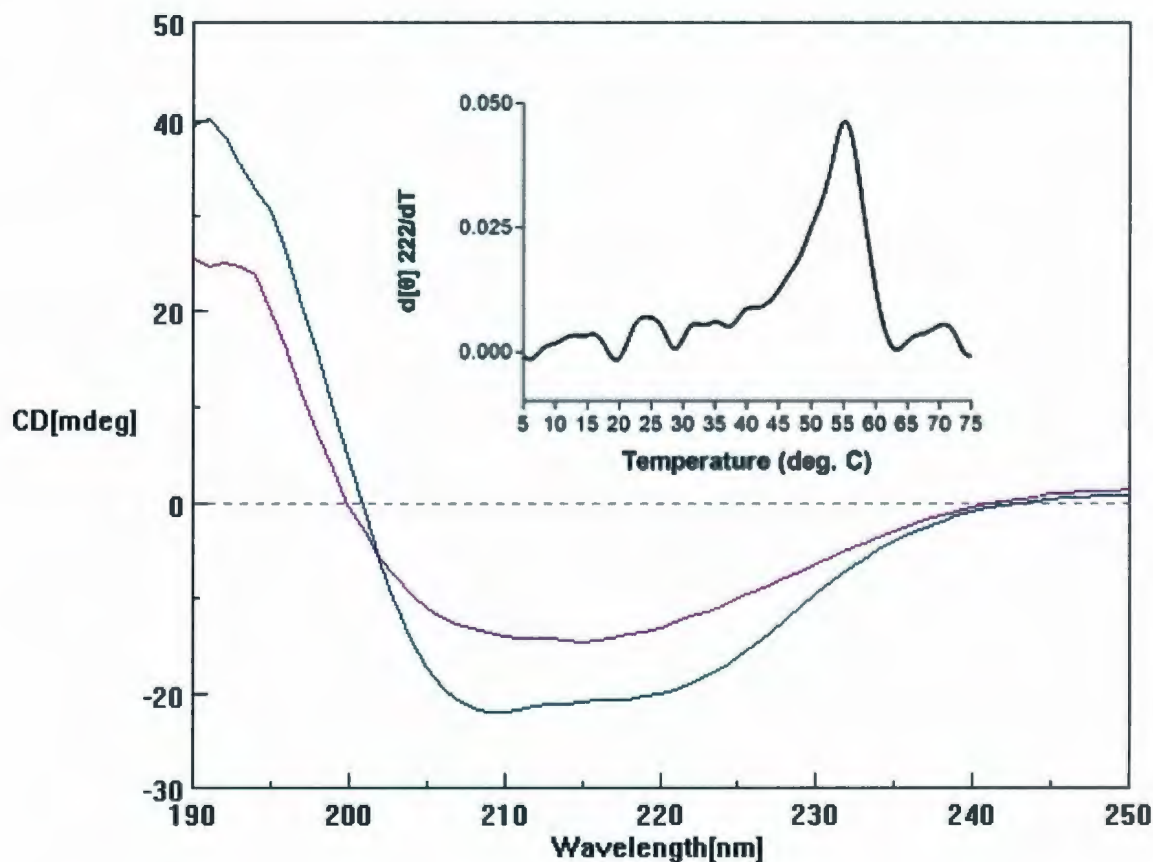
### **3.3 Spectroscopic techniques**

#### **3.3.1 Electronic circular dichroism**

##### 3.3.1.1 Thermal unfolding

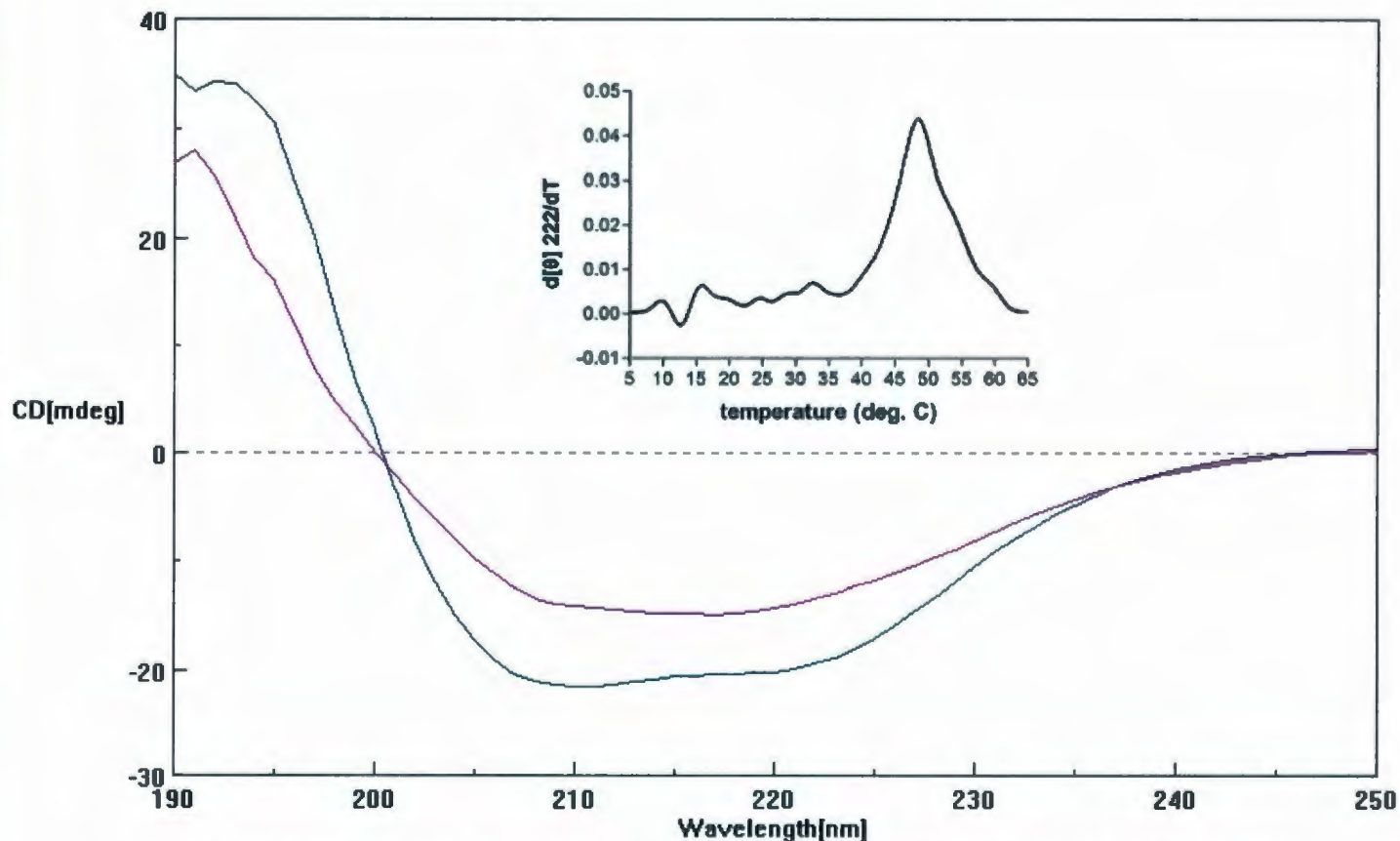
Figures 24 through 27 document the use of circular dichroism (CD) to observe the heat-induced unfolding of the various actin isoforms studied in this work. It is important to mention that when determining the concentration of slow skeletal muscle actin by UV spectroscopy there is a small but appreciable error when visually comparing the preparations banding intensity to that of a fast skeletal muscle actin on a SDS gel. This is, possibly, due to pigmentation that is co-purified with slow skeletal muscle actin that interferes with absorbance readings. To correct for this, the concentration of slow skeletal muscle actin was adjusted to give the same banding intensity and starting ellipticity as monitored by CD (an increase of ~25% was required). This is an important step, as too great a difference in protein concentration would cloud interpretation of CD

Figure 24: Thermally induced unfolding of the fast skeletal actin isoform from Atlantic herring as monitored by far-UV circular dichroism.



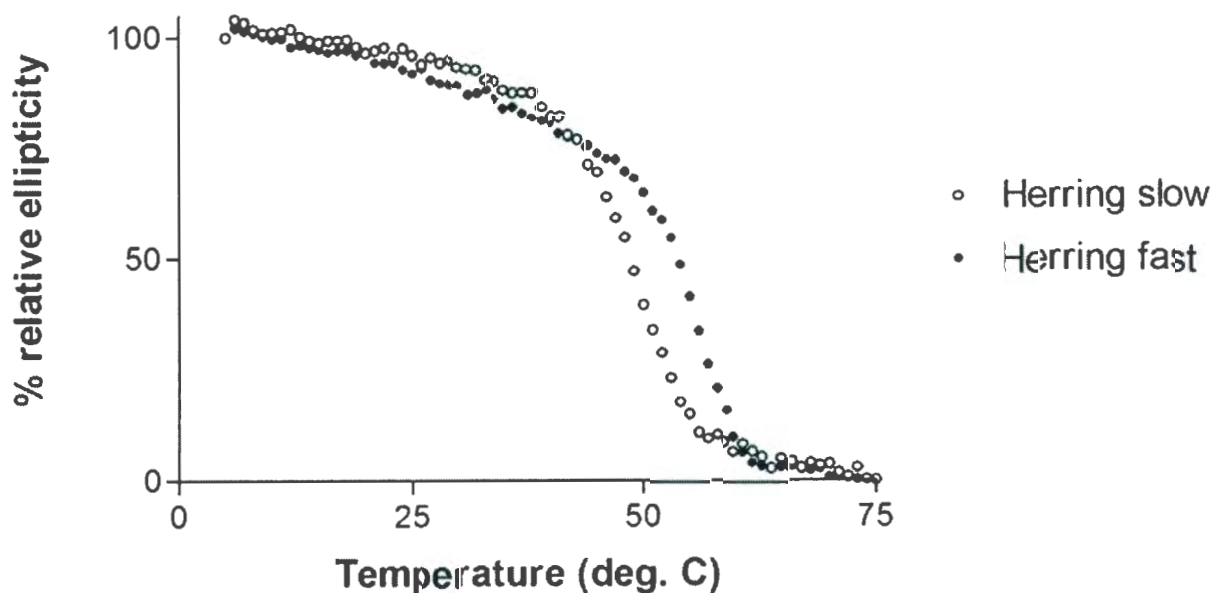
Ellipticity of G-actin ( $\sim 1.5$  mg/mL in 5 mM HEPES, 0.2 mM CaATP, 0.1 mM DTT, 0.01%  $\text{NaN}_3$ , pH 8.00) at 222 nm was monitored constantly over a linear temperature gradient of 5 - 75  $^{\circ}\text{C}$  using a Jasco-810 spectropolarimeter. Heating rate, either 30 or 60  $^{\circ}\text{C}$  per hour. Light path, 0.1 mm. Main graph is a wavelength scan at 5 $^{\circ}\text{C}$  (lower) and 75 $^{\circ}\text{C}$  (upper). Inset is the first differential of the ellipticity change monitored at 222nm over the temperature gradient. Starting ellipticity: -18.9046 mdeg. Ending ellipticity: -11.8646 mdeg.  $T_m$ , 55.26 $^{\circ}\text{C} \pm 0.709^{\circ}\text{C}$ . Experiment repeated at least three times with five separate protein preparations.

Figure 25: Thermally induced unfolding of the slow skeletal actin isoform from Atlantic herring as monitored by far-UV circular dichroism.



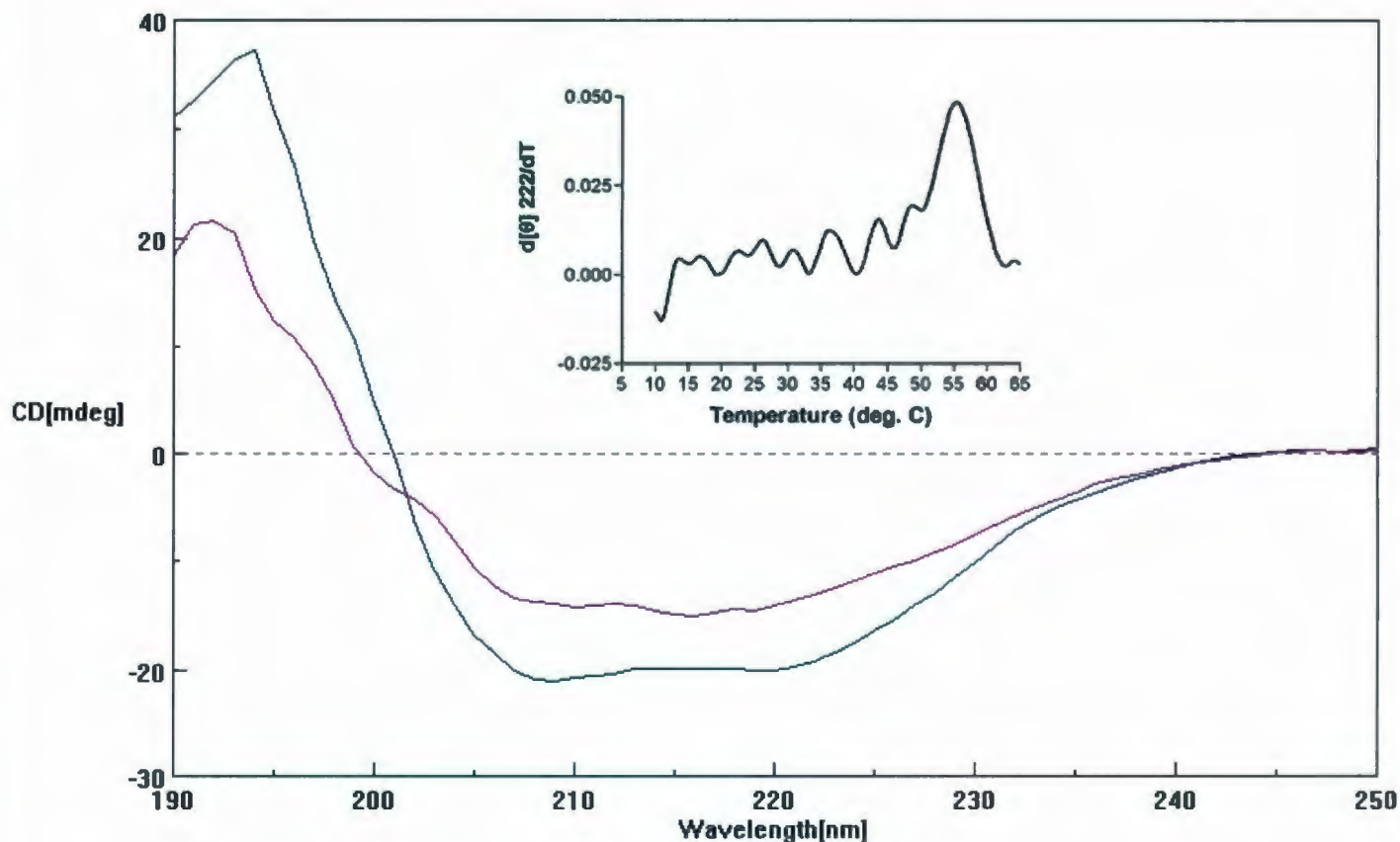
Ellipticity of G-actin ( $\sim 1.5$  mg/mL in 5 mM HEPES, 0.2 mM CaATP, 0.1 mM DTT, 0.01%  $\text{NaN}_3$ , pH 8.00) at 222 nm was monitored constantly over a linear temperature gradient of 5 - 65 °C using a Jasco-810 spectropolarimeter. Heating rate, either 30 or 60 °C per hour. Light path, 0.1 mm. Inset is the first differential of the ellipticity change monitored at 222nm over the temperature gradient. Starting ellipticity: -19.4434 mdeg. Ending ellipticity: -13.3911 mdeg.  $T_m$ , 49.74°C  $\pm$  0.599°C. Experiment repeated at least three times with five separate protein preparations.

Figure 26: Thermally induced unfolding of the skeletal muscle isoforms of actin isolated from the muscles of Atlantic herring plotted as the percent overall change in ellipticity.



Actins were considered to be in their native conformation at 5°C (relative ellipticity - 100%). Heat induced unfolding was considered to be complete at 75°C (relative ellipticity - 0%). Conversion from mdeg was performed using the following formula:  $(1 - [\theta^5 - \theta / \text{total change } \theta]) * 100\%$ . Data taken from Figures 24 and 25.

Figure 27: Thermally induced unfolding of the fast skeletal actin isoform from Atlantic mackerel as monitored by far-UV circular dichroism.



Ellipticity of G-actin (~ 1.5 mg/mL in 5 mM HEPES, 0.2 mM CaATP, 0.1 mM DTT, 0.01% NaN<sub>3</sub>, pH 8.00 at 222 nm was monitored constantly over a linear temperature gradient of 5 - 65 °C using a Jasco-810 spectropolarimeter. Heating rate, either 30 or 60 °C per hour. Light path, 0.1 mm. Inset is the first differential of the ellipticity change monitored at 222nm over the temperature gradient. Starting ellipticity: -19.1414 mdeg. Ending ellipticity: -13.007 mdeg. T<sub>m</sub>, 54.94°C ± 0.688°C. Experiment repeated at least three times with five separate protein preparations.

spectra. To this end, the starting ellipticities of all actin isoforms subjected to this treatment were within 1mdeg at 222 nm, centering at about -19 mdeg at a concentration of ~1.5 mg/ml and a path length of 0.1 mm. The total change in ellipticity when treating actin in this way is about 30%; the remaining 2° structure remains largely intact. Also of importance to note is that monitoring 2° structure at 222 nm focuses on the  $\alpha$ -helical content of the molecule and gives no information as to  $\beta$ -type structure. The wavelength used for monitoring (222 nm) was chosen because it is well known that the 2° structural elements of actin are principally  $\alpha$ -helical, ~45%, while the  $\beta$ -type structure accounts for ~27%; the rest, as actin is a globular protein, consists of turns and random coil [Wu & Yang 1976; Kabsch *et al.* 1990]. Figure 24 is representative of the unfolding of the fast skeletal muscle actin isolated from Atlantic herring over a range of temperature (5-75°C). In the main graph, wavelength scans of the sample at the beginning and end of the heating is presented. Inset is the first derivative of the progress curve at 222 nm, revealing the transition temperature ( $T_m$  - the temperature at which 50% of the protein is unfolded) of the fast skeletal muscle actin to be 55°C. Similarly, Figure 25 shows the thermally induced unfolding (5-65°C) of slow skeletal muscle actin from the same source revealing a transition temperature of 50°C. This 5°C difference

in the Tms of the two skeletal muscle actins found in *clupeiformes* is in stark contrast to the 10°C difference of the Tms of the skeletal muscle actins isolated from *salmonids* (Table 1; to be discussed). A comparison of the relative ellipticities of the two herring actins at 222 nm over the temperature gradient (Figure 26) makes the difference visually easier to ascertain and very clear.

The fast skeletal muscle actin isolated from Atlantic mackerel was subjected to the same treatment (Figure 27). It was expected from the digestion experiments that this actin would be similar to the fast skeletal muscle found in herring. This is indeed the case. A transition temperature of 55°C for the fast skeletal muscle of Atlantic mackerel is noted, further demonstrating that the substitutions present between the mackerel actin and other fast skeletal muscle actins have little or no effect on the 3° structure of the molecule.

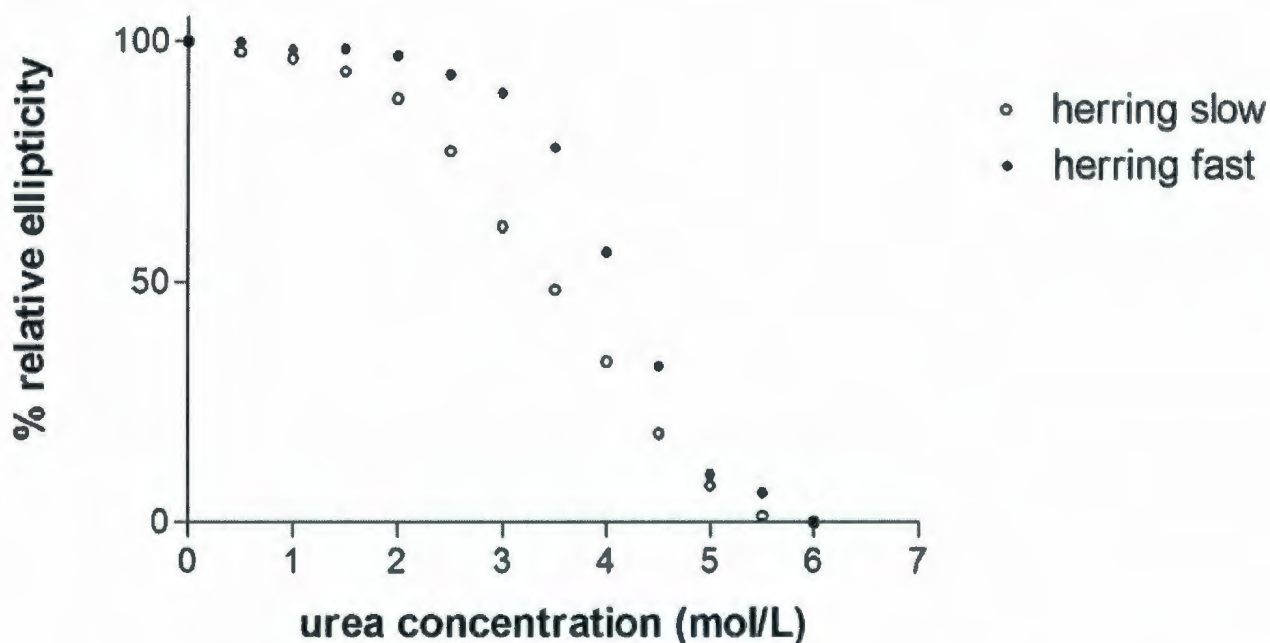
### 3.3.1.2 Chemical unfolding

#### 3.3.1.2.1 Urea induced unfolding

In the next set of experiments urea was be used to induce the unfolding of the various actin isoforms. In this instance the change in ellipticity is in the realm of 75% as opposed to the roughly 30% observed with an increase in temperature. Ellipticity was again recorded at RT at 222 nm while subjecting the actins to varying concentrations of urea. Just as varying the heating rate

was used to ensure equilibrium in the thermal denaturation experiments, these samples were allowed to incubate at RT for 30 minutes with their respective concentration of urea before spectral scans were taken. There was no further change in ellipticity if the samples were allowed longer incubation periods. Fast and slow actin isolated from the skeletal muscle of Atlantic herring yield unfolding midpoints of 4.0 M and 3.5 M, respectively (Figure 28). The slow skeletal muscle actin from herring, once again, exhibits an intermediate nature between the fast and slow skeletal muscle actins found in Atlantic salmon. In the *salmonid* fish, the fast actin transition is at 4.0 M and the slow muscle actin has a transition at 3.0 M [Mudalige et al. 2007]. Figure 12 shows a single amino acid substitution between the slow skeletal muscle actins isolated from these fish; Gln 354 Ala (herr:sal). Taken with the thermal unfolding data, Gln 354 can be concluded to stabilize the slow skeletal muscle actin isolated from Atlantic herring. It must be noted, however, that this stabilization appears to be conditional in nature. This same substitution exists between the fast skeletal muscle actin isoforms of herring and salmon yet the properties of each, when tested in this way, are the same. It is suggested through this that the stabilizing nature of this residue is dependent on the presence of other, destabilizing, substitutions.

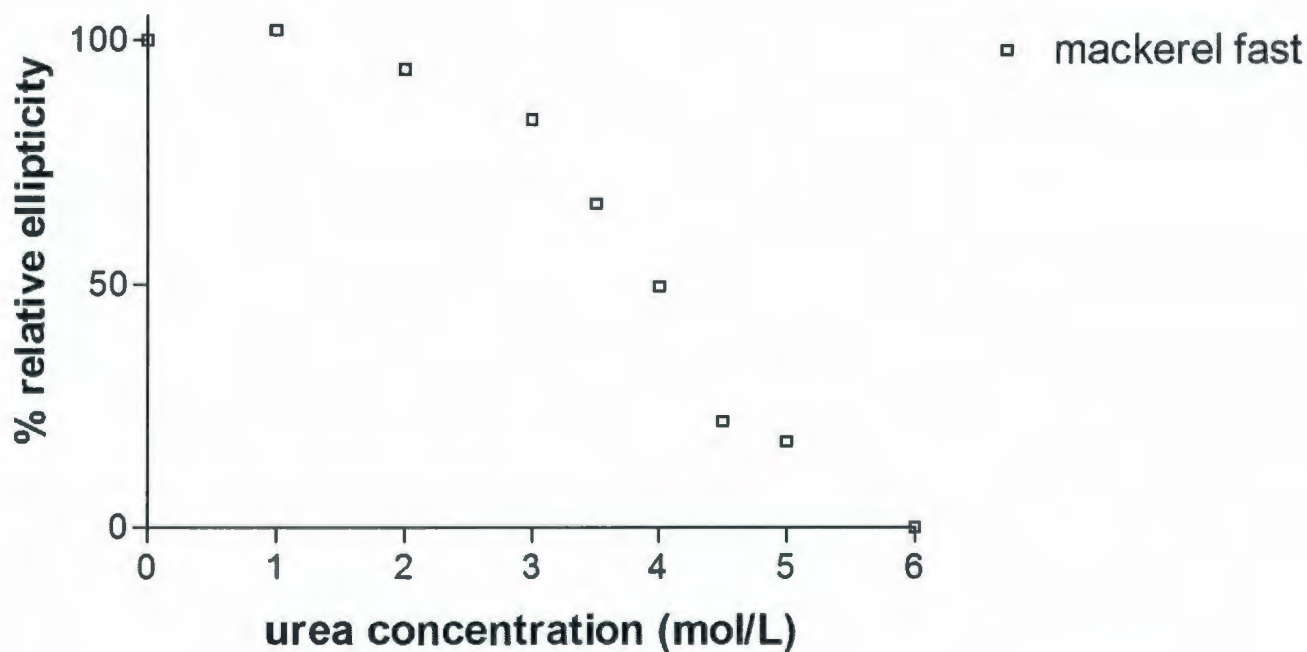
Figure 28: Dependence of relative ellipticity of actin isolated from Atlantic herring on the concentration of urea present.



Ellipticity of G-actin ( $\sim 2$  mg/mL; RT; TRIS buffer; light path, 0.1 mm) at 222 nm was measured using a Jasco-810 spectropolarimeter. [Urea] was increased in increments of 0.5 M using a freshly prepared 8 M stock. Starting ellipticities: fast  $-36.4562$  mdeg, slow  $-35.5392$  mdeg. Ending ellipticities: fast  $-7.7758$  mdeg, slow  $-6.4669$  mdeg. Midpoints of unfolding; herring fast, 4.0 M; herring slow, 3.5 M.

The digestion and thermal unfolding data have indicated that the substitutions present in the fast skeletal muscle actin isolated from mackerel (most notably Ser 155 Ala) have little to no consequence on actin conformation. The results presented in Figures 28 and 29 provide further support for this proposal; demonstrating a mid point of 4.0 M urea, consistent with the other fast skeletal muscle actin isoforms as well as the skeletal muscle actin found in rabbit. For ease of reference, heterogeneous amino acid identities and CD unfolding results of all discussed actin isoforms are summarized in Table 1 along with data pertaining to rabbit skeletal muscle actin.

Figure 29: Dependence of the relative ellipticity of actin isolated from Atlantic mackerel upon concentration of urea present.

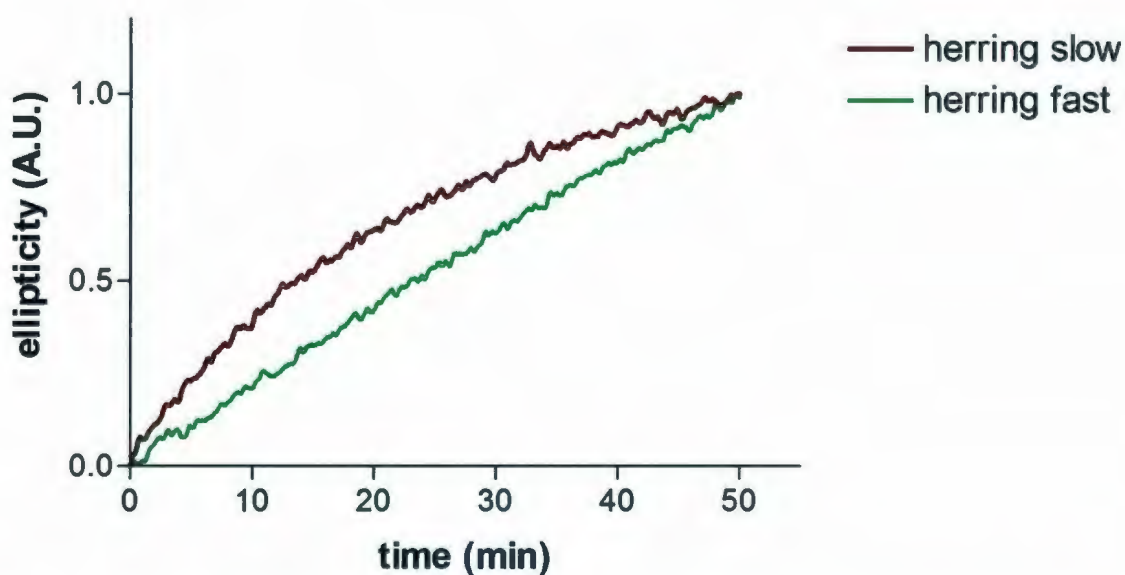


Ellipticity of G-actin (~ 1.5 mg/mL; RT; TRIS buffer; light path, 0.1 mm) at 222 nm was measured using a Jasco-810 spectropolarimeter. [Urea] was increased in increments of 0.5 M using a freshly prepared 8 M stock. Starting ellipticity: -22.4945 mdeg. Ending ellipticity: -6.5057 mdeg. Midpoint of unfolding, 4.0 M.

#### 3.3.1.2.2 EDTA induced unfolding

In some preliminary experiments, CD was used to monitor, at 222 nm, the EDTA induced unfolding of the two actins isolated from the skeletal muscles of Atlantic herring. The cleft of actin binds, in a mutually dependant manner, both divalent cation and ATP [Kabsch *et al.* 1990] that are required for the overall stability of secondary structure. In these experiments exposure to EDTA, a powerful  $\text{Ca}^{2+}$  chelator, was used to probe the stability of this cleft by observing the change in secondary structure of actin over time [Strzelecka-Golaszewska *et al.* 1985]. Actin isolated from the slow skeletal muscle of Atlantic herring, assuming a first order process, unfolds in the presence of EDTA with an observed rate of  $6.5 \times 10^{-4} \text{ sec}^{-1}$  (Figure 30). This compares with unpublished data from the Heeley laboratory pertaining to salmonid slow skeletal muscle actin treated in this way (a rate of  $1.7 \times 10^{-3} \text{ sec}^{-1}$ ). Under the same conditions herring fast skeletal actin exhibited a smaller change in ellipticity and it was not possible to obtain a rate from the progress curve. Nevertheless, these results clearly indicate that the slow skeletal muscle actin isoform is less resistant to the  $\text{Ca}^{2+}$  chelating activity of EDTA. This could be an indication that the slow actin isoform has a lower affinity for  $\text{Ca}^{2+}$ . These data are in full support of the thrombin exposure experiments, which indicate that slow skeletal muscle actin has a 3° conformation similar to EDTA exposed actin.

Figure 30: EDTA induced unfolding of actin isoforms isolated from the fast and slow skeletal muscles of Atlantic herring.

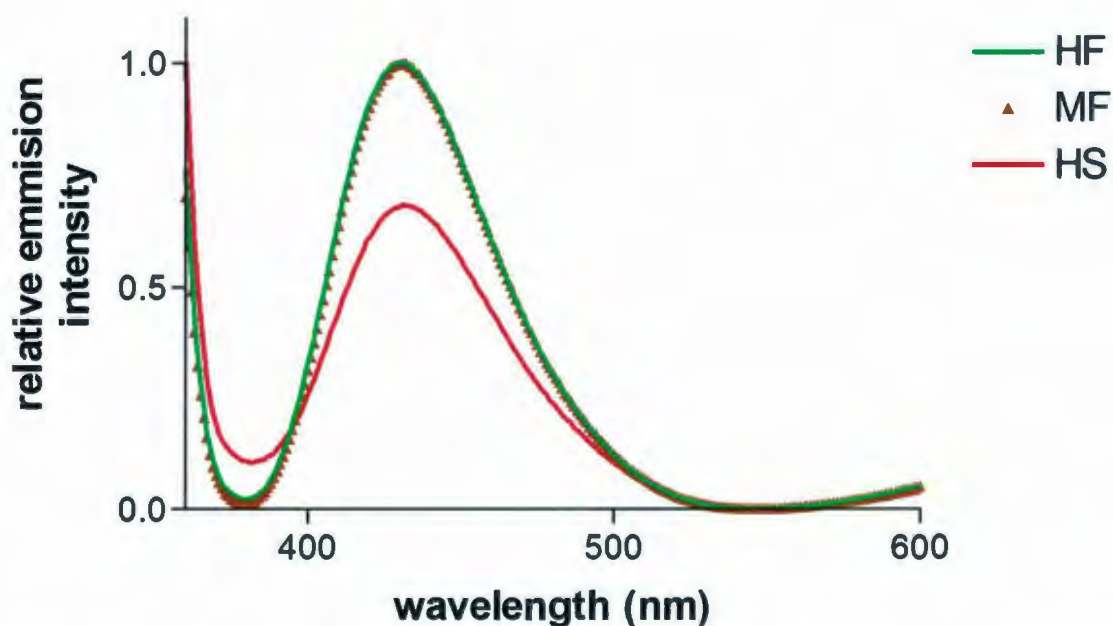


EDTA (0.1 M, pH 8.00) was added to a ~ 1 mg/ml actin solution to a final concentration of 1.0 mM. Temperature was maintained at 37°C by a circulating water bath. 0.2 mm water jacketed cells were used. The ellipticity at 222 nm was constantly monitored by a Jasco-810 spectropolarimeter. Slow skeletal muscle actin rate of unfolding:  $6.5 \times 10^{-4} \text{ sec}^{-1}$ . Data have been normalized and are presented in arbitrary units.

### 3.3.2 Fluorescence spectroscopy

A fluorescent ATP analogue, mant-ATP (a generous gift from Dr. Howard White, Eastern Virginia Medical School) was bound to the three actin isoforms identified in this study as outlined in section 2.17.3. It was chosen as it has been documented that this ATP analogue has a varying emission profile dependent on the polarity of its microenvironment [Hiratsuka 1982]. In these experiments, great care was taken to ensure the protein concentration in each sample was the same. To this end, the concentration of all samples obtained by UV spectroscopy was verified by the staining intensity on SDS PAGE gels before the mant-ATP binding procedure and by UV spectroscopy immediately prior to recording the emission spectra (data not shown). The results of the fluorescence emission are presented in Figure 31. These data confirm that the S155A substitution has no observable effect on the nucleotide binding of the mackerel fast skeletal muscle actin, as the two emission spectra are virtually identical. With regards to the slow skeletal muscle actin isolated from Atlantic herring it can be seen that while there is no horizontal shift in the fluorescence maxima (indicating no change in the polarity of the mant-ATP environment) the intensity of the peak is more than 25% less than that of the two fast skeletal muscle actins. This decreased intensity in the emission profile of the slow skeletal muscle actin isoform indicates that it has a lower affinity for mant-ATP than its fast counterparts while maintaining the hydrophobicity of the binding pocket.

Figure 31: Emission spectra of mant-ATP bound to various skeletal muscle actin isoforms.



~ 2 mg/ml solution of Ca-G-actin bound to mant-ATP was excited at 340 nm and emission was measured at 440 nm at RT. A wavelength scan from 360 nm to 600 nm was carried out using a Photon Technology International (PTI) model QM-2001-6 QuantaMaster emission spectrometer equipped with a Hamamatsu R-928 photomultiplier tube housed in a Products for Research Inc. PC177CE refrigerated chamber. All emission spectra were collected with a 1 mm slit width, 90° to excitation source and are uncorrected for instrument response.

## Chapter 4

### Conclusions & Future directions

#### 4.1 Conclusions

The work documented in this thesis is the first evidence that slow skeletal muscle actin is conserved through *teleost* evolution as a *bona fide* actin isoform. Through nucleotide sequencing, three inferred actin sequences were obtained: the fast and slow skeletal muscle actins found in Atlantic herring, a *cupeloforme*, (*Clupea harengus*; Acc# GQ455648, fast; Acc# EF495203, slow) and the fast skeletal muscle actin isoform found in Atlantic mackerel, a *perciforme* (*Scomber scombrus*; Acc# EF607093). Comparison of the slow skeletal muscle actin with one previously identified in Brown trout, a distantly related *salmonid* (*Salmo trutta*; Acc# AF267496) [Mudalige et al. 2007], revealed a single, inferred and non-conservative, amino acid substitution Q 354 A (herr:sal). Comparison of the fast skeletal muscle actin isoforms from Atlantic herring and Atlantic salmon, another *salmonid*, (*Salmo salar*, Acc# AF304406 [Mudalige et al. 2007]) follows the same trend with two inferred substitutions: Q 354 A and S 160 T (herr:sal). Interestingly, the identity of residue 354 is not unique to isotype but rather species; actin isoforms identified from *cupeloformes* have glutamine at 354 while alanine is found at this position in *salmonid* fish [Mudalige et al. 2007]. A comparison of the slow and fast skeletal muscle actin isoforms identified in Atlantic herring reveals 13 substitutions,

six that are non-conservative in nature. This is a record number of substitutions for a vertebrate skeletal muscle actin. The heterogeneity is considered real, as opposed to an artefact of cloning and sequencing, for the following reasons. First, the inferred sequence of herring slow actin is, with the exception of a single amino acid, identical to that of salmonid slow actin [Mudalige et al 2007]. It is significant that the two respective cDNA libraries were constructed by different members of the Heeley lab and that each cDNA was sequenced on both strands. Further, the predicted charge substitution (residue 360, Asp in slow, Gln in fast) is consistent with the observations derived from alkaline urea PAGE. The possibility that this substitution, as well as others, occurs at another position in the sequence can not be categorically ruled out, but against this the author again draws attention to the virtual identity between the two identified slow muscle actins.

Urea PAGE was also used as a method to screen for the presence of a charge substituted actin in the skeletal muscle of the following fish: Rainbow smelt, *Osmerus mordax*; Atlantic mackerel, *Scomber scombrus*; Atlantic halibut, *Hippoglossus hippoglossus*; tilapia, hagfish and lamprey (final three species unknown). With the exception of mackerel and smelt, these fish appear to utilize actins with the same net charge in their fast and slow skeletal muscle. This does not, however, preclude the possibility that these fish employ unique actins in their different skeletal

muscles. While the data in Figure 19 can be taken as an indication of skeletal muscle actin homogeneity, more sequencing must be performed. With regards to Rainbow smelt and Atlantic mackerel, two bands can be clearly seen in the slow skeletal muscle sample (Figure 18) indicating the slow skeletal muscle of these fish does not employ a single isoactin. While the data are not conclusive on this matter, it is unlikely in the case of Atlantic mackerel that this banding pattern is due to contamination by intermediate (pink) or fast muscle. While this could indeed be the case concerning Rainbow smelt, given the small nature of the species and the minute quantities of slow skeletal muscle isolated from the few available specimens; preparations of slow skeletal muscle from mackerel were carried out from much larger quantities of acetone powder. Minor contamination with intermediate skeletal muscle cannot account for the observed band intensity, and therefore presence of a second actin isoform. Taken with the fact that the fast skeletal muscle actin sequenced from Atlantic mackerel was obtained from a slow skeletal muscle library, it is concluded that the slow skeletal muscles of Atlantic mackerel contain two distinct actin isoforms.

Solution studies [Schwyter *et al.* 1989, Strzelecka-Golaszewska *et al.* 1992, Crosbie *et al.* 1994, Vahdat *et al.* 1995, Ooi & Mihashi 1996] have previously reported that changes in the nucleotide binding pocket (ATP/ADP bound in addition to analogues of these

nucleotides or a change in divalent metal cation) have an impact on the conformation of the molecule at distant sites; notably the enzymatic cleavage of the DNaseI binding loop (subtilisin) and the C-terminus (Arg 372/Lys 373 - trypsin). These regions can be thought of as a 'two-way-corridor': it has been demonstrated that changes to the C-terminus (the covalent attachment of a reporter probe or removal of two or three C-terminal residues) have an impact on nucleotide binding [Crosbie *et al* 1994]. Considering the sequence data in conjunction with established literature, two substitutions were considered as possible 'culprits' for the observed instability of the slow skeletal muscle actin isoform. Ser 155 Ala (fast:slow) and Gln 360 Asp (fast:slow) are located near the nucleotide binding pocket and C-terminus of actin, respectively. Again, for ease of reference the identity of heterogeneous residues as well as CD data for all actins used are presented in Table 1.

Obtaining the sequence of the fast skeletal muscle actin isolated from Atlantic mackerel allowed the non-conservative substitution S 155 A (fast:slow) to be ruled out as a contributor to the instability. This actin has, like slow actin, alanine at residue 155 and, unlike slow actin, glutamine at position 360. In spite of this, mackerel fast skeletal muscle actin responds as the other fast actin isoforms when exposed to subtilisin and thrombin, has the same melting temperature as the two fast skeletal muscle actins (55°C) and unfolds in the presence of urea

with a midpoint at the same concentration (4 M). Indeed, when examining the published crystal structures of actin it can be seen that serine 155 is pointing away from the nucleotide binding pocket, unable to contribute to nucleotide and divalent metal ion binding. This is supported further when observing fluorescence data presented in Figure 31 which show virtually identical emission spectra for the fast skeletal muscle actin isoforms isolated from Atlantic mackerel and Atlantic herring.

In support of a strong contribution of the C-terminal substitution to the observed instability is the curious case of the slow skeletal muscle actin isolated from Atlantic herring. While it is less stable than its fast muscle counterpart, it is appreciably more stable than the slow skeletal muscle actin isolated from Atlantic salmon (Tms: 45°C sal slow, 50°C herr slow, 55°C sal/herr fast; urea unfolding midpoint 3.0 M sal slow, 3.5 M herr slow, 4M sal/herr fast). The sole substitution between the two slow actins, residue 354, glutamine in herring skeletal muscle actins and alanine in salmonid skeletal muscle actins, must be the cause of this increased stability. Crystal structures show that residues 354 and 360 are 11 angstroms apart from each other, too far for a direct interaction (Figure 15). One then would have to infer that the presence of the larger side chain of glutamine is, somehow, stabilising this region of actin in some other way.

Limited exposure of the two skeletal muscle actin isoforms isolated from Atlantic herring to proteolytic enzymes demonstrates that slow skeletal muscle actin has a lower resistance to subtilisin (Figures 20 & 22) and thrombin (Figure 23). It can be unarguably stated that slow skeletal muscle actin is more accessible to protease cleavage and, therefore, has adopted a more open 3° structure compared to the fast skeletal muscle actin. This is supported not only by previous work done in the laboratory on the fast and slow skeletal muscles of Atlantic salmon, demonstrating altered cleavage patterns when V8 protease is employed [unpublished data from the Heeley laboratory] but by the circular dichroism data presented in this thesis (Figures 26 & 28).

The subtilisin digestion of the herring actins, while both highly susceptible to proteolysis, results in unique banding patterns for each isoactin. Most notably is the 36 kDa C-terminal peptide resulting from cleavage at M 47/G 48 in the DNaseI binding loop (indicated by arrows in Figure 20). This peptide accumulates when derived from fast skeletal muscle actin while maintaining a lower intensity band when produced from slow skeletal muscle actin.

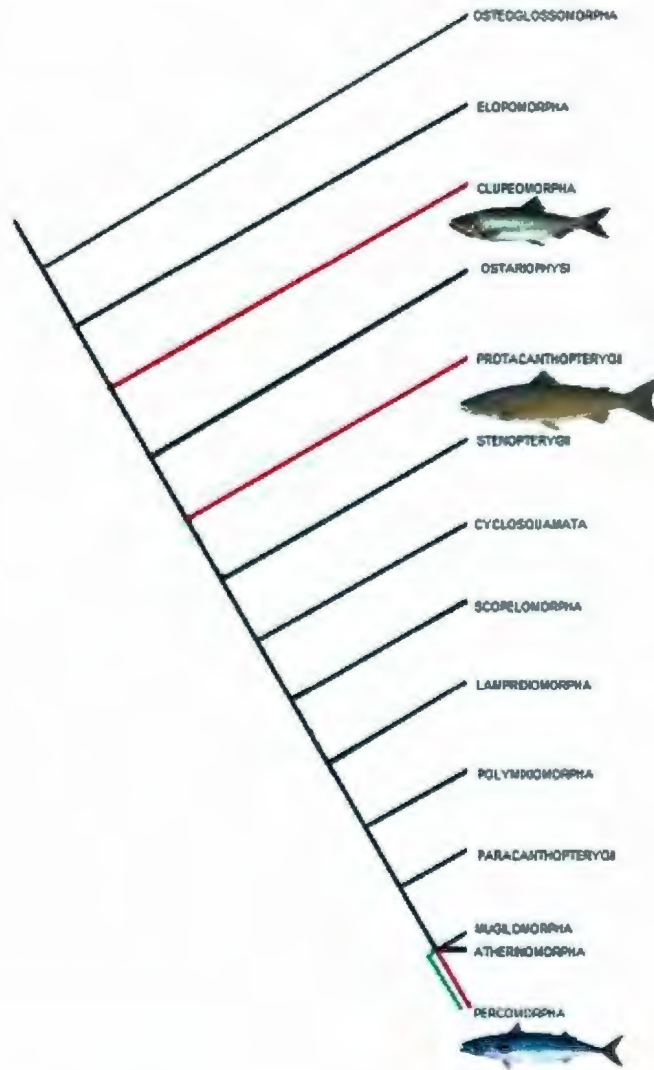
The work by Muszbek and Laki on the thrombin digestion of actin showed that the addition of EDTA to Ca<sup>2+</sup> bound G-actin facilitates its digestion whereas in the absence of EDTA there was no

detectable proteolysis [Muszbek & Laki 1974]. This clearly demonstrates that the binding of  $\text{Ca}^{2+}$  affects the 3° structure in such a way as to protect actin from cleavage by thrombin. Figure 23 shows the digestion of slow skeletal muscle actin isolated from Atlantic herring in the absence of EDTA while the fast skeletal muscle actin remains intact. It is conceivable, then, that the 3° structure of slow skeletal muscle actin is somewhat like EDTA-exposed actin in the paper presented by Muszbek and Laki. When considered with the work of Mudalige *et al.* demonstrating slow skeletal muscle actin isolated from Atlantic salmon to have a higher ATP exchange rate than its fast counterpart, the observed instability of the slow skeletal muscle actins could be explained by a weaker affinity for  $\text{Ca}^{2+}$  and, by extension, nucleotide. Figure 31 clearly demonstrates through the use of a fluorescent ATP analogue that slow skeletal muscle actin does, indeed, have a lower nucleotide affinity than its fast skeletal muscle counterparts. Divalent cation and nucleotide are dependent on each other for binding. That is, without one, the 3° structure of actin can be lost. It is impossible at this point to say with certainty if the data reflects a lower nucleotide affinity due to a lower affinity for divalent cation or *vice versa*.

## 4.2 Phylogenetic analysis

A rudimentary phylogenetic tree of teleost fish has been constructed and is presented in Figure 32. Lamprey and hagfish are the two most primitive fish known on our planet (Indeed, there is debate as to whether they even are fish at all). Results from the urea PAGE of lamprey and hagfish actin gave no indication that either 'fish' has an actin expressed solely in their slow skeletal muscles. It is demonstrated that in earlier teleost fish, *cupeloformes* and *salmonids*, the identified slow skeletal muscle actin appears to be the only actin isoform utilized in slow skeletal muscles. At some point during the evolution of these muscles, as noted in the more 'advanced' *perciformes*, it appears that teleost fish began to use both the fast and slow skeletal muscle actins in their slow skeletal muscle. This may be, however, a premature conclusion, as other species studied herein appear to utilise the same skeletal muscle actin in all skeletal muscles, notably tilapia, another *perciform* and Atlantic halibut, a *pleuronectiforme*, which is a suborder of *perciforms*. Neither species gave any indication of the charge variant documented herein.

Figure 32: Phylogenetic analysis of teleost fish for the presence of slow skeletal muscle actin.



Tree adapted from Nelson, 1994. Red bars indicate orders where slow skeletal muscle actin has been found. Green bars indicate the absence of a charge variant actin in the slow skeletal muscle of those fish.

While it was initially tempting to speculate that the slow skeletal muscle of teleost fish is moving towards a greater stability of the actin it employs, this is not in line with the phylogeny. Nor can the opposite be said, as there is currently no sequence of a 'higher' teleost slow skeletal muscle actin or definitive proof that these 'higher' teleosts utilise two actin isoforms in their slow skeletal muscles. Of these 'higher' teleosts only Atlantic mackerel and Rainbow smelt have shown any indication of a slow skeletal muscle actin. This gives some indication as to the functional role of this new actin isoform. Only species known to travel over distances, for food or spawning, have demonstrated a charge substituted actin in their skeletal muscles.

It is interesting to note in the phylogenetic tree of teleost fish that *cupeloformes* (Atlantic herring) are 'older' fish than the *salmonids* (Atlantic salmon). Why then is the slow skeletal muscle in Atlantic herring at an intermediate level of stability between the fast and slow skeletal muscle actins of *salmonid* fish? As mentioned in the introduction, slow skeletal muscle is used primarily for sustained swimming activities. The possibility that slow skeletal muscle actin is favored for these activities can be further examined with a continued sequencing effort. The evolutionary significance of the intermediate stability of the herring slow skeletal muscle actin remains elusive. Physiologically speaking, while unknown, the simplest

and, therefore, most likely explanation for slow skeletal muscle actin is thin (possibly thick) filament allostery. Clues to the differing properties of the two identified slow skeletal muscle actins may lie with the other thin filament proteins found in these fish. Muscle type specific isoforms for every other contractile protein have been well documented in the literature [Lehrer & Geeves 1998]; it would seem that now, after 67 years, skeletal muscle actin has, arguably, joined their ranks.

### 4.3 Future directions

- More skeletal muscle actin sequences need to be obtained. Notably, the slow skeletal muscle actin found in Atlantic mackerel and Rainbow smelt. The phylogenetic tree must be expanded to answer evolutionary questions.
  
- DNaseI binding experiments with the various actin isoforms would demonstrate any differences in the conformation of the DNaseI binding loop.
  
- Polymerization rates can be determined for the various actin isoforms. This would give informative and physiologically relevant information about the functionality of slow skeletal muscle actin.
  
- Thin filament reconstruction can be done *in vitro* using the various actin isoforms with a view to analysing the binding interactions between the various components of the thin filament (actin and tropomyosin, actin and troponin in the presence and absence of  $\text{Ca}^{2+}$ ).
  
- Site directed mutagenesis of rabbit skeletal muscle actin can be performed to examine the identified substitutions alone and partnered with others. This would clarify the relative

contributions of the 13 replacements found in slow skeletal muscle actin.

## REFERENCES

Alonso, S., Minty, A., Bourlet, Y., Buckingham, M. (1986) Comparison of three actin-coding sequences in the mouse; evolutionary relationships between the actin genes of warm-blooded vertebrates. *J. Mol. Evol.* **23**, 11

Aidley, D.J. (1998) *The physiology of excitable cells*, 3<sup>rd</sup> edition. Cambridge University Press.

Bailey, K. (1948) Tropomyosin; a new asymmetric protein component of the muscle fibril. *Biochem. J.* **43**, 271

Bailey, K. (1946) Tropomyosin: a New Asymmetric Protein Component of Muscle. *Nature.* **157**, 368

Belmont, L.D., Patterson, G.M., Drubin, D.G. (1999) New actin mutants allow further characterization of the nucleotide binding cleft and drug binding sites. *J. Cell. Sci.* **112**, 1325

Berg, J.S., Powell, B.C., Cheney, R.E. (2001) A millennial myosin census. *Mol. Biol. Cell.* **12**, 780

Betcher-Lange, S., Lehrer, S.S. (1978) Pyrene excimer fluorescence in rabbit skeletal alphaalphanatropomyosin labeled

with N-(1-pyrene) maleimide. A probe of sulfhydryl proximity and local chain separation. *J. Biol. Chem.* **253**, 3757

Biesiadecki, B., Chong, S.M., Nosek, T.M., Jin, J.P. (2007) Troponin T core structure and the regulatory NH2-terminal variable region. *Biochemistry (N.Y.)*. **46**, 1368

Bork, P., Sander, C., Valencia, A. (1992) An ATPase domain common to prokaryotic cell cycle proteins, sugar kinases, actin, and hsp70 heat shock proteins. *Proc. Nat. Acad. Sci. U.S.A.* **89**, 7290

Caspar, D.L., Cohen, C., Longley, W. (1969) Tropomyosin: crystal structure, polymorphism and molecular interactions. *J. Mol. Biol.* **41**, 87

Chang, C.T., Wu, C.S.C., Yang, J.T. (1978) Circular dichroic analysis of protein conformation: inclusion of the beta-turns. *Anal. Biochem.* **91**, 13

Chang, K.S., Zimmer Jr, W.E., Bergsma, D.J., Dodgson, J.B., Schwartz, R.J. (1984) Isolation and characterization of six different chicken actin genes. *Mol. Cell. Biol.* **4**, 2498

Collins, J.H., and Elzinga, M. (1975) The primary structure of actin from rabbit skeletal muscle. Completion and analysis of the amino acid sequence. *J. Biol. Chem.* **250**, 5915

Collins, J.H., Potter, J.D., Horn, M.J., Wilshire, G., Jackman, N. (1973) The amino acid sequence of rabbit skeletal muscle troponin C: gene replication and homology with calcium-binding proteins from carp and hake muscle. *FEBS Lett.* **36**, 268

Collins, J.H., Greaser, M.L., Potter, J.D., Horn, M.J. (1977) Determination of the amino acid sequence of troponin C from rabbit skeletal muscle. *J. Biol. Chem.* **252**, 6456-62

Conibear, P.B., Bagshaw, C.R., Fajer, P.G., Kovács, M., Málnási-Csizmadia, A. (2003) Myosin cleft movement and its coupling to actomyosin dissociation. *Nature Struct. Mol. Bio.* **10**, 831

Cooper, J.A., Pollard, T.D. (1982) Methods to measure actin polymerization. *Meth. Enzymol.* **85**, 182

Cooper, J.A., Walker, S.B., Pollard, T.D. (1983) Pyrene actin: documentation of the validity of a sensitive assay for actin polymerization. *J. Muscle Res. Cell Motil.* **4**, 253

de Couet, H.G., Mazander, K.D., Gröschel-Stewart, U. (1980) A study of invertebrate actins by isoelectric focusing and immunodiffusion. *Cellular and Molecular Life Sciences.* **36**, 404

De La Cruz, E.M., Ostap, E.M. (2004) Relating biochemistry and function in the myosin superfamily. *Curr. Opin. Cell Biol.* **16**, 61

De La Cruz, E.M., Pollard, T.D. (1995) Nucleotide-free actin: stabilization by sucrose and nucleotide binding kinetics. *Biochemistry (N.Y.)*. **34**, 5452

DeNofrio, D., Hooek, T.C., Herman, I.M. (1989) Functional sorting of actin isoforms in microvascular pericytes. *J. Cell Biol.* **109**, 191

Ebashi, S. (1963) Third Component Participating in the Super precipitation of natural actomyosin. *Nature*. **200**, 1010

Ebashi, S., Kodama, A. (2008) A new protein factor promoting aggregation of tropomyosin. *Biochem. Biophys. Res. Commun.* **369**, 13

Ebashi, S., Kodama, A., Ebashi, F. (1968) Troponin. I. Preparation and physiological function. *J. Biochem.* **64**, 465

Elzinga, M., Collins, J.H., Kuehl, W.M., Adelstein, R.S. (1973) Complete amino-acid sequence of actin of rabbit skeletal muscle. *Proc. Natl. Acad. Sci .U.S.A.* **70**, 2687

Estes, J., Selden, L.A., Kinosian, H.J., Gershman, L.C. (1992) Tightly-bound divalent cation of actin. *J. Muscle Res. Cell Motil.* **13**, 272

Fabiato, A., Fabiato, F. (1975) Contractions induced by a calcium-triggered release of calcium from the sarcoplasmic reticulum of single skinned cardiac cells. *J. Physiol. (Lond.)*. **249**, 469

Farah, C.S., Reinach, F.C. (1995) The troponin complex and regulation of muscle contraction. *The FASEB journal*. **9**, 755

Feng, L., Kim, E., Lee, W.H., Miller, C.J., Kuang, B. and Reisler, E. (1997) Fluorescence probing of yeast actin subdomain 3/4 hydrophobic loop 262-274. Actin-actin and actin-myosin interactions in actin filaments. *J. Biol. Chem.* **272**, 16829

Filatov, V.L., Katrukha, A.G., Bulargina, T.V., Gusev, N.B. (1999) Troponin: structure, properties, and mechanism of functioning. *Biochemistry (Moscow)*. **64**, 969

Flaherty, K.M., McKay, D.B., Kabsch, W. and Holmes, K.C. (1991) Similarity of the three-dimensional structures of actin and the ATPase fragment of a 70-kDa heat shock cognate protein. *Proc. Natl. Acad. Sci. U.S.A.* **88**, 5041

Flück, M., and Hoppeler, H. (2003) Molecular basis of skeletal muscle plasticity--from gene to form and function. *Rev. Physiol. Biochem. Pharmacol.* **146**, 159

Gabbiani, G., Schmid, E., Winter, S., Chaponnier, De Chastonay, C., Vandekerckhove, J., Weber, K., Werner, W. (1981) Vascular smooth muscle cells differ from other smooth muscle cells: predominance of vimentin filaments and a specific alpha-type actin. *Proc. Natl. Acad. Sci. U.S.A.* **78**, 298

Geeves, M.A., Holmes, K.C. (1999) Structural mechanism of muscle contraction. *Annu .Rev. Biochem.* **68**, 687

Gerson, J.H., Kim, E., Muhlrads, A. and Reisler, E. (2001) Tropomyosin-troponin regulation of actin does not involve subdomain 2 motions. *J. Biol. Chem.* **276**, 18442

Gillis, T., Marshall, C.R., Tibbits, G.F. (2007) Functional and evolutionary relationships of troponin C. *Physiological Genomics.* **32**, 16

Giulian, G.G., Moss, R.L., Greaser, M. (1984) Analytical isoelectric focusing using a high-voltage vertical slab polyacrylamide gel system. *Anal. Biochem.* **142**, 421

Goldschmidt-Clermont, P.J., Furman, M.I., Wachsstock, D., Safer, D., Nachmias, V.T., Pollard, T.D. (1992) The control of actin nucleotide exchange by thymosin beta 4 and profilin. A potential regulatory mechanism for actin polymerization in cells. *Mol. Biol. Cell.* **3**, 1015

Gomes, A.V, Potter, J.D., Szczesna-Cordary, D. (2002) The role of troponins in muscle contraction. *IUBMB Life*. **54**, 323

Gordon, A.M., Homsher, E., Regnier, M. (2000) Regulation of contraction in striated muscle. *Physiol. Rev.* **80**, 853

Graceffa, P., Lehrer, S.S. (1980) The excimer fluorescence of pyrene-labeled tropomyosin. A probe of conformational dynamics. *J. Biol. Chem.* **255**, 11296

Grand, R.J., Wilkinson, J.M. (1976) The amino acid sequence of rabbit cardiac troponin I. *Biochem. J.* **159**, 633

Greaser, M.L., and Gergely, J. (1971) Reconstitution of troponin activity from three protein components. *J. Biol. Chem.* **246**, 4226

Greaser, M.L., and Gergely, J. (1973) Purification and properties of the components from troponin. *J. Biol. Chem.* **248**, 2125

Greenfield, N.J., Huang, Y.J., Swapna, G.V.T., Bhattacharya, A., Rapp, B., Singh, A., Montelione, G.T., Hitchcock-DeGregori, S.E. (2006) Solution NMR structure of the junction between tropomyosin molecules: implications for actin binding and regulation. *J. Mol. Biol.* **364**, 80

Harford, J., Squire, J. (1986) " Crystalline" myosin cross-bridge array in relaxed bony fish muscle. Low-angle x-ray diffraction from plaice fin muscle and its interpretation. *Biophys. J.* **50**, 145

Hartshorne, D.J., Driezen, P. (1972) Studies on the subunit composition of troponin. *Cold Spring Harbor Symp. Quant. Biol.* **37**, 225

Hartshorne, D.J., Mueller, H. (1968) Fractionation of troponin into two distinct proteins. *Biochem. Biophys. Res. Commun.* **31**, 647

Head, J.F., Perry, S.V. (1974) The interaction of the calcium-binding protein (troponin C) with bivalent cations and the inhibitory protein (troponin I). *Biochem. J.* **137**, 145

Heeley, D.H., Golosinska, K., Smillie, L.B. (1987) The Effects of Troponin T Fragments T 1 and T2 on the Binding of Nonpolymerizable Tropomyosin to F-actin in the Presence and Absence of Troponin I and Troponin C. *J. Biol. Chem.* **262**, 9971

Heintz, D., Faulstich, H. (1996) Cross-Link Between cys 374 and cys 10 of Actin Abolishes Polymerizability and Allows Study of

the Properties of the F-actin monomer. *Biochemistry (N.Y.)*. **35**,  
258

Helper, D.J., Lash, J.A., Hathaway, D.R. (1988) Distribution of  
isoelectric variants of the 17,000-dalton myosin light chain in  
mammalian smooth muscle. *J. Biol. Chem.* **263**, 15748

Herman, I.M. (1993) Actin isoforms. *Curr. Opin. Cell Biol.* **5**, 48

Herzberg, O., James, M.N. (1988) Refined crystal structure of  
troponin C from turkey skeletal muscle at 2.0 Å resolution. *J.*  
*Mol. Biol.* **203**, 761

Hiratsuka, T. (1983) New ribose-modified fluorescent analogs of  
adenine and guanine nucleotides available as substrates for  
various enzymes. *Biochim. Biophys. Acta.* **742**, 496

Hoffman, R.M.B., Blumenschein, T.M.A., Sykes, B.D. (2006) An  
interplay between protein disorder and structure confers the Ca<sup>2+</sup>  
regulation of striated muscle. *J. Mol. Biol.* **361**, 625

Holmes, K.C. (1996) Muscle proteins-their actions and  
interactions. *Curr. Opin. Struct. Biol.* **6**, 781

Holmes, K.C., Geeves, M.A. (2000) The structural basis of muscle  
contraction. *Phil. Trans. Royal Soc. B: Biol. Sci.* **355**, 419

Holmes, K.C, Popp, D., Gebhard, W., Kabsch, W. (1990) Atomic model of the actin filament. *Nature*. **347**, 44

Houdusse, A., Kalabokis, V.N., Himmel, D., Szent-Györgyi, A.G., Cohen, C. (1998) Atomic Structure of Scallop Myosin Subfragment S1 Complexed with MgADP. *Cell*. **97**, 459

Houdusse, A., Szent-Györgyi, A.G., Cohen, C. (2000) Three conformational states of scallop myosin S1. *Proc. Nat. Acad. Sci. U.S.A.* **97**, 11238

Huang, X., Pi, Y., Lee, K.J., Henkel, A.S., Gregg, R.G., Powers, P.A., Walker, J.W. (1999) Cardiac troponin I gene knockout: a mouse model of myocardial troponin I deficiency. *Circ. Res.* **84**, 1

Hurley, J.H. (1996) The sugar kinase/heat shock protein 70/actin superfamily: implications of conserved structure for mechanism. *Annu. Rev. Biophys. Biomol. Struct.* **25**, 137

Huszar, G., Elzinga, M. (1971) Amino acid sequence around the single 3-methylhistidine residue in rabbit skeletal muscle myosin. *Biochemistry (N.Y.)*. **10**, 229

Huxley, A.F., Simmons, R.M. (1971) Proposed mechanism of force generation in striated muscle. *Nature*. **233**, 533

Huxley, H.E. (1969) The mechanism of muscular contraction. *Science (New York, N.Y.)*. **164**, 1356

Ikemoto, N. (1974) The calcium binding sites involved in the regulation of the purified adenosine triphosphatase of the sarcoplasmic reticulum. *J. Biol. Chem.* **249**, 649

Ikemoto, N., Nagy, B., Bhatnagar, G.M., Gergely, J. (1974) Studies on a metal-binding protein of the sarcoplasmic reticulum. *J. Biol. Chem.* **249**, 2357

Johnson, F., Smillie, L.B. (1975) Rabbit skeletal alpha-tropomyosin chains are in register. *Biochem. Biophys. Res. Commun.* **64**, 1316

Johnson, K.A., Taylor, E.W. (1978) Intermediate states of subfragment 1 and actosubfragment 1 ATPase: reevaluation of the mechanism. *Biochemistry (N.Y.)*. **17**, 3432

Kabsch, W., Holmes, K.C. (1995) The actin fold. *The FASEB journal*. **9**, 167

Kabsch, W., Vandekerckhove, J. (1992) Structure and function of actin. *Annu. Rev. Biophys. Biomol. Struct.* **21**, 49

Kabsch, W., Mannherz, H.G., Suck, D., Pai, E.F., Holmes, K.C.  
(1990) Atomic structure of the actin: DNase I complex. *Nature*.  
**347**, 37

Karn, J., Brenner, S., Barnett, L. (1983) Protein structural domains in the *Caenorhabditis elegans* unc-54 myosin heavy chain gene are not separated by introns. *Proc. Natl. Acad. Sci.U.S.A.*  
**80**, 4253

Kashina, A.S. (2006) Differential arginylation of actin isoforms: the mystery of the actin N-terminus. *Trends Cell Biol.* **16**, 610

Khaitlina, S.Y. (2007) Mechanisms of spatial segregation of actin isoforms. *Cell and Tissue Biology.* **1**, 293

Khaitlina, S.Y., Strzelecka-Gołaszewska, H. (2002) Role of the DNase-I-binding loop in dynamic properties of actin filament. *Biophys. J.* **82**, 321

Khaitlina, S.Y., Antropovaa, C., Kuznetsovaa, I., Turoverova, K., Collins, J.H. (1999) Correlation between Polymerizability and Conformation in Scallop  $\beta$ -Like Actin and Rabbit Skeletal Muscle  $\alpha$ -Actin. *Arch. Biochem. Biophys.* **368**, 105

Kim, E., Motokia, M., Seguroa, K., Muhlrada, A., Reisler, E.  
(1995) Conformational changes in subdomain 2 of G-actin:

fluorescence probing by dansyl ethylenediamine attached to Gln-41. *Biophys. J.* **69**, 2024

Kim, E., Wriggers, W., Phillips, M., Kokabil, K., Rubenstein, P.A., Reisler, E. (2000) Cross-linking constraints on F-actin structure. *J. Mol. Biol.* **299**, 421

Kretsinger, R.H., Barry, C.D. (1975) The predicted structure of the calcium-binding component of troponin. *Biochim. Biophys. Acta.* **405**, 40

Leavis, P.C., Rosenfeld, S.S., Gergely, J., Grabarek, Z., Drabikowski, W. (1978) Proteolytic fragments of troponin C. Localization of high and low affinity Ca<sup>2</sup> binding sites and interactions with troponin I and troponin T. *J. Biol. Chem.* **253**, 5452

LeBlanc, P., Gillis, T.E., Gerrits, M.F., Ballantyne, J.S. (1995) Metabolic organization of liver and somatic muscle of landlocked sea lamprey, *Petromyzon marinus*, during the spawning migration. *Canadian Journal of Zoology / Revue canadienne de zoologie.* **73**, 916

Lees-Miller, J.P., Helfman, D.M. (1991) The molecular basis for tropomyosin isoform diversity. *Bioessays.* **13**, 429

Lehman, W., Hatch, V., Korman, V., Rosol, M., Thomas, L., Maytum, R., Geeves, M.A., Van Eyk, J.E., Tobacman, L.S., Craig, R. (2000) Tropomyosin and actin isoforms modulate the localization of tropomyosin strands on actin filaments. *J. Mol. Biol.* **302**, 593

Lehrer, S.S. (1994) The regulatory switch of the muscle thin filament: Ca<sup>2+</sup> or myosin heads? *J. Muscle Res. Cell Motil.* **15**, 232

Lehrer, S.S., Geeves, M.A. (1998) The muscle thin filament as a classical cooperative/allosteric regulatory system. *J. Mol. Biol.* **277**, 1081

Lehrer, S.S., Kerwar, G. (1972) Intrinsic fluorescence of actin. *Biochemistry (N.Y.)*. **11**, 1211

Lehrer, S.S., Betteridge, D.R., Graceffa, P., Wong, S., Seidel, J.C. (1984) Comparison of the fluorescence and conformational properties of smooth and striated tropomyosin. *Biochemistry (N.Y.)*. **23**, 1591

Lionikas, A., Li, M., Larsson, L. (2006) Human skeletal muscle myosin function at physiological and non-physiological temperatures. *Acta Physiologica*. **186**, 151

Lowey, S., and Cohen, C. (1962) Studies on the structure of myosin. *J. Mol. Biol.* **4**, 293

Lowey, S., Slayter, H.S., Weeds, A.G., Baker, H. (1969) Substructure of the myosin molecule. I. Subfragments of myosin by enzymic degradation. *J.Mol.Biol.* **42**, 1

Lu, R.C., Elzinga, M. (1977) Partial amino acid sequence of brain actin and its homology with muscle actin. *Biochemistry (N.Y.)*. **16**, 5801

Lymn, R.W, Taylor, E.W. (1971) Mechanism of adenosine triphosphate hydrolysis by actomyosin. *Biochemistry (N.Y.)*. **10**, 4617

Lyons, G.E., Ontell, M., Cox, R., Sassoon, D. and Buckingham, M. (1990) The expression of myosin genes in developing skeletal muscle in the mouse embryo. *J. Cell Biol.* **111**, 1465

MacLeod, C., Firtel, R.A., Papkoff, J. (1980) Regulation of actin gene expression during spore germination in *Dictyostelium discoideum*. *Dev. Biol.* **76**, 263

Mak, A.S., Smillie, L.B., Stewart, G.R. (1980) A comparison of the amino acid sequences of rabbit skeletal muscle alpha-and beta-tropomyosins. *J. Biol. Chem.* **255**, 3647

Martin, D.J., Rubenstein, P.A. (1987) Alternate pathways for removal of the class II actin initiator methionine. *J. Biol. Chem.* **262**, 6350

McLachlan, A.D., and Stewart, M. (1975) Tropomyosin coiled-coil interactions: evidence for an unstaggered structure. *J. Mol. Biol.* **98**, 293

McLaughlin, P.J., Gooch, J.T., Mannherz, H.G., Weeds, A.G. (1993) Structure of gelsolin segment 1-actin complex and the mechanism of filament severing. *Nature.* **364**, 685

Menetrey, R. (2007) Crystal Structure of a Vertebrate Smooth Muscle Myosin Motor Domain and Its Complex with the Essential Light Chain. *Cell.* **131**, 300

Mercer, R.C.C., Mudalige, W.A.K.A., Heeley, D.H. (2009) Slow skeletal muscle actin. *Biophys. J.* **96**, 124a

Moraczewska, J. (2002) Structural determinants of cooperativity in acto-myosin interactions. *Acta Biochim.Pol.* **49**, 805

Moraczewska, J., Strzelecka-Gołaszewska, H., Moens, P.D., dos Remedios, C.G. (1996) Structural changes in subdomain 2 of G-actin observed by fluorescence spectroscopy. *Biochem. J.* **317**, 605

Moraczewska, J., Wawro, B., Seguro, K., Strzelecka-Golaszewska, H. (1999) Divalent cation-, nucleotide-, and polymerization-dependent changes in the conformation of subdomain 2 of actin. *Biophys. J.* **77**, 373

Moraczewska, J., Gruszczynska-Biegala, J., Redowicz, M.J., Khaitlina, S.Y., Strzelecka-Golaszewska, H. (2004) The DNase-I binding loop of actin may play a role in the regulation of actin-myosin interaction by tropomyosin/troponin. *J. Biol. Chem.* **279**, 31197

Morita, T. (2000) Amino acid sequences of  $\alpha$ -skeletal muscle actin isoforms in two species of rattail fish, *Coryphaenoides acrolepis* and *Coryphaenoides cinereus*. *Fisheries Science.* **66**, 1150

Morita, T. (2003) Structure-based Analysis of High Pressure Adaptation of  $\alpha$ -Actin. *J. Biol. Chem.* **278**, 28060

Mornet, D., and Ue, K. (1984) Proteolysis and structure of skeletal muscle actin. *Proc. Natl. Acad. Sci. U.S.A.* **81**, 3680

Mounier, N., Sparrow, J.C. (1997) Structural comparisons of muscle and nonmuscle actins give insights into the evolution of their functional differences. *J. Mol. Evol.* **44**, 89

Mudalige, W.A.K.A., Jackman, D.M., Waddleton, D.M., Heeley, D.H.  
(2007) A vertebrate slow skeletal muscle actin isoform. *FEBS Journal*. **274**, 3452

Mueller, H., Perry, S.V. (1962) The degradation of heavy meromyosin by trypsin. *Biochem. J.* **85**, 431

Muszbek, L., Laki, K. (1974) Cleavage of Actin by Thrombin. *Proc. Natl. Acad. Sci. U.S.A.* **71**, 2208

Nakajima-Iijima, S., Hamada, H., Reddy, P., Kakunaga, T. (1985) Molecular structure of the human cytoplasmic beta-actin gene: interspecies homology of sequences in the introns. *Proc. Natl. Acad. Sci. U.S.A.* **82**, 6133

Nelson, J.S. (1994) *Fishes of the world*. pp. 624, Wiley, New York, USA

Nyman, T., Schüler, H., Korenbaum, E., Schutt, C.E., Karlsson, R., Lindberg, U. (2002) The role of MeH73 in actin polymerization and ATP hydrolysis. *J. Mol. Biol.* **317**, 577

Oda, T., Iwasa, M., Aihara, T., Maéda, Y., Narita, A. (2009) The nature of the globular-to fibrous-actin transition. *Nature*. **457**, 441

Oefner, C., and Suck, D. (1986) Crystallographic refinement and structure of DNase I at 2 Å resolution. *J. Mol. Biol.* **192**, 605

Ohtsuki, I. (1979) Molecular arrangement of troponin-T in the thin filament. *J. Biochem.* **86**, 491

Ohtsuki, I. (2007) Troponin: structure, function and dysfunction. *Adv. Exp. Med. Biol.* **592**, 21

Ohtsuki, I., Morimoto, S. (2008) Troponin: regulatory function and disorders. *Biochem. Biophys. Res. Commun.* **369**, 62

Ooi, A., Mihashi, K. (1996) Effects of Subtilisin Cleavage of Monomeric Actin on Its Nucleotide Binding. *J. Biochem.* **120**, 1104

Ooi, A., Yano, F., Okagaki, T. (2008) Thermal stability of carp G-actin monitored by loss of polymerization activity using an extrinsic fluorescent probe. *Fisheries Science.* **74**, 193

Orbán, J., Lőrinczy, D., Nyitrai, M., Hild, G. (2008) Nucleotide dependent differences between the  $\alpha$ -skeletal and  $\alpha$ -cardiac actin isoforms. *Biochem. Biophys. Res. Commun.* **368**, 696

Otey, C.A., Kalnoski, M.H., Bulinski, J.C. (1988) Immunolocalization of muscle and nonmuscle isoforms of actin in myogenic cells and adult skeletal muscle. *Cell Motil. Cytoskeleton.* **9**, 337

Otterbein, L., Graceffa, P., Dominguez, R. (2001) The crystal structure of uncomplexed actin in the ADP state. *Science.* **293**, 708

Page, R., Lindberg, U., Schutt, C.E. (1998) Domain motions in actin. *J. Mol. Biol.* **280**, 463

Papp, G., Bugyi, B., Ujfalusi, Z., Halasi, S., Orbán, J. (2005) The effect of pH on the thermal stability of  $\alpha$ -actin isoforms. *J. Therm. Anal. Calori.* **82**, 281

Parry, D.A., Squire, J.M. (1973) Structural role of tropomyosin in muscle regulation: analysis of the x-ray diffraction patterns from relaxed and contracting muscles. *J. Mol. Biol.* **75**, 33

Pato, M.D., Mak, A.S., Smillie, L.B. (1981a) Fragments of rabbit striated muscle alpha-tropomyosin. II. Binding to troponin-T. *J. Biol. Chem.* **256**, 602

Pato, M.D., Mak, A.S., Smillie, L.B. (1981b) Fragments of rabbit striated muscle alpha-tropomyosin. I. Preparation and characterization. *J. Biol. Chem.* **256**, 593

Pearlstone, J.R., Carpenter, M.R., Johnson, P., Smillie, L.B. (1976) Amino-acid sequence of tropomyosin-binding component of rabbit skeletal muscle troponin. *Proc. Natl. Acad. Sci. U.S.A.* **73**, 1902

Perrie, W.T., Perry, S.V. (1970) An electrophoretic study of the low-molecular-weight components of myosin. *Biochem. J.* **119**, 31

Perry, S.V. (2001) Vertebrate tropomyosin: distribution, properties and function. *J. Muscle Res. Cell Motil.* **22**, 5

Perutz, M.F. (1984) Species adaptation in a protein molecule. *Adv. Protein Chem.* **36**, 213

Phillips Jr, G.N., Fillers, J.P., Cohen, C. (1986) Tropomyosin crystal structure and muscle regulation. *J. Mol. Biol.* **192**, 111

Pollard, T.D. (1986) Rate constants for the reactions of ATP- and ADP-actin with the ends of actin filaments. *J. Cell Biol.* **103**, 2747

Pollard, T.D., Cooper, J.A. (1986) Actin and actin-binding proteins. A critical evaluation of mechanisms and functions. *Annu. Rev. Biochem.* **55**, 987

Rayment, I., Holden, H.M., Whittaker, M., Yohn, C.B., Lorenz, M., Holmes, K.C., Milligan, R.A. (1993a) Structure of the actin-myosin complex and its implications for muscle contraction. *Science*. **261**, 58

Rayment, I., Rypniewski, W.R., Schmidt-Base, K., Smith, R., Tomchick, D.R., Benning, M.M., Winkelmann, D.A., Wesenberg, G., Holden, H.M. (1993b) Three-dimensional structure of myosin subfragment-1: a molecular motor. *Science (New York, N.Y.)*. **261**, 50

Reisler, E., Egelman, E.H. (2007) Actin's structure and function: What we still do not understand. *J. Biol. Chem.* **282**, 36133

Robinson, R.C., Mejillano, M., Le, V.P., Burtnick, L.D., Yin, H.L., Choe, S. (1999) Domain movement in gelsolin: a calcium-activated switch. *Science*. **286**, 1939

Rould, M.A., Wan, Q., Joel, P.B., Lowey, S., Trybus, K.M. (2006) Crystal structures of expressed non-polymerizable monomeric actin in the ADP and ATP states. *J. Biol. Chem.* **281**, 31909

Rubenstein, P.A., Martin, D.J. (1983) NH<sub>2</sub>-terminal processing of *Drosophila melanogaster* actin. Sequential removal of two amino acids. *J. Biol. Chem.* **258**, 11354

Rubenstein, P.A., Spudich, J.A. (1977) Actin microheterogeneity in chick embryo fibroblasts. *Proc. Natl. Acad. Sci. U.S.A.* **74**, 120

Saeki, K., Sutoh, K., Wakabayashi, T. (1996) Tropomyosin-Binding Site(s) on the Dictyostelium Actin Surface As Identified by Site-Directed Mutagenesis. *Biochemistry (N.Y.)*. **35**, 14465

Schaub, M.C., Perry, S.V. (1969) The relaxing protein system of striated muscle. Resolution of the troponin complex into inhibitory and calcium ion-sensitizing factors and their relationship to tropomyosin. *Biochem. J.* **115**, 993

Schutt, C.E, Myslik, J.C., Rozycki, M.D., Goonesekere, N.C.W., Lindberg, U. (1993) The structure of crystalline profilin  $\beta$ -actin. *Nature*. **365**, 810

Schwaiger, I., Sattler, C., Hostetter, D.R., Rief, M. (2002) The myosin coiled-coil is a truly elastic protein structure. *Nature Materials*. **1**, 232

Schwyster, D., Phillips, M., Reisler, E. (1989) Subtilisin-cleaved actin: polymerization and interaction with myosin subfragment 1. *Biochemistry (N.Y.)*. **28**, 5889

Schwyster, D.H, Kron, S.J., Toyoshima, Y.Y., Spudich, J.A., Reisler, E. (1990) Subtilisin cleavage of actin inhibits in vitro sliding movement of actin filaments over myosin. *J.Cell Biol.* **111**, 465

Selden, L.A., Estes, J.E., Gershman, L.C. (1989) High affinity divalent cation binding to actin. Effect of low affinity salt binding. *J. Biol. Chem.* **264**, 9271

Sheterline, P., Clayton, J., Sparrow, J.C. (1998) *Protein Profile. Actin*. Oxford University Press.

Sin, I.L., Fernandes, R., Mercola, D. (1978) Direct identification of the high and low affinity calcium binding sites of troponin-C. *Biochem. Biophys. Res. Commun.* **82**, 1132

Smillie, L.B. (1976) Tropomyosin: structure and function of a coiled-coil protein in muscle contraction. *PAABS Revista*. **5**, 183

Spudich, J.A., Watt, S. (1971) The regulation of rabbit skeletal muscle contraction. I. Biochemical studies of the interaction of the tropomyosin-troponin complex with actin and the proteolytic fragments of myosin. *J. Biol. Chem.* **246**, 4866

Spyracopoulos, L., Li, M.X., Sia, S.K., Gagné, S.M., Chandra, M., Solaro, R.J., Sykes, B.D. (1997) Calcium-Induced Structural Transition in the Regulatory Domain of Human Cardiac Troponin C. *Biochemistry (N.Y.)*. **36**, 12138

Squire, J.M. (1997) Architecture and function in the muscle sarcomere. *Curr.Opin.Struct.Biol.* **7**, 247

Straub, F.B. (1942) Actin. *Studies of the Med. Inst. Szeged.* **2**, 3

Strzelecka-Golaszewska, H., Venyaminov, S.Y., Zmorzyski, S., Mossakowska, M. (1985) Effects of various amino acid replacements on the conformational stability of G-actin. *FEBS.* **147**, 331

Strzelecka-Golaszewska, H., Moraczewska, J., Khaitlina, S.Y., Mossakowska, M. (1993) Localization of the tightly bound divalent-cation-dependent and nucleotide-dependent conformation changes in G-actin using limited proteolytic digestion. *FEBS.* **211**, 731

Strzelecka-Golaszewska, H., Wozniak, A., Hult, T., Lindberg, U. (1996) Effects of the type of divalent cation, Ca<sup>2+</sup> or Mg<sup>2+</sup>, bound at the high-affinity site and of the ionic composition of the solution on the structure of F-actin. *Biochem. J.* **316**, 713

Suck, D., Oefner, C., Kabsch, W. (1984) Three-dimensional structure of bovine pancreatic DNase I at 2.5 Å resolution. *EMBO J.* **3**, 2423

Swezey, R.R., Somero, G.N. (1982) Polymerization thermodynamics and structural stabilities of skeletal muscle actins from vertebrates adapted to different temperatures and hydrostatic pressures. *Biochemistry (N.Y.)*. **21**, 4496

Takeda, S., Yamashita, A., Maeda, K., Maéda, Y. (2003) Structure of the core domain of human cardiac troponin in the Ca<sup>2+</sup> state. *Nature*. **424**, 35

Talbot, J.A., Hodges, R.S. (1981) Synthetic studies on the inhibitory region of rabbit skeletal troponin I. Relationship of amino acid sequence to biological activity. *J. Biol. Chem.* **256**, 2798

Tanaka, H., Maezawa, Y., Ojima, T., Nishita, K. (2004) Cloning and sequencing of cDNAs encoding walleye pollack  $\alpha$ -skeletal actin isoforms. *Fisheries Science*. **70**, 198

Turoverov, K.K., Verkhusha, V.V., Shavlovsky, M.M., Biktashev, A.G., Povarova, O.I., Kuznetsova, I.M. (2002) Kinetics of actin unfolding induced by guanidine hydrochloride. *Biochemistry (N.Y.)*. **41**, 1014

Vahdat, A., Millera, C., Phillippsa, M., Muhlradb, A., Reisler, E. (1995) A novel 27 & 16 kDa form of subtilisin cleaved actin: structural and functional consequences of cleavage between Ser234 and Ser235. *FEBS Lett.* **365**, 149

Van Eerd, J.P., Takahshi, K. (1976) Determination of the complete amino acid sequence of bovine cardiac troponin C. *Biochemistry (N.Y.)*. **15**, 1171

Van Eyk, J.E., Strauss, J.D., Hodges, R.S., Rüegg, J.C. (1993) A synthetic peptide mimics troponin I function in the calcium-dependent regulation of muscle contraction. *FEBS Lett.* **323**, 223

Vandekerckhove, J. (1981) A Highly Sensitive Protein-Chemical Procedure Able to Distinguish Different Actins. *FEBS*. **113**, 595

Vandekerckhove, J., Weber, K. (1978) At least six different actins are expressed in a higher mammal: an analysis based on the amino acid sequence of the amino-terminal tryptic peptide. *J. Mol. Biol.* **126**, 783

Vandekerckhove, J., Weber, K. (1979) The complete amino acid sequence of actins from bovine aorta, bovine heart, bovine fast skeletal muscle, and rabbit slow skeletal muscle. A protein-chemical analysis of muscle actin differentiation. *Differentiation*. **14**, 123

Vandekerckhove, J., Weber, K. (1984) Chordate muscle actins differ distinctly from invertebrate muscle actins. The evolution of the different vertebrate muscle actins. *J. Mol. Biol.* **179**, 391

Vassilyev, D.G., Takeda, S., Wakatsuki, S., Maeda, K., Maéda Y. (1998) Crystal structure of troponin C in complex with troponin I fragment at 2.3-Å resolution. *Proc. Natl. Acad. Sci. U.S.A.* **95**, 4847

Vibert, P., Cohen, C. (1988) Domains, motions and regulation in the myosin head. *J. Muscle Res. Cell Motil.* **9**, 296

Vibert, P., Craig, R., Lehman, W. (1997) Steric-model for activation of muscle thin filaments. *J. Mol. Biol.* **266**, 8

von Schalburg, K.R., Leong, J., Cooper, G.A., Robb, A., Beetz-Sargent, M.R., Lieph, R., Holt, R.A., Moore, R., Ewart, K.V., Driedzic, W.R., ten Hallers, B.F.H., Zhu, B., de Jong, P.J.,

Davidson, W.S., Koop, B.F. (2008) Rainbow smelt (*Osmerus mordax*) genomic library and EST resources. *Marine Biotechnology*. **10**, 487

Wang, Y.L. (1985) Exchange of actin subunits at the leading edge of living fibroblasts: possible role of treadmilling. *J. Cell Biol.* **101**, 597

Wasko, A.P., Severino, S.E., Presti, F.T., Poletto, A.B., Martins, C. (2007) Partial molecular characterization of the Nile tilapia (*Oreochromis niloticus*)  $\alpha$ -cardiac muscle actin gene and its relationship to actin isoforms of other fish species. *Gene. Mol. Biol.* **30**, 1089

Weeds, A.G, Taylor, R.S. (1975) Separation of subfragment-1 isoenzymes from rabbit skeletal muscle myosin. *Nature*. **257**, 54

Weihing, R.R, Korn, E.D. (1972) *Acanthamoeba* actin. Composition of the peptide that contains 3-methylhistidine and a peptide that contains N e-methyllysine. *Biochemistry (N.Y.)*. **11**, 1538

Whalen, R.G., Butler-Browne, G.S., Gros, F. (1976) Protein synthesis and actin heterogeneity in calf muscle cells in culture. *Proc. Natl. Acad. Sci. U.S.A.* **73**, 2018

White, S., Cohen, C., Phillips Jr, G.N. (1987) Structure of co-crystals of tropomyosin and troponin. *Nature*. **325**, 826

White, H.D., Belknap, B., Webb, M.R. (1997) Kinetics of Nucleoside Triphosphate Cleavage and Phosphate Release Steps by Associated Rabbit Skeletal Actomyosin, Measured Using a Novel Fluorescent Probe for Phosphate. *Biochemistry (N.Y.)*. **36**, 11828

Wilkinson, J.M. (1974) The preparation and properties of the components of troponin B. *Biochim. Biophys. Acta*. **359**, 379

Wolska, B.M., Vijayan, K., Arteaga, G.M., Konhilas, J.P., Phillips, R.M., Kim, R., Naya, T., Leiden, J.M., Martin, A.F., de Tombe, P.P., Solaro, R.J. (2001) Expression of slow skeletal troponin I in adult transgenic mouse heart muscle reduces the force decline observed during acidic conditions. *J. Physiol. (Lond.)*. **536**, 863

Wu, C.S, Yang, J.T. (1976) Reexamination of the conformation of muscle proteins by optical activity. *Biochemistry (N.Y.)*. **15**, 3007

Zechel, K., Weber, K. (1978) Actins from mammals, bird, fish and slime mold characterized by isoelectric focusing in polyacrylamide gels. *FEBS*. **89**, 105

Zhang, R., Zhao, J., Mandveno, A., Potter, J.D. (1995) Cardiac troponin I phosphorylation increases the rate of cardiac muscle relaxation. *Circ. Res.* **76**, 1028

Zimmerle, C.T., Patane, K., Frieden, C. (1987) Divalent cation binding to the high-and low-affinity sites on G-actin. *Biochemistry (N.Y.)*. **26**, 6545

Zot, A.S., Potter, J.D. (1987) Structural aspects of troponin-tropomyosin regulation of skeletal muscle contraction. *Ann. Rev. Biophys.* **16**, 535





